OUKA
The University of Osaka
Institutional Knowledge Archive

Title	Research on Supporting Data-driven Analysis on Animal Behavioral Big Data
Author(s)	田, 一鳴
Citation	大阪大学, 2021, 博士論文
Version Type	VoR
URL	https://doi.org/10.18910/85437
rights	© 2021, The Author(s). This article is licensed under a Creative Commons Attribution 4.0 International License, which permits use, sharing, adaptation, distribution and reproduction in any medium or format, as long as you give appropriate credit to the original author(s) and the source, provide a link to the Creative Commons licence, and indicate if changes were made. The images or other third party material in this article are included in the article's Creative Commons licence, unless indicated otherwise in a credit line to the material. If material is not included in the article's Creative Commons licence and your intended use is not permitted by statutory regulation or exceeds the permitted use, you will need to obtain permission directly from the copyright holder. To view a copy of this licence, visit http://creativecommons.org/licenses/by/4.0/. The Creative Commons Public Domain Dedication waiver (http://creativecommons.org/publicdomain/zero/1.0/) applies to the data made available in this article, unless otherwise stated in a credit line to the data.
Note	

The University of Osaka Institutional Knowledge Archive : OUKA

https://ir.library.osaka-u.ac.jp/

The University of Osaka

Research on Supporting Data-driven Analysis on Animal Behavioral Big Data

Submitted to
Graduate School of Information Science and Technology
Osaka University

July 2021

Yiming TIAN

List of Publications

1. Journal Paper

1. Y. Tian, T. Maekawa, D. Amagata, T. Hara, S. Matsumoto, K. Yoda, E. Fujioka, F. Hamai, D. Fukui, S. Hiryu. Discovering Frequent Co-occurrence Rules from Multi-modal Animal Locomotion Data, *IPSJ Journal*, 60(3): 859–869, 2019.

2. Y. Tian, T. Maekawa, J. Korpela, D. Amagata, T. Hara, S. Matsumoto, K. Yoda. Automatic Identification of Differences in Behavioral Co-occurrence between Groups, *Animal Biotelemetry*, 9(21): 1–15, 2021.

3. Y. Tian, T. Maekawa, T. Hara, S. Matsumoto, K. Yoda. Data-driven approach to understand decision-making: Machine learning predicts trip decision-making from initial trajectory segments in seabirds, *Biology Letters* (revision submitted).

2. International Conference Paper

1. Y. Tian, T. Maekawa, J. Korpela, D. Amagata, T. Hara, S. Matsumoto and K. Yoda. Preliminary investigation of co-occurrence rule extraction for sex-specific behavior of Streaked Shearwater, *ACML2019 Workshop on Machine Learning for Trajectory, Activity, and Behavior*, 2019.

2. Y. Tian, T. Maekawa, T. Hara, Y. Yokomori and T. Kitagawa. NaviMine: A tool for mining trajectories through behavior prediction, *PerCom2021 Workshop on Pervasive Information Flow*, 2021.

3. Domestic Conference Paper

(Oral presentation)

1. Y. Tian, T. Maekawa, D. Amagata, T. Hara, S. Matsumoto, K. Yoda, E. Fujioka, F. Hamai, D. Fukui, S. Hiryu. A Study on Fast Extraction of Frequent

Co-occurrence Rules from Animal Movement Behavior Data. In *Proc. of DEIM Forum*, 2018.

2. Y. Tian, T. Maekawa, D. Amagata, T. Hara, S. Matsumoto, K. Yoda, E. Fujioka, F. Hamai, D. Fukui, S. Hiryu. Preliminary Investigation of Co-Occurrence Rule Extraction from Multi-Modal Animal Locomotion Data, In *Proc. of The 80th National Convention of IPSJ*, 2018.

3. Y. Tian, T. Maekawa, T. Hara, S. Matsumoto and K. Yoda. A Study on the Discovery of Factors Related to Decision-making in Animals Using Behavioral Prediction. In *Proc. of The Society of Instrument and Control Engineers*, 2020.

(Poster presentation)

1. Y. Tian, T. Maekawa, D. Amagata, T. Hara, S. Matsumoto, K. Yoda, E. Fujioka, F. Hamai, D. Fukui, S. Hiryu. Frequent Rule Discovery and Validation from Migration Behavior Data of Japanese Large-footed Bat and Streaked Shearwater, In *The Zoological Society of Japan*, 2018.

Abstract

Navigation is an essential ability of many animals, and it can help animals find their way accurately without maps or instruments. Through constant research by biologists, the capabilities of navigation are becoming more apparent; for example, in long distance navigation, birds use the earth's magnetic field or sky, and in short distance navigation, many animals use the surrounding environment and their memory to find the right way. However, the mechanisms of navigation are not yet fully understood, especially the processes by which animals deal with their external/internal information. For example, how do animals set their destinations? How do animals choose the appropriate path to reach their destinations? How do animals follow paths based on their surrounding environment? Thanks to recent advances in sensing technology and batteries, more and finer data on animal behavior can be recorded from animal borne sensor devices, such as trajectory as well as body and environmental information, for example, heart rate and water temperature. These data can help biologists learn more about navigation. Therefore, biologists have tried to build a model to explain the mechanism of navigation by using the data from sensors. If we can understand, clarify, and predict navigation, human can coexist with animals and deal with the spread of infectious diseases by animals. However, the collected data is big animal behavioral data, including a lot of sensor modalities and long-term time-series, making it difficult for biologists to analyze navigation in identifying the essential sensor modalities and timings.

Therefore, the goal of the study is to develop methods to support biologists in understanding animal navigation using big animal behavioral data. In this study, we (i) find important sensing modalities from multi-modal sensor data in the task of detecting frequent co-occurrence behavioral modes and (ii) determine important timings from long-term sensor data in the task of identifying clues of animals' decision-making. (i) Different sensing modality contains different behavioral modes, such as resting and cruising modes in speed, and tensing and relaxing modes in heart rate. If an animal in the cruising mode also in the relaxing mode simultaneously, we call the cruising mode and relaxing mode as frequent co-occurrence behavioral modes. Detecting co-occurrence behavioral modes can help us understand animal behavior and its relationship with internal states/surrounding environments. To detect the frequent co-occurrence behav-

ioral modes, we need to analyze all possible behavioral modes from the whole sensor modalities, which incurs an expensive computational time. (ii) As for the detection of important timings, this study focuses on the analysis of decision-making by animals. Analyzing decision-making during locomotion by animals can help us understand the navigation mechanisms. However, it is difficult for biologists to find out clues related to decision-making. First, it is difficult to detect when an animal makes a decision because the data becomes huge in the observation over long period of time. Second, a lot of sensor modalities are recorded, making it difficult to find out clues that animals use to make their decisions.

In this thesis, we aim to solve these two problems to support biologists to understand the mechanism of animal navigation. This thesis consists of 5 chapters. We introduce the research background of animal navigation and discuss research issues in Chapter 1.

In Chapter 2, we propose a frequent co-occurrence behavioral modes detection method. The proposed method achieves high-speed time-series segmentation & clustering and automatically detects co-occurrence behavioral modes. The proposed method first uses Symbolic Aggregate approXimation (SAX), a symbolization method, to segment time-series. We reduce the computation time of SAX by reusing previous results of SAX when different parameter (number of symbols) was used. We then apply spectral clustering to cluster the segments. Spectral clustering is a graph partition method, which regards data points as vertices in a graph; in our case, we assume segments as nodes in a graph. To speed up the clustering, we reduce the graph size by merging segments with the same symbol into one node; we verify that the clustering result of the merged graph is identical to the result of the original graph. Compared with comparison methods, our method significantly improves the speed of time-series segmentation and clustering. We applied the proposed method to Japanese Large-footed Bats in order to analyze their behavior while foraging. The results revealed that the bats use their uropatagium (the membrane that extends between the thighs of a bat) to slow down when foraging since they are easier to control the body when the speed is low.

In Chapter 3, we continue our study on frequent co-occurrence behavioral modes. Here we introduce comparative analysis into the analysis of behavioral co-occurrence, and we study on the difference in co-occurrence behavioral modes between groups, such as male group vs. female group. In our method, we first identify the frequent

co-occurrence behavioral modes using the method in Chapter 2. Then, we calculate the correlation of the behavioral modes for each group. Next, we compute the absolute values of the differences (the difference in correlation between groups) between the two groups. Finally, the co-occurrence of behavioral modes that differed in frequency between the two groups is obtained. We applied our method to streaked shearwaters (*Calonectris leucomelas*), in order to reveal behavioral difference between male and female birds. The results revealed that females dive more frequently than males between 10:00 and 17:00 to catch fish for chicks, suggesting the sex-specificity in the roles of breeding chicks.

In Chapter 4, we propose a trajectory mining tool, NaviMine, to find the important timings and clues related to decision-making by using behavior prediction. To find the time and clues related to decision-making, we focus on the initial t hours segment of trajectories. If we can predict animals' future movement by using an initial t hours segment with a high probability, we can assume that factors related to future decision-making are hidden in the initial t hours segments. We applied the tool to chum salmon (*Oncorhynchus keta*) and streaked shearwaters (*Calonectris leucomelas*). The results obtained by the proposed method indicate that the changes in water temperature in the early period play a crucial role in determining the destination of salmon. Our method also revealed that the foraging activities in the initial 5 hours affect the trip duration of seabirds.

Finally, in Chapter 5, we summarize this thesis and discuss our future work.

Contents

1 Introduction **1**

1.1 Research issues 3

1.1.1 Analysis of multi-modal sensor data 4

1.1.2 Analysis of long-term sensor data 6

1.2 Research contents 6

1.3 Contribution of thesis 9

1.4 Organization of thesis 10

2 Detecting co-occurrence behavioral modes in animal behavioral data **13**

2.1 Introduction 13

2.2 Preliminary 16

2.2.1 Time-series segmentation and clustering 16

2.2.2 First passage time 18

2.3 Proposed method 19

2.3.1 Problem definition 19

2.3.2 Overview 20

2.3.3 Segmentation 22

2.3.4 Clustering 25

2.3.5 Score 30

2.4 Experiment 31

2.4.1 Dataset 31

2.4.2 Feature extraction 33

2.4.3 Comparison method and environment 34

2.4.4 Result 35

2.5 Discussion . . . 37
2.5.1 Efficiency of the proposed method . . . 37
2.5.2 Insight obtained from the results . . . 40
2.6 Conclusion . . . 41

3 Detecting difference in co-occurrence behavioral modes between groups in animal behavioral data 43
3.1 Introduction . . . 43
3.2 Preliminary . . . 45
3.2.1 Big data mining technology for comparative analysis . . . 45
3.2.2 LSTM autoencoder . . . 45
3.3 Proposed method . . . 46
3.3.1 Problem definition . . . 47
3.3.2 Algorithm . . . 47
3.3.3 Feature extraction/learning . . . 48
3.3.4 Identifying co-occurrences in behavioral modes and diversification . . . 51
3.3.5 Identifying the co-occurrence of behavioral modes that differs between groups . . . 51
3.4 Experiment . . . 51
3.4.1 Dataset . . . 51
3.4.2 Feature extraction . . . 52
3.4.3 Comparison methods and environment . . . 53
3.4.4 Result . . . 54
3.5 Discussion . . . 56
3.6 Conclusion . . . 65

4 NaviMine: A tool for detecting important timing and clues related to animal decision-making 67
4.1 Introduction . . . 67
4.2 Preliminary . . . 69
4.3 Proposed method . . . 70
4.3.1 Assumption . . . 70

4.3.2 Overview 70
4.3.3 Behavior prediction 71
4.3.4 Accuracies series analysis 72
4.4 Experiment 76
4.4.1 Dataset 76
4.4.2 Feature extraction 81
4.4.3 Environment 82
4.4.4 Result 83
4.5 Discussion 86
4.6 Conclusion 90

5 Summary **93**
5.1 Summary of contributions 93
5.2 Future work 95

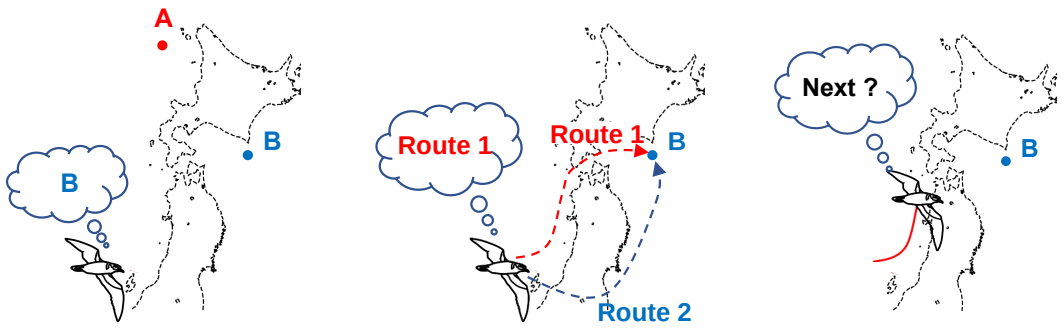
Acknowledgment **97**

Chapter 1

Introduction

Navigation is an ability of many animals that allows them to recognize their location and reach their destinations accurately without instruments (e.g., compass). Through continuous researches by biologists, the capabilities of animal navigation are becoming more apparent. Animal navigation can be broadly grouped into landmark-based navigation, celestial navigation, magnetic navigation, and sensory navigation [4].

The selection of landmarks varies for different animals; its homogeneity lies in the fact that the landmarks selected by animals often depend on the size of the animal and the environment in which they live [10, 16, 17]. The nest-return behavior of Bienenwolfes (*Philanthus triangulum*) is a typical example of landmark-based navigation [95]. Celestial bodies can provide direction for animals, and the sun and starry sky have all been found to play an important supporting role in animal navigation [25, 26, 46, 103]. The sun, as a relatively stable, regularly changing, and predictable reference, has been used by many animals as a compass to accomplish a range of navigational behaviors. The first experiments using the sun for navigation were conducted by Gustav Kramer, who showed experimentally that migratory birds use the sun as a compass for their migratory behavior [47]. Bio-magnetism is a phenomenon that exists in many animals, which are able to perceive magnetic fields and can produce responses from the molecular level to the individual biological level [75, 107, 108, 109]. The occurrence of migratory behavior in many animals is the result of bio-magnetism. For example, the European robin adopts a navigation method based on the use of solar navigation, supplemented by the use of magnetic fields, combined with the bird's nesting experience



(a) Destination setting (b) Path selection (c) Behavioral control

Figure 1.1: The process animals deal with information from surrounding environment.

and familiarity with the destination [63].

In addition to the standard navigation using the above senses, there is also navigation using the senses of smell and hearing [101, 119]. Some animals have a keen sense of smell, and they are able to perceive the odor of specific chemicals and leave an imprint for a long time or even a lifetime. These animals can then navigate with their imprints. After entering freshwater from the ocean, salmon rely on their sense of smell to navigate successfully back to their natal river for spawning [23]. Sensory deprivation experiments validated this idea [110]. Experiments with salmon with blocked nasal passages and blinded salmon showed that the former could not return accurately to their natal river, while the latter were unaffected. On the other hand, auditory navigation is a way of obtaining navigation information by making and receiving sounds. Bats are representative of a creature that can use echolocation [84]. Bats emit and receive ultrasonic, which allows them to search for prey and travel at night.

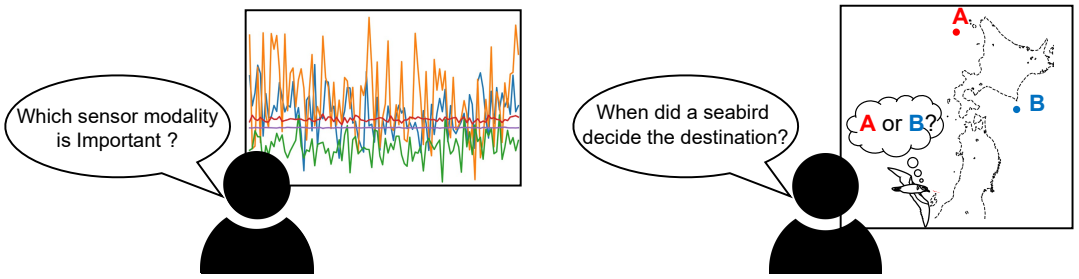
However, there is still much that is unknown about the mechanisms of animal navigation, such as how animals deal with information from surrounding environments (Figure 1.1). For example, in destination setting, how do animals determine their destination for foraging (Figure 1.1a)? In path selection, how do they choose their route after they had decided on their destination (Figure 1.1b)? In behavioral control, how do they determine their location and can follow a set route as they travel to their destination (Figure 1.1c)?

On the other hand, due to the development of sensor and battery technologies, more and more detailed data can be recorded; for example, GPS tracks can be recorded every minute. At the same time, sensors can also record a wide range of information about the animal's surrounding environment and its body condition, such as water temperature and heart rate. This information records the animals' behavior in detail. By analyzing these data, biologists can gain a deeper understanding of the animals' navigation mechanisms. Thus, biologists use the information regarding the surrounding environment as input and trajectory information as output to construct models that explain the mechanisms of animal navigation.

If the navigation of animals can be understood, clarified, and predicted, humans can achieve coexistence with animals. By understanding the navigation of animals, humans are able to prevent the spread of infectious diseases. Many deadly infectious diseases are now transmitted through animals. For example, plague can be transmitted by fleas, and the coronavirus disease 2019 (COVID-19) that began last year was transmitted from bats to humans through other animals [106]. Suppose that the human can understand the behavior of animals that may carry those potentially deadly infectious diseases. In that case, it can be possible to propose counter measures based on the behavior, e.g., setting up a sanctuary.

1.1 Research issues

Due to the recent advances in sensor, battery, and memory technologies, we can now collect big animal behavioral data includes a lot of sensor modalities and is long periods. However, it is difficult for biologists to find out the important sensor modalities (Figure 1.2a) and timings (Figure 1.2b) from the big animal behavioral data. For example, there are two possible destinations of seabirds in Figure 1.2b, A and B, it is difficult to detect when the seabirds made their decision to go to A or B by manually analyzing long-term multi-modal trajectory data (example trajectory data is shown below). Therefore, it is important to develop methods to solve these problems to support biologists in revealing animal navigation from the big animal behavioral data (Figure 1.3). In this section, we detail the research problems of detecting important information from big data on animal behavior.



(a) analysis of multi-modal sensor data (b) analysis of long period record

Figure 1.2: Problems biologists face when analyzing sensor data: (a) multi-modal sensor data. (b) long period record.

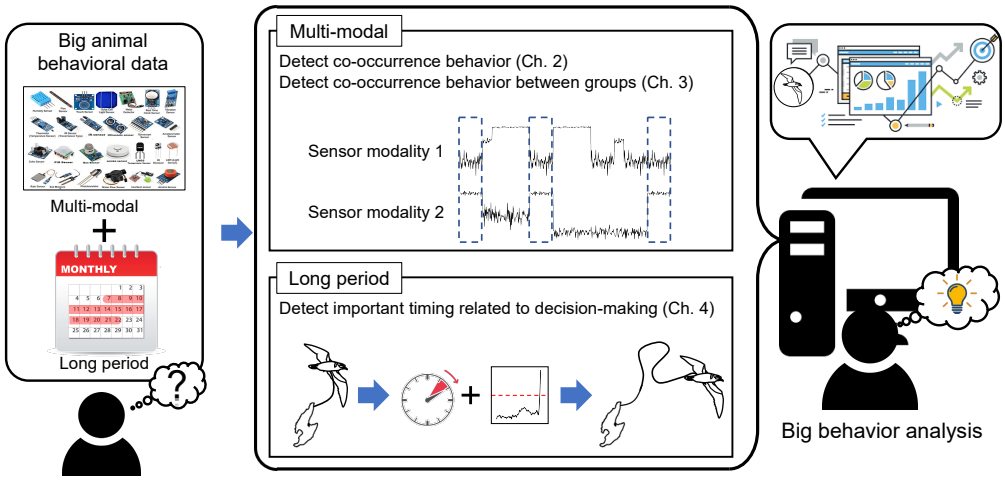


Figure 1.3: The objectives of the study. We try to solve two problems : difficulties in analyzing (1) multi-modal sensor data and (2) long period record to support biologists realize big behavioral analysis.

1.1.1 Analysis of multi-modal sensor data

Recent animal borne sensor loggers allow fine-grained measurement of the animals' behavior along with associated environmental and physiological data, enabling the biologists to unravel the adaptive significance of the behavior. However, because animal-borne loggers can now record multi-modal time-series information from a variety of sensors, it is becoming increasingly difficult to identify biologically important patterns

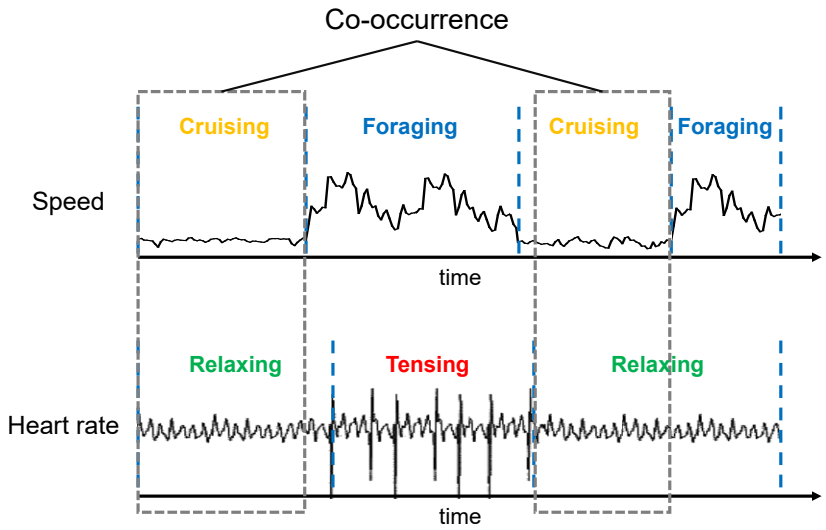


Figure 1.4: A hypothetical example of co-occurrence of behavioral modes. The cruising mode extracted from the time-series speed data and the relaxing mode extracted from the time-series heart rate data co-occur frequently.

hidden in the high-dimensional long-term data. In particular, it is important to identify co-occurrences of several behavioral modes recorded by different sensors in order to understand behavioral responses caused by external stimuli and/or an internal hidden state of an animal. Figure 1.4 shows an example of co-occurrence behavioral modes. There are two modes: the cruising mode and the forging mode, in the speed data. In the heart rate data, there are relaxing mode and tensing mode. From the figure, we can find that the cruising mode and the relaxing mode are co-occurred, which means that when an animal is cruising, it is relaxing. However, the previous studies select sensor modalities to analyze (and parameters for mode detection algorithm) based on the experience of biologists. In our research, we try to find the best combination of two behavioral modes from all sensor modalities as well as the best parameters from all possible values, resulting in an expensive computational time. Therefore, we develop a computationally efficient method to detect frequent co-occurrence of behavioral modes by automatically selecting the parameters and sensor modalities.

1.1.2 Analysis of long-term sensor data

Animal movement plays an important role in determining the foraging, reproductive, and survival success of a species [64, 96]. In particular, the timing and direction of travel play a crucial role in survival, for example, arriving at nest at right time or safely avoiding predators, which are affected by various internal, external, and social factors [18, 61]. Although sensor data of animals in the wild enable a computational analysis of animal movement, it is difficult to identify the timing of decision-making from long-duration time-series data. Figure 1.5 shows the first 5 hours of seabirds' trajectories after departure from the colony. After that, the seabirds start either one of the two kinds of trips; the long-term trips in blue over one day or short-term trips in red less than one day. In the long-term trips, seabirds fly to Hokkaido for foraging, while in the short-term trips, seabirds just fly around the colony. As shown in Figure 1.5, it seems that there is no visual difference between long-term trips and short-term trips in the first 5 hours. However, because animals make the decision based on experienced external/internal events in many cases, it is likely that something affecting the decision-making is hidden in the past sensory data. Therefore, we develop a method to detect important timings and clues related to animal destination determination.

1.2 Research contents

In this thesis, we propose methods for supporting the detection of important information from big animal behavioral data. Our methods, which utilize various techniques, such as clustering, deep learning, statistical analysis, address and solve the research issues stated in Section 1.1. The outline of the proposed methods is as follows.

- Detecting co-occurrence behavior

  Chapter 2 addresses the problem of finding the best combination of two behavioral modes from all sensor modalities and segmentation/clustering parameters. The behavioral modes can be extracted by time-series segmentation and clustering. Finding the best combination of two behavioral modes from all sensor modalities and parameters means that we have to iterate time-series segmentation and clustering many times, resulting in huge computational costs. To solve the problem,

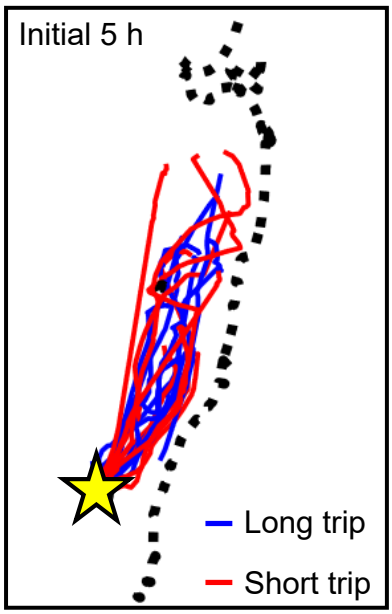


Figure 1.5: An example of initial 5 hours of seabirds' trajectories after departure from the colony. Blue lines indicate long-term trips and red lines indicate short-term trip. Yellow star mark measures the colony.

we develop a co-occurrence behavioral modes extraction method that efficiently computes the iterations of time-series segmentation and clustering. We develop a method for extracting co-occurrence behavioral modes that efficiently executes iterations of time series segmentation and clustering. In the proposed method, we employ Symbolic Aggregate approXimation (SAX) to segment sensor time-series efficiently. After obtaining the segmentation results, we use spectral clustering, which is a graph-based clustering method. Spectral clustering constructs a similarity graph where each segment corresponds to a node in the graph. To reduce the computational cost of the clustering, we use node similarity to reduce the size of the graph. Finally, we calculate co-occurrence scores between different modes and find out the co-occurrence behavioral modes. We apply the method on the Japanese Large-footed Bat to understand its foraging strategy, that enables it to capture insects moving with high speed. After discussion with biologists, some new insights related to prey capture behavior are found by the proposed method.

- Detecting co-occurrence behavior between groups

  In Chapter 3, we modify the methods in Chapter 2 by trying to identify the co-occurrence behavioral modes that differ substantially between groups. Because animals belonging to different groups, e.g., male group and female group, behave differently, finding the co-occurrence behavioral modes that differ between groups can help biologists to understand action strategies caused by differences in the groups, e.g., sexual size dimorphism. Therefore, we introduce comparative analysis into the method in Chapter 2 to detect co-occurrence behavioral modes with significant differences in frequency between two groups. After we get the co-occurrence behavioral modes, we separate corresponding data into two groups (e.g., male and female). For each group, we compute the correlation of the co-occurred modes and compute the difference between the correlations. We iterate this process over the co-occurrence behavioral modes with high scores and finally get a rank list. The higher the score, the more significant the difference between groups. We apply the method to streaked shearwaters (*Calonectris leucomelas*), which is a kind of seabird. Since there is a sex-specificity between males and females, e.g., body size and roles in breeding chicks, we want to determine how the sex-specificity influences their behaviors. After discussion with biologists, some new findings related to foraging behavior in the parenting period are found through the proposed method.

- Detecting important timings related to animal decision-making

  In Chapter 4, we aim to detect the timings and clues of animals' decision-making. To solve the problems we mentioned in Section 1.1.2, we set an assumption that animals decide their destination according to their past internal/external events. If we can use the past trajectory to predict future destinations, for example, there should be some clues related to destination determination in the past trajectories. In this study, to reveal the timing of destination determination, we focus on the initial short segments of trajectories of animals and predict future destinations using these segments. If we can predict the destination of animals by using the first t hours of the initial segments, it can be considered that the primary reasons for determining destination are hidden in the first t hours of the initial segments.

To find out appropriate t, the proposed method computes prediction accuracies of future destinations by varying different t values. Then, by fusing the prediction accuracies of different t values, we can obtain a series of the accuracies. To detect the meaningful time when factors related to destination determination may exist, we focus on three kinds of timings: i) sudden increase, ii) peak, and iii) increase before the plateau in the accuracy series. We apply the method to behavioral data from seabirds (streaked shearwater) and salmon. There are two kinds of trips for seabirds, short-term trips are less than one day, while long-term trips are over than one day. On long-term trips, seabirds fly to Hokkaido for foraging. However, long-term trips consume much energy. The research question is to find out the reason why seabirds travel long distances to forage by consuming their energy. Although previous researches show that salmon use their smell to find their natal river, the way of using their sense of smell to identify their natal river has not yet been revealed. Our method shows that the foraging activities in the initial hours may affect the trip duration of seabirds, and salmon may determine their destinations in an early period.

1.3 Contribution of thesis

Attempts to enhance science by leveraging computer technologies are called e-science [39], that applies computer technologies to scientific investigations, including data preparation, experimentation, data collection, and analysis of the data. For the e-science study, this study proposes two computational approaches to analyze animal navigation: i) detecting co-occurrence behavioral modes and ii) detecting decision-related factors. First, while previous methods have used multiple time-series as inputs to detect co-occurrence behavioral modes using the clustering method, this study proposes a new cluster analysis method for multi-modal time-series data, resulting in the ability to find co-occurrence behavioral modes. Secondly, we provide a tool to detect the timing and the important clues of animal decision-making based on behavioral prediction, and this method offers a new way of animal behavior analysis. The above techniques can be applied not only to biological studies but also to other natural science studies that analyze multi-modal time-series such as analysis of earthquake and time-series gene expression.

We believe that this study will contribute to e-science in terms of knowledge extraction from multi-modal long-term time-series using computational methods. In detail, the contributions of this study are as follows.

- We propose a method for automatically detecting frequent co-occurrence of behavioral modes that differ in frequency between two groups from big animal behavioral data. We have developed an efficient calculation method to find the optimal hyperparameters (combinations of sensor modalities used and clustering parameters). We extend the method to find the behavioral mode that differs in frequency between two groups. The proposed method can find behavioral modes from different sensor modalities that are frequently co-occurred and then identifies co-occurrence behavioral modes with great differences between two groups. To our knowledge, this is the first study that can automatically detect the co-occurrence of behavioral modes from big animal behavioral data.
- We validate the effectiveness of the methods using actual data obtained from bat and seabirds, including the relationship between movement behavior and capture events of bats and sex-specific differences in seabirds related to co-occurrences between horizontal (i.e., GPS positions) and vertical (i.e., diving depths) movements.
- We develop a tool that can automatically detect potential times and important clues related to the destination determination of animals. Biologist only needs to prepare data on the trajectory of the target animal in order to formulate hypotheses related to the destination decision. The tool can also be used to mine important information from the data to reveal the causality between the data.
- We apply our tool to seabirds and salmon, and find some new insights that allow biologists to understand mechanisms of decision-making regarding navigation.

1.4 Organization of thesis

This thesis consists of five chapters, and the remainder of the thesis is organized as follows.

In Chapter 2, we introduce and discuss the problem of detecting co-occurrence behavioral modes from multi-modal sensor data in Section 2.1. Section 2.2 reviews the related work of this topic. Our proposed method is described in Section 2.3. In this section, we first describe the overview of our method. Then, we introduce our idea about reducing the computational time of time-series segmentation and clustering and describe how the proposed method can detect co-occurrence behavioral modes. The experiment setup and co-occurred behavioral modes found by our proposed method are described in Section 2.4. In Section 2.5, we present the results of our discussions with biologists Finally, we conclude our work in this chapter in Section 2.6. The study in this chapter is based on our works published in [87, 88, 89, 90].

In Chapter 3, we introduce and discuss the problem of the co-occurrence behavioral modes with great difference in frequency between two groups in Section 3.1. Section 3.2 reviews the related work of this topic. In Section 3.3, we describe our proposed methods. The details of the experiment and the co-occurrence behavioral modes with great differences in groups found by the proposed method are discussed in Section 3.4. We show the discussion result and the new insights discovered in Section 3.5. Finally, this chapter is summarized in Section 3.6. The study in this chapter is based on our works published in [94, 93]

In Chapter 4, we focus on detecting the timing of animals' decision-making from long period data in Section 4.1. In Section 4.2, we review related works of this topic in the chapter. Section 4.3 shows our assumption and proposed method. We conduct experiments to clarify our hypothesis, and the setting and results of experiments are described in Section 4.4. Section 4.5 describes the clues found in the results related to the animals' decision-making. Finally, our work in this chapter is concluded in Section 4.6. The study in this chapter is based on our work published in [91, 92].

Finally, in Chapter 5, we summarize this thesis and discuss future work.

Chapter 2

Detecting co-occurrence behavioral modes in animal behavioral data

2.1 Introduction

Thanks to advanced sensing and microcomputer technologies, more detailed animal behavioral data are collected at intervals of minutes or even seconds by sensor devices, such as micro GPS loggers attached to seabirds for recording trajectory information [31]. As a result, a large number of interdisciplinary studies have been conducted focusing on understanding animal behavior related to the fields of biology, neuroscience, information science, and engineering [73, 78, 98]. In addition to animal behavioral data, sensors are used to collect environmental (e.g., surrounding images, sounds, smells) and biological (e.g., blood sugar level, neural activity, and heart rate) data to elucidate the interrelationships between behavioral responses and environmental changes.

Animal behavioral data generally include several behavioral modes, such as foraging mode and cruising mode obtained from speed time-series data. Similarly, environmental and biological time-series data include several behavioral modes, including relaxing and tensing modes in heart rate time-series data. It is possible to understand animal behavior and its relationship with surrounding environments or internal states of animals by extracting frequent co-occurrence behavioral modes from multi-modal sensor data.

An example of a standard frequent co-occurrence behavioral mode is that animals

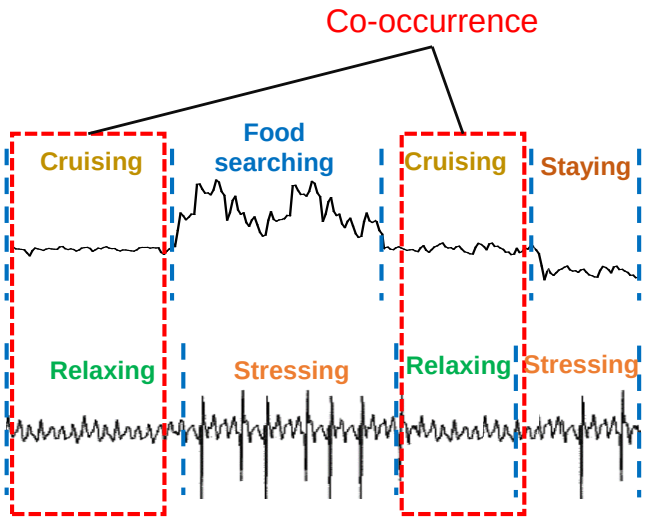


Figure 2.1: A hypothetical example of co-occurrence of behavioral modes. The cruising mode extracted from the time-series speed data and the relaxing mode extracted from the time-series heart rate data co-occur frequently.

are presented in both cruising and relaxing modes as shown in Figure 2.1. Time-series segmentation and clustering methods have been used to extract behavioral modes from animal behavioral data. In the example of Figure 2.1, after segmenting and clustering the time-series of the speed, it is assumed that the time-series are divided into three clusters: cruising, food searching and staying. Each cluster can be considered as a behavioral mode. On the other hand, there are two modes in the heart rate data: relaxing mode and stressing mode. Comparing these two time-series data, it is clear that when the animal is cruising, it is in the relaxing mode. This study attempts to find such co-occurrence behavioral modes from multi-modal sensor data.

Supervised and unsupervised methods have been used to detect behavioral modes from the time-series of behavioral data. Supervised methods, such as random forests, are trained on labeled data and predict a category label for each data point on a time slice [72, 83]. Unsupervised methods such as clustering methods and Hidden Markov Models (HMMs) have been actively studied due to the difficulty of collecting labeled data from wildlife [7, 86]. However, the use of unsupervised methods for multi-modal data is problematic. In unsupervised methods, data are grouped based on the distance

between data points, which makes it difficult to group data points correctly in multi-modal sensor data. Suppose a data point is composed of an acceleration value and an ambient temperature value. In this case, even if the animal performs the same activity, as reflected in the acceleration data, data points collected in high-temperature conditions can be grouped into different clusters than those collected in low-temperature conditions; this makes it difficult to interpret such meaningless clustering. Although Adam et al. [1] used hierarchical Hidden Markov Models (HHMMs) to estimate the latent state of each sensor modality, the latent state of the sensor was dominated by the latent state of the primary sensor, which was specified by the researcher. As a result, previous studies could only deal with multi-modal data with high correlation, e.g., multivariate data consisting of displacement and accelerometer data.

In addition to the aforementioned problem, in previous studies, the sensor modalities (or sensor data features such as speed and acceleration extracted from raw sensor data such as GPS trajectory) and clustering parameters (e.g., thresholds) used for analysis were selected subjectively by researchers based on their experience [21, 86], resulting in biased analysis.

In this study, we propose a method to discover frequent co-occurrence behavioral modes by automatically selecting the clustering parameters and sensor modalities that maximize the co-occurrence score (the score is calculated based on the time correlation between the two behavioral modes, which will be defined in detail later). In order to find the best combination of clustering parameters and sensor modalities, we iterate time-series clustering by varying these inputs, i.e., parameters and sensor modalities, and then output co-occurrence behavioral modes with high scores. Since each parameter can have multiple values and a number of features can be extracted from trajectories (e.g., speed, acceleration, and angular speed) and time-series sensor data (e.g., water depth), it increases the number of iterations of the time-series segmentation/clustering process. In this study, a frequent co-occurrence behavioral modes extraction method is proposed to compute the iterations of time-series segmentation and clustering efficiently.

The contributions of this study are as follows:

- A new task of discovering frequent co-occurrence behavioral modes from multi-modal animal locomotion data is defined.

- We propose a computationally efficient method for discovering frequent co-occurrence behavioral modes from animal locomotion data.
- The effectiveness of the proposed method is confirmed using actual data obtained from bats.

The structure of this chapter is as follows. Section 2.2 provides a review of some related works, including clustering and biological analysis methods. In Section 2.3, we describe detail of our approach. Section 2.4 shows experiments of the proposed method and results. The discussions with biologists are introduced in Section 2.5. Finally, in Section 2.6, we conclude this paper and discuss future work.

2.2 Preliminary

This section reviews related work on time-series segmentation and clustering and introduces a trajectory feature used in the study.

2.2.1 Time-series segmentation and clustering

Clustering is a data mining technique that divides data into several groups so that the similarity between data from the same group will be high, while the similarity between data from different groups will be small [38]. Sensory information observed by a sensor has been stored in the order of its timestamp, such as animals' behavior and environmental data (e.g., water depth), which are called time-series data [50]. By analyzing behavioral time-series, biologists can understand how an animal's behavior at one time step affects the behavior at the next time step. Specifically, time-series clustering has been widely used to understand animal behavioral modes [13, 20].

Time-series clustering methods are categorized into three types depending on the object being clustered, including whole time-series clustering, subsequence time-series clustering, and timepoint clustering [3]. Whole time-series clustering is the clustering of a set of time-series based on the similarity between these time-series. Subsequence time-series clustering (Figure2.2) indicates that it is the clustering of a set of subseries in a single time-series data; in other words, it clusters segments of a time-series data.

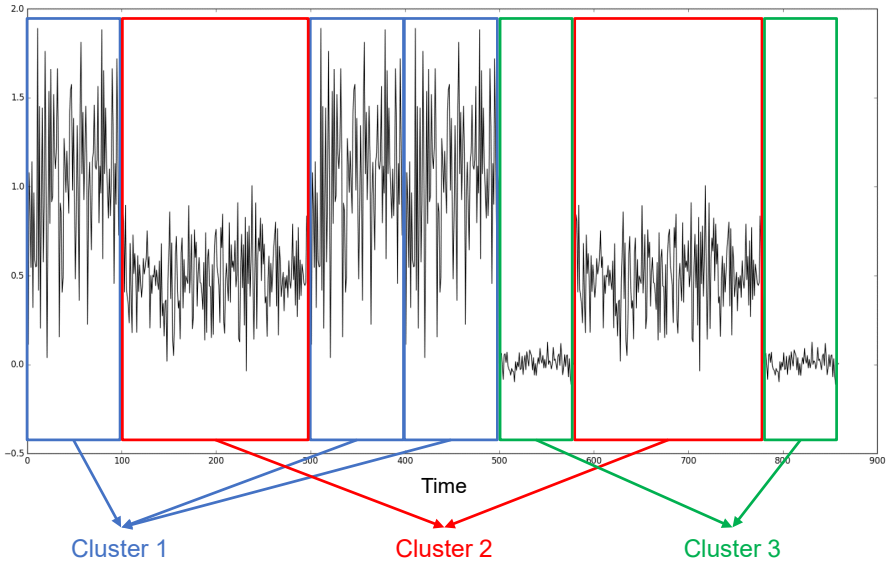


Figure 2.2: A sample of subsequence time-series clustering and there are 3 clusters.

Timepoint clustering is similar to the segmentation of a time-series. However, the difference is that it does not cluster all data points [30, 62, 97].

Considering that this study aims to find frequent co-occurrence behavioral modes from animal trajectory time-series, subsequence time-series clustering is described in detail next. Moreover, in this study, "time-series clustering" refers to subsequence time-series clustering. In subsequence time-series clustering, K-means [38] is commonly used.

Given a same dimensional dataset $X = \{X_1, X_2, , ...X_n\}$ with size of n, K-means clustering aims to partition X into k clusters $S = \{S_1, S_2, , ...S_k\}$ in order to minimize the sum of the intra-cluster distances. That is to say, the objective is to find

$$\arg\min_{S} \sum_{i=1}^{k} \sum_{x \in S_i} \parallel x - \mu_i \parallel^2$$

where μ_i is the mean in S_i [15].

Despite the high-speed advantage of K-means, time-series clustering is complex due to the enormous amount of data, which will lead to a sharp decrease in clustering speed [2, 49]. There are some studies that preprocess time-series data before performing time-

series clustering, e.g., performing time-series segmentation (merge similar adjacent data into a segment) to reduce the length of the data, significantly reducing the computation time.

Zhou et al. studied time-series clustering of the human motion time-series [116]. They first performed time-series segmentation using K-means before time-series clustering. If consecutive data belong to the same cluster, they are merged into one data. After the temporal reduction, they applied spectral clustering to the reduced data. They continued the study of human motion using kernel K-means instead of K-means because K-means is most beneficial only for spherical clustering [117].

Sequential models have also use for subsequence time-series clustering. A Bayesian nonparametric version of the hidden Markov model (HMM) called the hierarchical Dirichlet process HMM (HDP-HMM) was proposed in [41]. The authors segmented (decoded) time-series data using an HMM and estimated the number of states of the HMM using the Bayes estimation.

The goal of the above studies was to cluster time-series data only, and they focused on one-time clustering. In contrast, our goal is to mine valuable co-occurrence behavioral modes, which required repetitive clustering. To achieve this goal in a reasonable amount of time, we propose a method that reduced the total computational cost when repeatedly clustering.

2.2.2 First passage time

First passage time (FPT) shows the time an object takes to pass for the first time through a circle of fixed radius r centered at a point on the trajectory [40], and is used in this study as a locomotion feature. FPT can be used to measure the effort of animals to search for prey along a trajectory, with a longer FPT likely indicating that there is a large amount of food in an area; in comparison, a shorter FPT indicates that the animal is moving [27].

Fauchald et al. applied FPT to the trips of Antarctic Petrel (*Thalassoica antarctica*) [27], in order to analyze the changes in the behavioral modes of the seabird. For each trip, they calculated the variance of FPT by varying different radius (from 0 to 400 km). They selected the radius with the largest FPT variance among all trips and studied the

spatial relationship of search effort among trips within this area. In [68], the authors analyzed 26 seals from the Baltic Sea during the autumn in 2011–2013. The GPS location was recorded two or three times per hour with two kinds of conditions, 'at-sea' and 'haul-out'. They applied the FPT to each point on the trajectory, varying the circle's radius from 1.5 to 80 km (in 0.5 km increments). They also chose the radius that maximized the variance of the FPT and analyzed the seals' foraging habitat.

2.3 Proposed method

2.3.1 Problem definition

As we mentioned before, the features (or sensor modalities) and parameters used for time-series segmentation and clustering were based on the experience of biologists. Therefore, the extracted behavioral modes might be biased. Moreover, this experience does not apply to all species because we cannot infer the behavioral modes of non-studied species. In our approach, we used all parameters and features for the segmentation and clustering of time-series data. Since obtaining behavioral modes required expensive computational time, our study aimed to design a computationally efficient algorithm to obtain behavioral modes from sensor modalities. First, we achieved fast time-series segmentation and clustering. Second, we found frequent co-occurrence behavioral modes between movement and environmental (or biological) data.

Let L and E be a location information dataset and an environmental sensor dataset, respectively. More specifically, $L = \{\langle l_1, t_1\rangle, ..., \langle l_{|L|}, t_{|L|}\rangle\}$, where l_i is two-dimensional (or three-dimensional) location information and t_i is the time when l_i is observed. Also, $E = \{\langle e_1, t_1\rangle, ..., \langle e_{|E|}, t_{|E|}\rangle\}$, where e_i is d-dimensional sensor data and d is one or more. For example, when we observe atmospheric pressure and temperature, $d = 2$. Our inputs were obtained from L and E. Given L, we can extract multiple kinds of one-dimensional feature time-series, L_1, L_2, ..., L_n. For example, L_1 is a time-series of speed. Similarity, given E, E_1, E_2, ..., E_m are obtained, and for example, E_1 is a time-series of derivative of atmospheric pressure. Detailed feature information is described in Section 2.4.

Note that co-occurrence behavioral modes were found as a result of specific time-

series segmentation/clustering. In the following, we define several terms related to clustering.

Segment. Given a time-series X and a parameter (set) α, a segment s, which is computed based on α, is a subsequence of X. If $s = \{\langle x_i, t_i\rangle, \langle x_{i+1}, t_{i+1}\rangle, ..., \langle x_j, t_j\rangle\}$, the time length of s, denoted by $s.t$, is $[t_i, t_j]$.

Cluster. Given a time-series X and a parameter set θ consisting of α and β, a cluster, which is computed based on β, is a set of segments that follow Definition **Segment**. One cluster can be considered as one behavioral mode.

2.3.2 Overview

Given a set of feature time-series, trajectory features $(L_1, ..., L_n)$, and environmental (or biological) features $(E_1, ..., E_m)$ and the range of clustering parameters. We needed to perform clustering for each time-series using all parameters and calculate the co-occurrence scores of all cluster pairs obtained from L_i and E_j. Note that naively enumerating all cluster pairs is infeasible if the number and the length of time-series are large. Therefore, we propose an efficient method which overcomes this challenge.

An overview of our approach is shown in Figure 2.3. For input data, we assume time-series locomotion features extracted from trajectories (e.g., speed, acceleration time-series), for more detailed information on input data, please refer to Subsection 2.4.2. For each feature time-series (extracted from trajectory, environmental or biological data), we first perform time-series segmentation by using each segmentation parameter value. After that, we iterate the clustering analysis for each segmentation result by using each clustering parameter value to obtain different behavioral modes. Finally, we calculate the co-occurrence score between two behavioral modes (one obtained from trajectory features and the other from environmental features) and identify the highest one.

To effectively segment the time-series, we apply Symbolic Aggregate approXimation (SAX) [51], which is a symbolization method. In addition, as a clustering tool, we employed spectral clustering [65]. Spectral clustering first construct a similarity graph; in our case, each segment correspond to a node of the graph and calculate its feature vector. Then, the nodes are clustered according to the feature vectors using some clustering

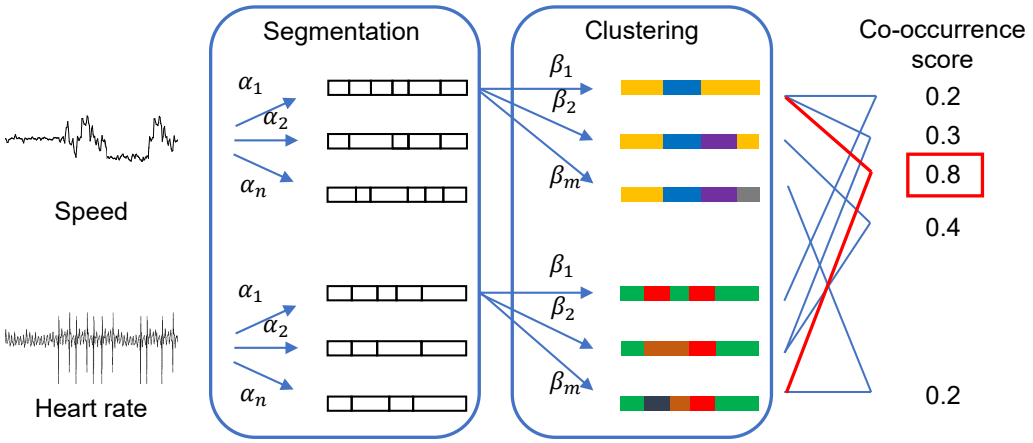


Figure 2.3: Overview of proposed method.

Algorithm 1: `Proposed method`

Input: $\mathcal{X}$: a set of time-series, α_{max}: maximum #symbols, α_{min}: minimum #symbols, β_{max}: maximum cluster number, β_{min}: minimum cluster number

```
/* Clustering time-series */
for ∀X_i ∈ 𝒳 do
    μ, σ² ← COMPUTE-MEAN-VARIANCE(X_i)        ▷ μ is mean and σ² is variance
    for α = α_max to α_min do
        SAX(X_i, μ, σ², α)
        MERGE-SYMBOLS(·)
        SIMILARITY-GRAPH-CONSTRUCTION()
        LAPLACIAN-EIGENMAPS()
        for β = β_min to β_max do
            X_{i,α-β} ← k-MEANS++
            R ← R ∪ {X_{i,α-β}}                ▷ store the clustering result
```

method (we use K-means++ [5]).

The detailed segmentation and clustering for one feature time-series are described in Algorithm 1. We were given a feature time-series $\mathcal{X}$, a range of SAX parameter $[\alpha_{min}, \alpha_{max}]$, and a range of cluster number $[\beta_{min}, \beta_{max}]$. For each time-series X_i, we first computed its mean μ and variance σ^2 to enable SAX-based segmentation. Next, for

each parameter $\alpha \in [\alpha_{min}, \alpha_{max}]$, we executed time-series segmentation with SAX and then performed spectral clustering for each $\beta \in [\beta_{min}, \beta_{max}]$, i.e., a segmentation result using α could be reused when β was varied in our algorithm.

This framework was effective because we could reuse previously computed results. Specifically, suppose we executed SAX with a parameter $\alpha = c \cdot \alpha_i$ (c is a positive constant). In that case, we could obtain the result of SAX with α_i from the previously obtained results with α. In addition, we reduced the graph size based on the symbolizing result to accelerate spectral clustering. These facts provided the efficiency of our method.

2.3.3 Segmentation

The SAX algorithm takes an input time-series of length n and converts it to a string of length w [51]. In our case, let $n = w$ since we did not want to lose useful information. The size of the alphabet was an integer α, where $\alpha > 2$ (e.g., for an alphabet = {`a, b, c`}, $\alpha = 3$). Assume that the normalized time-series follows a Gaussian distribution, breakpoints can be identified to produce regions with equal size under the Gaussian curve for α [48].

Breakpoints. The breakpoints are a list of numbers, $B = \{b_1, b_2, ..., b_{\alpha-1}\}$ ($b_i < b_{i+1}$). These numbers divide the area under the Gaussian curve by α equal parts. Thus, the area under the Gaussian curve from b_i to b_{i+1} is $1/\alpha$. Table 2.1 gives the breakpoints for value α from 2 to 10.

Given a time-series, we calculated its mean μ and variance σ^2 and then computed breakpoints by using the mean and variance. For example, Table 2.1 shows the breakpoints under the normal distribution, and we transformed the breakpoints in the table with mean and variance to get the breakpoints of the input data. These mean and variance were used for all parameters α ($\alpha \in [\alpha_{min}, \alpha_{max}]$). Once the breakpoints were obtained, we could discretize the time-series. All points in the time-series with values less than the minimum breakpoint were mapped to `a`. All points with values greater than the minimum breakpoint and less than the second smallest breakpoint were mapped to `b`, and so on. The symbols of the neighbor space were called neighbor symbols. The symbolic version of the time-series in Figure 2.4 is `ccccd...bbbbc`. The neighbor

Table 2.1: Breakpoints under the standard normal distribution (α from 2 to 10).

		α								
		2	3	4	5	6	7	8	9	10
$Breakpoints$	b_1	0	-0.43	-0.67	-0.84	-0.97	-1.07	-1.15	-1.22	-1.28
	b_2		0.43	0	-0.25	-0.43	-0.57	-0.67	-0.76	-0.84
	b_3			0.67	0.25	0	-018	-0.32	-0.43	-0.52
	b_4				0.84	0.43	0.18	0	-0.14	-0.25
	b_5					0.97	0.57	0.32	0.14	0
	b_6						1.07	0.67	0.43	0.25
	b_7							1.15	0.76	0.52
	b_8								1.22	0.84
	b_9									1.28

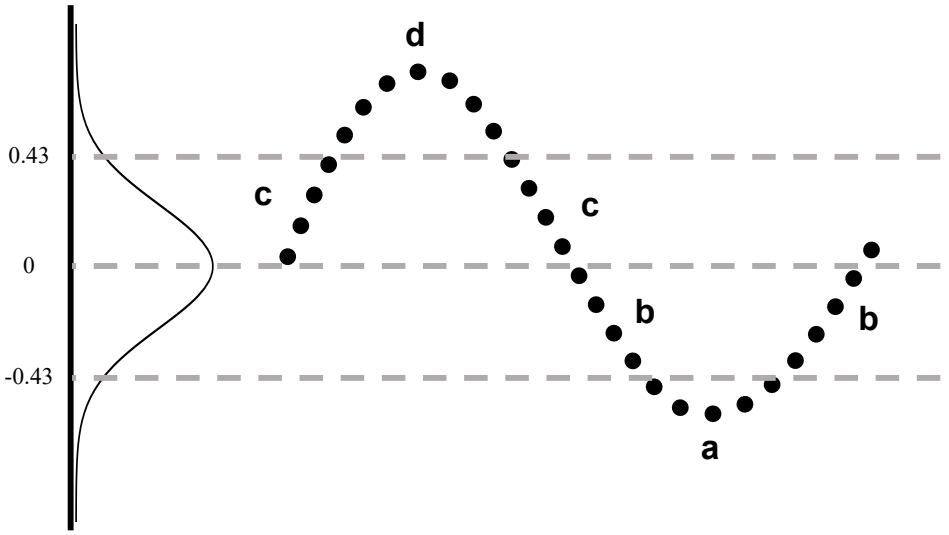
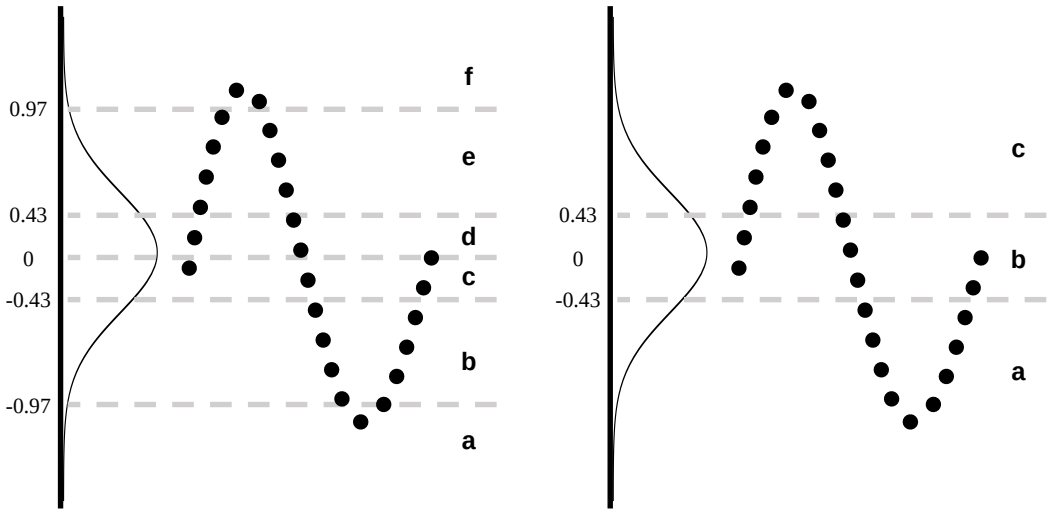


Figure 2.4: An example of SAX. The result after applied SAX ($\alpha = 3$) is `ccccd...bbbbc`.

symbols of `c` were `b` and `d`.

Note that the segmentation was executed in the descending order of α to reuse the previously obtained results (Algorithm 1 line 4). Considering the case of $\alpha = 6$ and



(a) An example that a time-series is symbolized by SAX ($\alpha = 6$)

(b) An example that a time-series is symbolized by SAX ($\alpha = 3$)

Figure 2.5: We can reuse the SAX result when the parameter is 2α to obtain the result when the parameter is α.

$\alpha = 3$, we could find that the first and second breakpoints when $\alpha = 3$ were equal to the second and fourth breakpoints when $\alpha = 6$ (Table 2.1). In other words, if x was converted to `a` or `b` when $\alpha = 6$ (Figure 2.5a), x was absolutely converted to `a` when $\alpha = 3$, just converting `a` and `b` to `a`, `c` and `d` to `b`, `e` and `f` to `c` in the results of $\alpha = 6$, we could obtain the results of $\alpha = 3$ (Figure 2.5b).

Next, let $X_i(\alpha, \mathtt{z})$ be the set of $x \in X_i$ where x was converted to `z` when the parameter of SAX was α. We computed the average value of $X_i(\alpha, \cdot)$, for each symbol:

$$avgX_i(\alpha, \cdot) = \frac{\sum x}{|X_i(\alpha, \cdot)|}$$

This is because this was one of the inputs of spectral clustering. As well as the above symbolizing, this averaging could utilize the previous results to save computation cost. In the example of Figure 2.5, we computed avg $X_i(3, \mathtt{a})$ when $\alpha = 3$ based on avg $X_i(6, \mathtt{a})$, avg $X_i(6, \mathtt{b})$, $|X_i(\mathtt{a})|$ and $|X_i(\mathtt{b})|$ computed when $\alpha = 6$ by the formula:

$$|X_i(3,\mathtt{a})| = \frac{|X_i(6,\mathtt{a})|avgX_i(6,\mathtt{a}) + |X_i(6,\mathtt{b})|avgX_i(6,\mathtt{b})}{|X_i(6,\mathtt{a})| + |X_i(6,\mathtt{b})|}$$

Then, we segmented X_i (Algorithm 1 line 6). Each repeating symbol was coded once together, for example, the segments of the time-series in Figure 2.5b was b, c, b, a, and b.

2.3.4 Clustering

After segmenting the time-series X_i, we performed spectral clustering [65] to cluster these segments. The main idea of spectral clustering is to consider all the segments as nodes in a graph and to achieve clustering by cutting the graph. Each edge between two nodes has a weight, which indicates the similarity between the two nodes. The edge weight between two nodes with low similarity has a small value, while the edge weight between two nodes with high similarity has a large value. The graph partitioning is achieved by minimizing the sum of edge weights between subgraphs and maximizing the sum of edge weights within subgraphs.

Based on the segments obtained from time-series segmentation, we first constructed a similarity graph; the definition is as follows.

Similarity graph. Given a set of segments of X_i ($\{s_1, s_2, ...s_n\}$), a similarity graph $G = (V, E)$ constructed by the segment set is a weighted graph which has a node set V and an edge set E. Nodes correspond to the segments, and an edge is created between two nodes with the same symbol or neighbor symbols. Assume that two nodes s_i and s_j has an edge and their symbols are respectively z and z′. The weight of the edge $w_{i,j}$, which corresponds to the similarity between nodes, is defined below.

$$w_{i,j} = \frac{1}{|\text{avg } X_i(\alpha, \mathrm{z}) - \text{avg } X_i(\alpha, \mathrm{z}')|}$$

One might think that edges should be created between all nodes. In fact, if we did this, we got a strange cluster: some symbols are not adjacent to each other with other

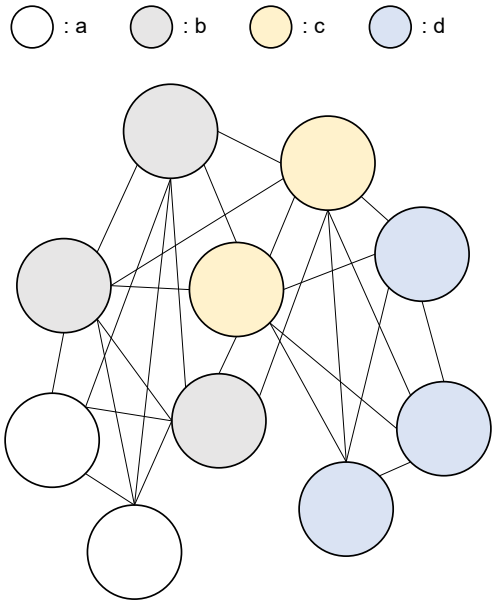


Figure 2.6: Construct a graph based on the result of time-series segmentation ($\alpha = 4$)

symbols. To avoid this, we only considered symbols that are identical and adjacent (Figure 2.6).

After that, we calculated the weighted adjacency matrix W and degree matrix D from the similarity graph.

Weighted adjacency matrix. A weighted adjacency matrix is a matrix used to represent the adjacency relationships between vertices in a graph.

$$W = \begin{pmatrix} w_{11} & \cdots & w_{1n} \\ \vdots & & \vdots \\ w_{n1} & \cdots & w_{nn} \end{pmatrix}$$

Degree matrix. The degree matrix is a diagonal matrix, and the elements on the diagonal are the degrees of the individual vertices. The degree of a vertex indicates the number of edges associated with that vertex.

$$D = \begin{pmatrix} d_1 & 0 & \cdots & 0 \\ 0 & d_2 & \cdots & 0 \\ \vdots & \vdots & & \vdots \\ 0 & 0 & \cdots & d_n \end{pmatrix}$$

where

$$d_i = \sum_{j=1}^{n} w_{ij}$$

In addition, given a subset of vertices $A \subset V$, its complement is defined as $\overline{A}$. For two subset A, B ($A \cap B = \varnothing$), the similarity between A and B is defined as follow.

$$W(A, B) = \sum_{i \in A, j \in B} w_{ij}$$

The main tool for spectral clustering is graph Laplacian matrix L, it is defined as

$$L = D - W$$

and has the following properties:

The Laplacian matrix L is positive semi-definite and has n non-negative eigenvalues, the smallest eigenvalue is 0, $0 = \lambda_1 \leq \lambda_2 \leq \cdots \leq \lambda_n$.

Once the graph Laplacian matrix L was obtained, we computed its eigenvalues and eigenvectors. We then divided the graph G into k subgraphs $\{A_1, A_2, \cdots, A_k\}$, where $A_i \cap A_j = \varnothing$ $(i, j = 1, 2, \cdots, k)$ and $A_1 \cup A_2 \cup \cdots \cup A_k = V$. We applied RatioCut [32] to cut the graph:

$$RatioCut(A_1, A_2, \cdots, A_k) = \sum_{i=1}^{k} \frac{cut(A_i, \overline{A}_i)}{|A_i|}$$

where

$$\begin{aligned} cut(A_i, \overline{A}_i) &= \frac{1}{2} W(A_i, \overline{A}_i) \\ &= \frac{1}{2} \sum_{i \in A_i, j \in \overline{A}_i} w_{ij} \end{aligned}$$

and $|A_i|$ shows the number of vertices in a subset A. Therefore, we could get graph partitions by minimizing RatioCut. In some studies [56, 102], it has been proved that minimize RatioCut can be transformed to construct a matrix $H \in \mathbb{R}^{n \times k}$ which the first k eigenvectors (based on the eigenvalues) and performed K-means on the rows of H. However, it can be intuitively observed that the above operations incur a high computational cost and memory usage (for calculating eigenvalues and eigenvectors of L) if the graph size is large. Therefore, we reduced the computational cost by graph size reduction. In fact, we merged nodes with the same symbol into a single node. This merged similarity graph is defined below.

Merged similarity graph. A merged similarity graph of G, $\hat{G}$, consists of nodes with different symbols and edges, which are created between nodes with neighbor symbols. Assume two nodes $\hat{s}_i$ and $\hat{s}_j$ in $\hat{G}$ have an edge and their symbols are respectively $\mathtt{z}$ and $\mathtt{z'}$. Let $V(\mathtt{z})$ be the set of nodes which have symbol $\mathtt{z}$, of V (a node set of G). The weight of the edge $\hat{w}_{i,j}$ is

$$\hat{w}_{i,j} = \sum_{i \in V(\mathtt{z}), j \in V(\mathtt{z'})} w_{ij}$$

From the above definition, we could find that the number of vertices and edges in $\hat{G}$ are α and $O(\alpha)$, respectively. Note that $\alpha \ll \|V\|$ and α was a small integer in practice, which suggests an efficiency of the graph size reduction. Furthermore, we showed that this graph size reduction does not lose the correctness:

Theorem 1 (Correctness). Merged similarity graph $\hat{G}$ provides the same partition result with the origin similarity graph G.

Proof. First, we would like to prove that the vertices with the same symbol must be divided into the same subgraph. From the definition of the similarity between nodes, we can find that the weight of edges (similarity) between vertices with the same symbol is ∞. If we cut the vertices (e.g., v_i, v_j) with the same symbol into different subgraphs (e.g., A_i, A_j), the $cut(A_i, A_j)$ becomes ∞. As a result, the RatioCut also changes into ∞, and we cannot minimize it. This is a violation of the idea of a graph partition. Therefore, the vertices with the same symbol are never partitioned into different subgraphs; in other words, vertices with the same symbol must be divided into the same subgraph.

Second, we had to verify that the two graphs $\hat{G}$ and G have the same graph partitioning result. From the above proof and equations, we can see that.

$$\begin{aligned} cut(V(\mathtt{z}), V(\mathtt{z'})) &= \hat{w}_{i,j} \\ &= cut(\{\hat{s}_i\}, \{\hat{s}_j\}) \end{aligned}$$

This indicates that the cutting results of $\hat{G}$ and G were the same. Therefore, Theorem 1 has been proved.

After we obtained the graph $\hat{G}$ and computed its eigenvalues and eigenvectors, we chose the second and third eigenvectors (because the first eigenvector is $\mathbb{1}$) and applied K-means++ [5] to cluster them instead of K-means (Algorithm 1 line 8–11) since the K-means algorithm starts by randomly selecting k points in the dataset as cluster centers. In contrast, when setting cluster centers, K-means++ lets the k initial cluster centers be as far apart from each other as possible, resulting in better separation of data points. Owing to Theorem 1, we used $\hat{G}$ instead of G, and thereby we could efficiently execute spectral clustering. Finally, we introduced the time complexity of our clustering.

Theorem 2 (Time complexity). Given a time-series X_i, our clustering needs

$$O(\sum_{\alpha}(|X_i| + \alpha^3 + \sum_{\beta}\alpha\beta))$$

time.

Proof. SAX and MERGE-SYMBOLS$(\cdot)$ need $O(|X_i|)$ time. Similarity graph construction incurs $O(\alpha^2)$ time, while computing eigenvectors need $O(\alpha^3)$ time [54]. For a

fixed iteration number, K-means++ need $O(\alpha\beta)$ time [12]. Recall that K-means++ is executed $(\beta_{max} - \beta_{min} + 1)$ time, so for a given α, we need $O(|X_i| + \alpha^3 + \sum_\beta \alpha\beta)$ time. Therefore, in total, the time complexity of our clustering is $O(\sum_\alpha(|X_i| + \alpha^3 + \sum_\beta \alpha\beta))$, which completes the proof.

Because α and β were practically small integers, our method could obtain all cluster pairs quickly.

2.3.5 Score

Given a trajectory feature time-series L_i and an environmental time-series E_j, after applied our method to these two time-series, we can get $L_i = \{L_i^1, L_i^2, \cdots, L_i^p\}$ and $E_j = \{E_j^1, E_j^2, \cdots, E_j^q\}$, where L_i^p (E_j^q) is p-th (q-th) cluster (mode) in L_i (E_j). Then we define the score of pair of modes (L_i^p, E_j^q):

Score(L_i^p, E_j^q). Given $L_i^p = \{s_1^p, s_2^p, \cdots\}$ and $E_j^q = \{s_1^q, s_2^q, \cdots\}$,

$$Score(L_i^p, E_j^q) = Corr(L_i^p, E_j^q) - Freq(L_i^p, E_j^q)$$

where

$$Corr(L_i^p, E_j^q) = \frac{\sum_{n,m} |s_n^p.t \cap s_m^q.t|}{\sum_m |s_m^q.t|}$$

and

$$Freq(L_i^m, E_j^n) = \frac{C \cdot \max(\sum_n |s_n^p.t|, \sum_m |s_m^q.t|)}{|L_i|}$$

Note that $Corr(L_i^p, E_j^q)$ measures the time correlation between L_i^p and E_j^q (between two behavioral modes extracted from trajectory feature L_i and environmental feature E_j, respectively). In addition, $Freq(L_i^m, E_j^n)$ works as a penalty if the relation between L_i^p and E_j^q was a simply a steady activity (e.g., when the animal is resting, it is in the relaxing mode).

2.4 Experiment

In this section, we presented experiments based on our proposed approach. We described in detail the subjects of our study, as well as the dataset used in the experiments and the corresponding processing.

2.4.1 Dataset

We applied the proposed method to a synthetic dataset as well as to a real dataset.

Synthetic dataset

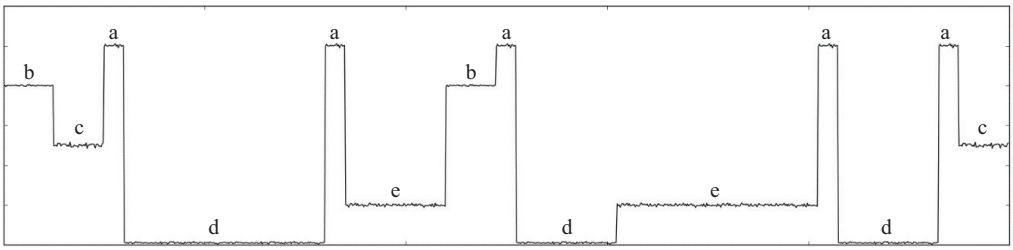
To validate the quality/correctness of the co-occurrence score calculation method proposed in Section 2.3.5, we used synthetic data to test whether we could find the frequent co-occurrence of two clusters. We generated multiple time-series data obeying Gaussian distribution with a different mean (μ) and variance (σ^2).

- **Synthetic sequence** a: $\mu = 100$, $\sigma^2 = 0.4$.
- **Synthetic sequence** b: $\mu = 80$, $\sigma^2 = 0.2$
- **Synthetic sequence** c: $\mu = 50$, $\sigma^2 = 0.6$
- **Synthetic sequence** d: $\mu = 1$, $\sigma^2 = 0.3$
- **Synthetic sequence** e: $\mu = 20$, $\sigma^2 = 0.5$

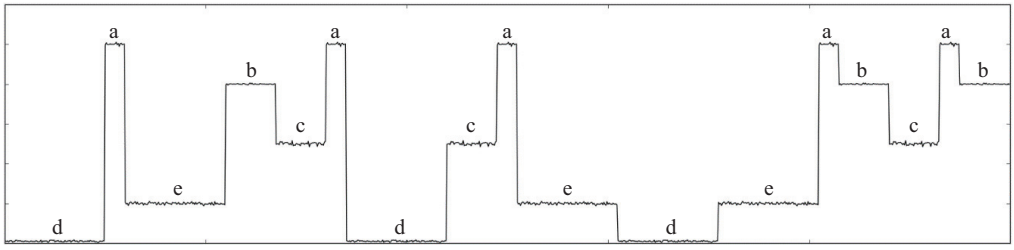
We used these five synthetic sequences to splice into two synthetic time-series with a length of 100,000. We set sequence a as the frequent sequence that appears and ends simultaneously in the two synthetic time-series (Figure 2.7). The total length of sequence a was 10,000.

Real dataset

We further compared our method using a dataset collected from Japanese Large-footed Bat (*Myotis macrodactylus*), a species of vesper bats. The bats can emit ultrasonic



(a) First synthetic time-series



(b) Second synthetic time-series

Figure 2.7: Synthetic time-series for testing. The co-occurrence clusters are synthetic sequence a in each time-series.

waves from 40Hz to 70Hz. We obtained three-dimensional trajectory time-series data of Japanese Large-footed Bats during foraging flight using a 16ch microphone array at Tomakomai Experimental Forest of Hokkaido University (The experiment was conducted by Faculty of Life and Medical Sciences, Doshisha University [29].) The bats feeding pond was surrounded by four units of Y-shaped four-microphone array, and 3D trajectories and the intervals of ultrasound emissions of bats were observed. The 3D coordinates were measured using trilateration when the bats emitted ultrasound. We employed linear interpolation to generate trajectories with a uniform sampling interval (1,000 Hz). In addition, since bats emitted ultrasonic waves at a high frequency of about 150 Hz when attacking insects, we could know the time and location of bat attacks. For details of data collection, please refer to [29]. The number of trajectories was 6, the average duration of the trajectories was 68.0 seconds, and the average number of data points in a trajectory was 67,208. We used a video recorder to record the bats' behaviors and found the time of bat predation by analyzing the video. In summary, we obtained

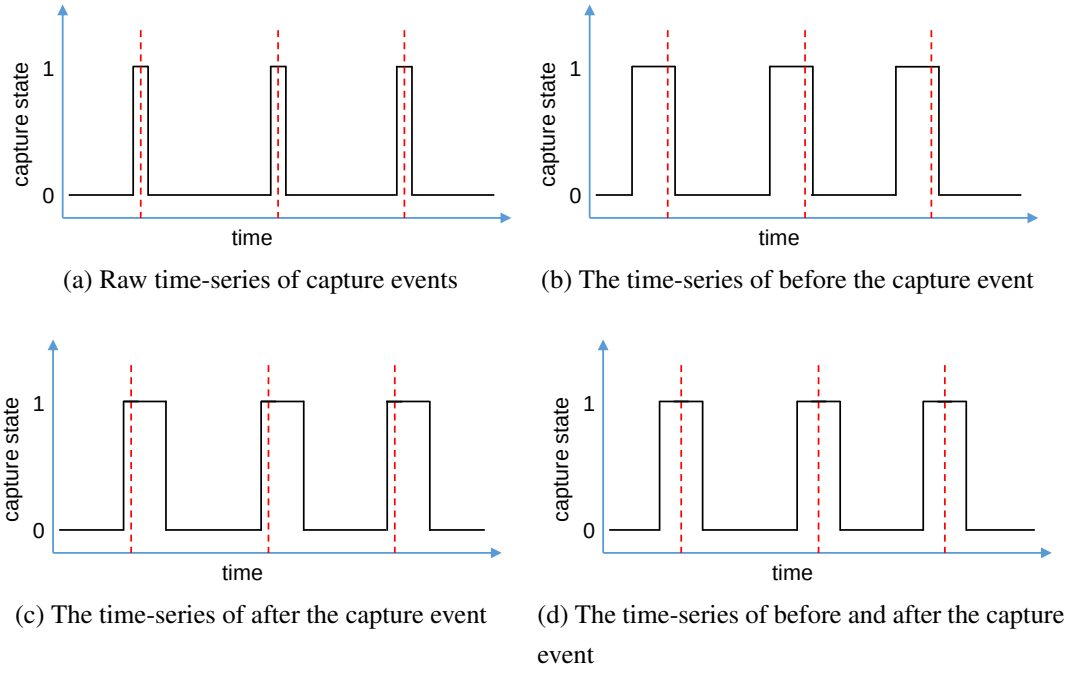
two kinds of data from the bat: 3D trajectory and predation information.

2.4.2 Feature extraction

We extracted speed (speed in 3D space, speed in horizontal plane and vertical speed) (m/s), absolute acceleration (absolute acceleration in 3D space, absolute acceleration in horizontal plane, and absolute vertical acceleration) (m/s^2), angular speed in the horizontal plane (rad/s), moving average and variance of speed, moving average and variance of absolute acceleration and moving average and variance of angular speed from 3D trajectories. We computed the moving average and variance using each window size of 0.1s to 0.5s with an interval of 0.1s, and the FPT varied radius of 1m to 5m with an interval of 1m. That is, 82 feature time-series were extracted from each 3D trajectory data.

We also computed a time-series representation of when a bat caught insects, the value equals to 1 at the moment of capturing a prey. Otherwise, it is 0 (Figure 2.8a). The broken red lines in Figure 2.8a indicate the time bat captured an insect. In addition, we computed three different extensions of the time-series: (1) w_s sec preceding the capture event, (2) w_s sec following the capture event, and (3) $w_s/2$ sec preceding and following the capture event. A capturing event occurs at time t, for example, the values between $t - w_s$ and t becomes 1 in the first case (Figure 2.8b).

By analyzing the time-series of preceding the capture events, we could understand the state of the bat before capturing the prey. The time-series following the capture events showed the state of the bat after capturing the insect, while the time-series preceding and following capture events exhibited the state of the bat when capturing the insect. Since we did not know the appropriate w_s for analyzing, we changed the value of w_s from 0.1 sec to 1 sec with an interval of 0.1 sec. That is, 30 extended capture state time-series were extracted. Since there were only two values (clusters) in the time-series, we did not apply the proposed method on the time-series of capture states, and we just used the clusters (capture state is 1) to calculate the co-occurrence score with the behavioral modes obtained from the movement features.



(a) Raw time-series of capture events

(b) The time-series of before the capture event

(c) The time-series of after the capture event

(d) The time-series of before and after the capture event

Figure 2.8: Capture event time-series and its extensions, broken red lines measure the time when a bat capture an insect.

2.4.3 Comparison method and environment

We designed the following comparison methods to test the computation time and memory usage.

- **Proposed**. The proposed method in this paper.
- **w/o symbol**. The method without reusing previous SAX results.
- **w/o reduce**. The method without using a merged similarity graph.
- **Naive**. A method simply repeats each iteration without our proposed techniques.

All the above method provided the same output. We omitted computing cluster pairs that do not satisfy $Corr(L_i^p, E_j^q) > \gamma$ in order to filter out co-occurrence behavioral modes with low correlation before calculating the scores. In our experiments, we set

Table 2.2: Results of synthetic data. Running time [sec], and average precision and recall.

	Running time	Avg. precision	Avg. recall
Proposed	1.1	1.00	1.00
HDP-HMM	19.0	1.00	0.98
w/o reduce	19.0×10^4	1.00	1.00

$\gamma = 0.4$. For the parameters setting, we set α from 4 to 20 and β from 3 to 7. All methods were implemented in C++, Ubuntu, and all experiments were performed on a computer with a 3.4GHz Intel Core i7 processor and 16GB RAM.

2.4.4 Result

Result of synthetic dataset

We compared the proposed method to HDP-HMM [41], which is a time-series segmentation/clustering method based on the Bayes estimation, and w/o reduce. The result of running time, average precision, and average recall are shown in Table 2.2.

Result of Bat

The result of computation time and memory usage are shown in the Tables 2.3 and 2.4. The numerical values recorded in Table 2.4 are the peak of memory usage.

Since the number of output was enormous, biologists investigated top-3 co-occurrence behavioral modes.

Co-occurrence of behavioral modes with the best score: "A behavioral mode of low speed (lower than approximately 3.0 (m/s))" extracted from moving average of speed (window size: 0.2s) and "a behavioral mode of 0.2s following capture events" were highly correlated. The $Corr$ and $Freq$ were 0.401 and 57363/403249, respectively.

Table 2.3: Efficiency evaluation of bats: Running time [sec]

	Segmentation	Clustering	Total
Proposed	6.12	6.44	12.56
w/o symbol	8.93	6.47	15.40
w/o reduce	6.20	1.00×10^4	1.00×10^4
Naive	13.08	2.62×10^4	2.62×10^4

Table 2.4: Efficiency evaluation of bats: Memory usage [MB]

	Peak of memory
Proposed	11.02
w/o symbol	11.15
w/o reduce	750.18

Figure 2.9 shows entire 3D trajectories and feature time-series, identified behavioral modes are highlighted in red.

Co-occurrence of behavioral modes with the 2nd best score: "A behavioral mode of low speed (lower than approximately 4.0 (m/s))" extracted from "moving average of speed (window size: 0.5s)" and "a behavioral mode of 0.4s following capture events" had the second-highest co-occurrence score. The $Corr$ and $Freq$ were 0.456 and 78812/403249, respectively. We could find that these features are similar to features with the highest score; the difference was that the time after capturing extends from 0.2 seconds to 0.4 seconds. We did not draw the 3D trajectories and feature time-series since it is similar to Figure 2.9.

Co-occurrence of behavioral modes with the 3rd best score: "A behavioral mode of low moving variance of acceleration (lower than approximately 60 $(\mathrm{m/s^2})^2$)" extracted from moving variance of acceleration (window size is 0.3s) and "a behavioral mode of

0.1s following capture events" had the third-highest occurrence score. The $Corr$ and $Freq$ were 0.450 and 70284/403249, respectively. Figure 2.10 shows 3D trajectories and feature time-series, extracted modes are highlighted in red.

2.5 Discussion

2.5.1 Efficiency of the proposed method

The proposed method could successfully detect the co-occurrence modes generated by the target distribution (Table 2.2). Since the proposed method reduced the number of data points (graph nodes), the running time of the proposed method was significantly shorter than that of HDP-HMM. The accuracy for HDP-HMM was not perfect because the method failed to detect few segments from the target distribution. We could also confirm that Proposed outputs the same results as w/o reduce, which did not perform graph size reduction. As for w/o reduce, it takes a long time to compute eigenvectors from large graphs.

By comparing the Proposed with the w/o symbol, we saw that utilizing the previous SAX results can reduce computation time (Table 2.3). Recall that $\alpha_{max} = 20$, so Proposed utilized the previous SAX results when $\alpha \leq 10$ (As α_{max} increases, we obtain benefits of reusing the previous results). In addition, by comparing Proposed with w/o reduce, our graph size reduction efficiency could be confirmed. The graph size reduction provides a significant impact on computational cost.

Actually, w/o reduce did not function and incurred run out of memory because the similarity graph size was too large, and this caused the matrix to be too large, which will require large space to compute eigenvectors and eigenvalues. The running time of w/o reduce and Naive showed the estimated lower bound of running time, which was obtained by the running time in the setting where α and β were minimum. The proposed method was faster than w/o reduce by a factor of at least four orders of magnitude (Table 2.3).

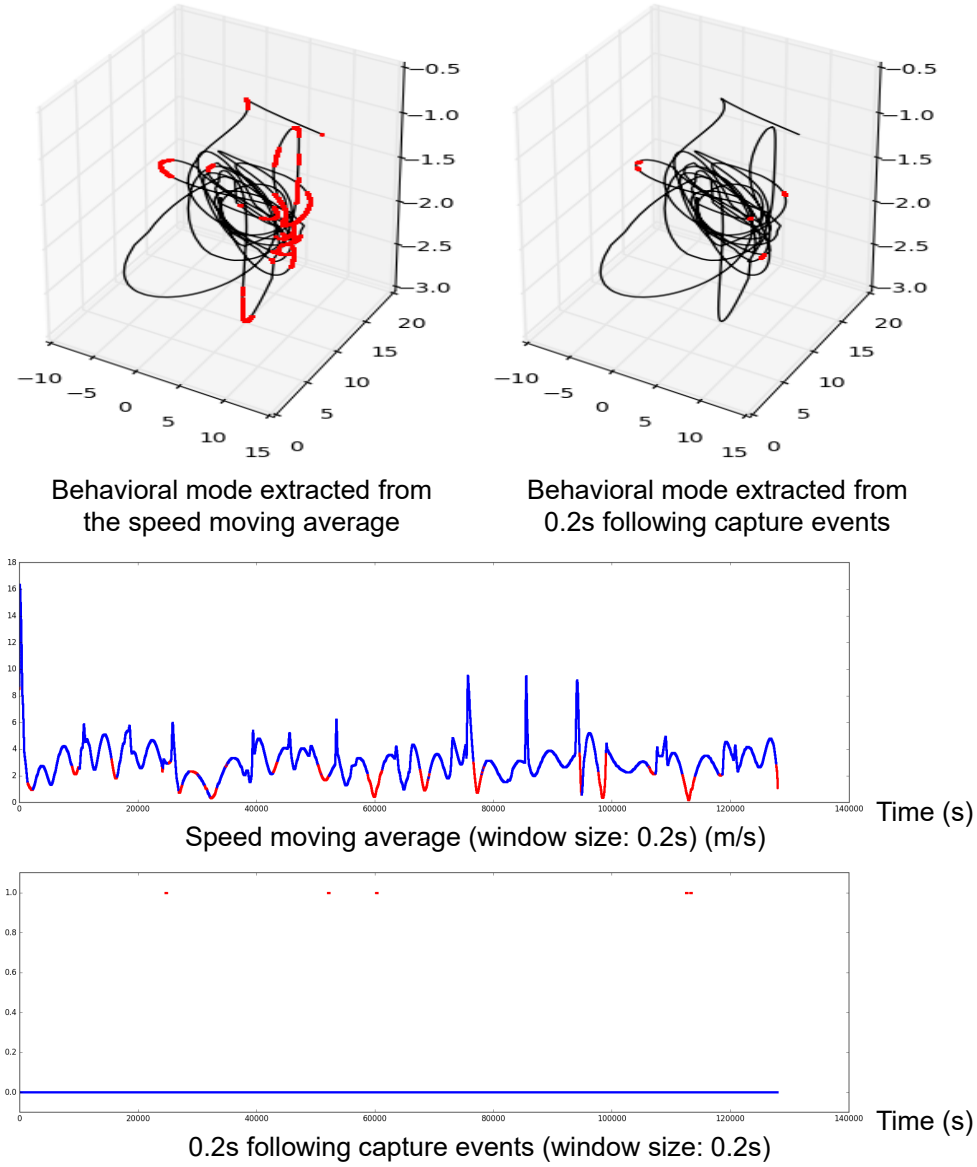


Figure 2.9: Example result of bats with the highest co-occurrence score. The correlated behavioral modes are the behavioral mode of low speed and the behavioral mode of 0.2s following capture events. The upper maps show bat trajectories. The black lines show the trajectory, and the red segments represent identified behavioral modes. The lower graphs show the time-series of features, and the red segments show the identified behavioral mode.

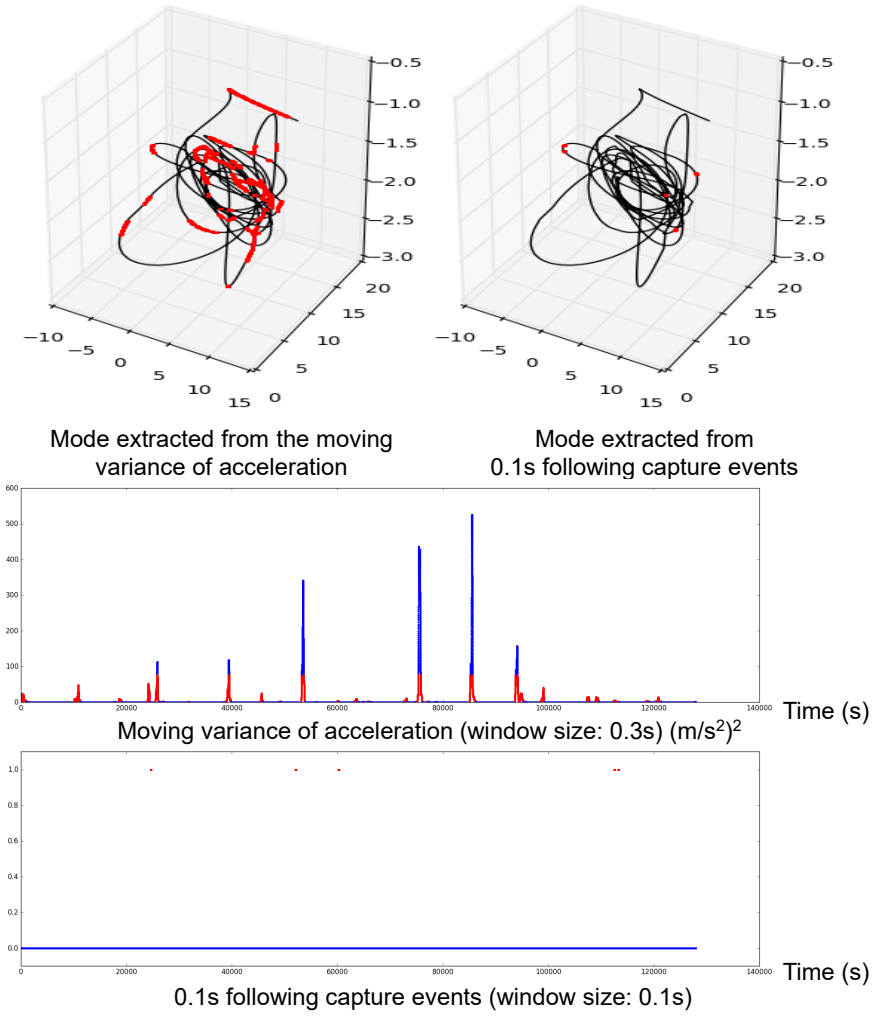


Figure 2.10: Example result of bats with the third-highest score. The correlated behavioral modes are the behavioral mode of low moving acceleration and the behavioral mode of 0.1s following capture events. The upper maps show bat trajectories. The black lines show the trajectory, and the red segments represent identified behavioral modes. The lower graphs show time-series of features, and the red segments show the identified behavioral mode

Compared with two methods, Proposed and w/o symbol, it shows that reusing the previous SAX result can save some memory because the parameter α is so small that the promotion is not very obvious (Table 2.4).

On the other hand, when we applied w/o reduce, since the size of the similarity graph was so large that it took an amount of space to compute eigenvalues and eigenvectors and it incurred run out of memory in some cases. To avoid this, we applied our method on one feature time-series and set α to make the number of vertices in the similarity graph are 6805 when we analyzed bats. In addition, 6805 is not the maximum number of nodes in the w/o reduce (they are less than the average number of vertices). By comparing Proposed with w/o reduce, using the merged similarity graph has greatly improved memory saving.

2.5.2 Insight obtained from the results

We presented these results of bats to biologists and obtained the following insights and findings.

Investigation of the co-occurrence of behavioral modes with the best and second-best score indicates that the behavioral mode of low speed and the behavioral mode of 0.2s following capture events were highly correlated. These co-occurrence behavioral modes can be translated as a slow-speed foraging mode. We confirmed that there is a significant difference between the speed for 0.2 seconds after the capture event and the speed outside those 0.2 seconds using the t-test (2.91 m/s vs. 3.28 m/s; $P < 0.001$). While an investigation of the speed of movement before capturing has been performed on other bats [42, 43, 79], this is the first study revealing that Japanese Large-footed bats continue in slow-speed after capturing events. This result indicates that the bats concentrate on eating the captured insects.

Investigation of the co-occurrence of behavioral modes with third-best score indicates that the behavioral mode of low acceleration and the behavioral mode of 0.1s following capture events were highly correlated. We confirmed that there is a significant difference between the absolute acceleration 0.1 sec following capture events and that preceding capture events using the t-test (0.67 m/s^2 vs. 1.36 m/s^2; $P < 0.001$). The absolute acceleration before capturing is larger than that after capturing. This may be because the bats drastically reduce their speed by stopping fluttering as well as the air resistance of the uropatagium[1]. Low speed provides sufficient time for the bats to

[1]It is the membrane that stretches between the legs and tail and is used to capture insects.

precisely grasp their situations, e.g., locations of surrounding insects. In addition, low speed may enable the bats to precisely control their movements [67]. This is the first study that revealed the difference in the acceleration of the bat before and after capturing a prey.

2.6 Conclusion

In this chapter, we focused on detecting co-occurrence behavioral modes from multi-modal sensor data collected from animals. We proposed a method to automatically find co-occurrence behavioral modes. To find the co-occurrence behavioral modes, we designed a score computation method. In the experiment, we first used synthetic data to test whether our proposed method can find out co-occurrence behavioral modes or not. The result shows our method could discover frequent co-occurrence behavioral modes from synthetic data. Second, we selected Japanese Large-footed Bats as our research subjects. We recorded the running time and memory usage of the proposed method. Compared with other methods, our method runs the shortest time and occupies the least memory. We obtained top-3 co-occurrence behavioral modes of bats with the highest score and put forward hypotheses. Finally, we discussed these results with biologists.

As part of our future work, we plan to apply the proposed method to other animals that cannot be directly observed.

Chapter 3

Detecting difference in co-occurrence behavioral modes between groups in animal behavioral data

3.1 Introduction

Animal behavior is expressed with a continuous stream of events that can be divided into discrete behavioral modes (e.g., resting and foraging), as mentioned in Chapter 2. These behavioral modes are measured for each sensor modality (i.e., different sensors used when observing behavior and environment, such as sound and position). Some behavioral modes obtained from different sensor modalities may co-occur, and the probability of co-occurrence of different behavioral modes depends on the different groups or environments.

Sexual dimorphism refers to the fact that the two sexes of the same species exhibit different characteristics in addition to the differences in their sexual organs. This condition is widespread in animals, and differences may include secondary sexual characteristics, size, weight, coloration, markings, but also behavioral and cognitive differences, and has attracted great interest among evolutionary biologists [70, 77, 81, 118]. For example, chimpanzees make grunts while foraging, and the co-occurrence probability of grunts and foraging behavior depends mainly on sex and individual circumstances

[44]. Behavioral co-occurrence reflects the decision-making of each group and thus provides insight into sex-specificity foraging strategies, polymorphisms with corresponding strategies, and life history strategies of different populations. Therefore, identifying behavioral co-occurrence and its variation between groups from a large amount of behavioral data is vital for understanding animal behavior and/or its relationship with the surrounding environment.

In this chapter, we develop a method to detect the co-occurrence of behavioral modes that differ in frequency between two groups (e.g., males and females) by introducing a comparative analysis based on the method in Chapter 2. In addition, we use deep learning to automatically extract meaningful features from behavioral data.

The contributions of this study are as follows.

- We propose a method to automatically detect frequent co-occurrence of behavioral modes that differ in frequency between two groups from multi-modal animal behavioral data. Our method can detect behavioral modes that frequently co-occur from different sensor modalities and then identify behavioral modes that differ in frequency of co-occurrence between the two groups. To the best of our knowledge, this is the first study to automatically detect knowledge related to the co-occurrence of behavioral modes from multi-modal animal behavioral data.

- We validate the method using actual data obtained from seabirds, including co-occurrence-related sex differences between horizontal (i.e., GPS position) and vertical movements (i.e., dive depth) of seabirds.

The structure of Chapter 3 is as follows. In Section 3.2, we provide a review of some related works. In Section 3.3, we describe detail of our approach. Section 3.4 shows experiments of the proposed method and results. The discussions with biologists are introduced in Section 3.5. Finally, in Section 3.6, we conclude this paper and discuss future work.

3.2 Preliminary

3.2.1 Big data mining technology for comparative analysis

Data mining is a technique for discovering meaningful patterns from big data. It can be used in various fields to find yet undiscovered, interesting patterns. Previously, researchers attempted to find the interesting parts by plotting the data. As the volume and dimensionality of data increases, it becomes challenging to manually analyze the data. Therefore, researchers use tools, such as classification, clustering, and neural networks, to find useful information from the big data. Vartak et al. proposed SeeDB [99] to find the most "interesting" or "useful" patterns from database. The authors developed SeeDB [100] to make it possible to find "interesting" that differs between groups by comparing the distributions of different groups. However, the SeeDB could only detect descriptive statistics (e.g., count, sum, average) from the data. Maekawa et al. [57] applied deep learning to comparative analysis to detect the difference in trajectories features (e.g., speed, angular speed) between groups. In contrast, our study focuses on the difference in behavior co-occurrence between groups.

3.2.2 LSTM autoencoder

In the research, we used Long Short Term Memory (LSTM) autoencoder to extract representations of each time step in the sensor modalities. The definition of LSTM and autoencoder are as following.

LSTM. LSTM is a kind of recurrent neural network (RNN) and first proposed in [37]. LSTM is capable for learning long-term dependence information and processing time-series due to its special structure.

Autoencoder. Autoencoder is a kind of artificial neural network used for unsupervised learning [52, 53]. It is a data compression algorithm, aimed at learning the representation of data. Autoencoder includes two processes: encode and decode. As is shown in Figure 3.1, the autoencoder first uses an encoder to compress the input into a potential representation and then uses a decoder to reconstruct the output from this representation. By limiting the number of hidden units to fewer than the number of input and output

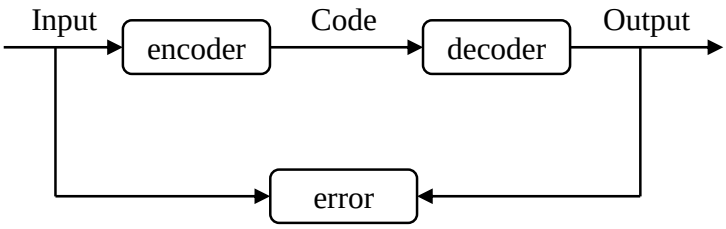


Figure 3.1: An autoencoder is a neural network that learns the latent representation of an input. The encoder converts the input into the latent representation, the hidden layer contains the latent representation of the input data, and the decoder reconstructs the original input from the latent representation.

units, the network can obtain a compressed representation of the input while retaining the important information about the input that is necessary for its reconstruction (i.e., the output of the autoencoder).

LSTM autoencoder is often used for analyzing time-series sequences. In [58], they used LSTM autoencoder to detect anomaly by just training normal data. The anomalous information can be detected if the LSTM autoencoder could not reconstruct well. In [82], they designed a model based on LSTM autoencoder to learn representation of video. First, they used these representations to reconstruct the input video. After that, they predicted serval future frames based on the representations.

3.3 Proposed method

Our method comprised of four steps (Figure 3.2): 1) feature extraction/learning, 2) behavioral mode extraction using a clustering method, 3) identifying co-occurrence behavioral modes, and 4) identifying behavioral co-occurrence differences between groups. The method started with original sensor data (e.g., GPS coordinates) and calculated or learned features (e.g., speed) in the first step. Then, the method extracted behavioral modes (e.g., cruising mode and relaxing mode) from the time-series of features in the second step. In the third step, the method identified pairs of behavioral modes that frequently co-occur. In the fourth step, the method output pairs of behavioral modes that

differ between given two groups in terms of the frequency of co-occurrence. Compared to the method in Chapter 2, the improvements of the proposed method in this chapter are as follows.

- We used deep learning to learn the representation of the features extracted from the trajectory through feeding features into the LSTM auto-encoder.
- We could find in the results of Chapter 2 that the method will output similar co-occurrence behavioral modes. Therefore, we improved the algorithm so that it can merge similar results.
- We added the function to calculate the differences between groups.

Since the proposed method in this chapter is based on the improved method in Chapter 2, we only present the improved parts.

3.3.1 Problem definition

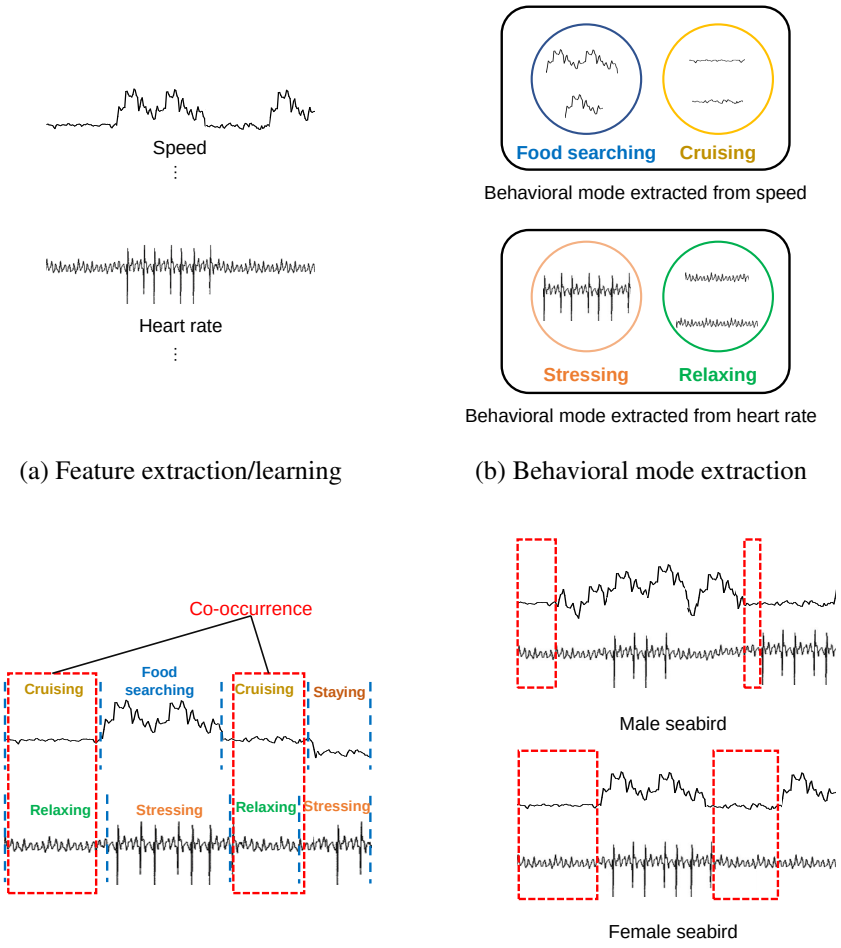
DEFINITION 1 (DIFF($L^{p,A}_{i,\theta_n}, E^{q,A}_{j,\theta_m}, L^{p,B}_{i,\theta_n}, E^{q,B}_{j,\theta_m}$)).

$$Diff(L^{p,A}_{i,\theta_n}, E^{q,A}_{j,\theta_m}, L^{p,B}_{i,\theta_n}, E^{q,B}_{j,\theta_m}) = \|Corr(L^{p,A}_{i,\theta_n}, E^{q,A}_{j,\theta_m}) - Corr(L^{p,B}_{i,\theta_n}, E^{q,B}_{j,\theta_m})\|$$

$Diff(L^{p,A}_{i,\theta_n}, E^{q,A}_{j,\theta_m}, L^{p,B}_{i,\theta_n}, E^{q,B}_{j,\theta_m})$ measures the difference of co-occurrence between groups. $Corr(L^{p,A}_{i,\theta_n}, E^{q,A}_{j,\theta_m})$ and $Corr(L^{p,B}_{i,\theta_n}, E^{q,B}_{j,\theta_m})$ are the correlation in group A and group B, respectively. $L^{p,A}_{i,\theta_n}$ ($E^{q,A}_{j,\theta_m}$) shows segments in the p-th (q-th) cluster obtained from individuals belonging to group A. The greater the value of $Diff(L^{p,A}_{i,\theta_n}, E^{q,A}_{j,\theta_m}, L^{p,B}_{i,\theta_n}, E^{q,B}_{j,\theta_m})$, the greater the difference in the frequencies of the co-occurrence between the two groups.

3.3.2 Algorithm

Algorithm 2 shows the procedures of this method. Line 1–11 of Algorithm 2 are same as the method in Chapter 2. After the scores of all cluster pairs were computed, results diversification was then performed to remove similar co-occurrence behavioral modes (Algorithm 2 Line 13). We then divided the data according to the type of group, calculated correlations in each group, and ranked the correlated behavioral modes based on the difference in correlation between the two groups (Algorithm 2 Line 15–16).



(a) Feature extraction/learning

(b) Behavioral mode extraction

(c) Find co-occurrence behavioral modes

(d) Find behavioral co-occurrence differs between groups

Figure 3.2: Overview of the proposed method. (a) Feature extraction/learning. (b) Behavioral mode extraction using a clustering method. (c) Identifying co-occurrence of behavioral modes. (d) Identifying behavioral co-occurrence differences between groups.

3.3.3 Feature extraction/learning

We first extracted artificially designed features from the time-series, (i.e., motion features, such as speed and angular speed, which were extracted from the trajectory time-

Algorithm 2: `Proposed method`

Input: $\mathcal{X}$: a set of time-series, α_{max}: maximum #symbols, α_{min}: minimum #symbols, β_{max}: maximum cluster number, β_{min}: minimum cluster number

```
/* Feature learning */
```
$\mathcal{X} \leftarrow \mathcal{X} \cup$ LSTM-AUTOENCODER$(\mathcal{X})$
```
/* Clustering time-series */
```
for $\forall X_i \in \mathcal{X}$ **do**
  $\mu, \sigma^2 \leftarrow$ COMPUTE-MEAN-VARIANCE(X_i) ▷ μ is mean and σ^2 is variance **for** $\alpha = \alpha_{max}$ *to* α_{min} **do**
    SAX$(X_i, \mu, \sigma^2, \alpha)$
    MERGE-SYMBOLS$(\cdot)$
    SIMILARITY-GRAPH-CONSTRUCTION()
    LAPLACIAN-EIGENMAPS()
    for $\beta = \beta_{min}$ *to* β_{max} **do**
      $R \leftarrow R \cup \{\text{k}-means++()\}$ ▷ store the clustering result

```
/* Diversification */
```
$\mathcal{R} \leftarrow$ DIVERSIFICATION(R)
```
/* Find the co-occurrence behavioral mode that differ
   greatly in frequency between two groups */
```
for $\forall \mathcal{R}_i \in \mathcal{R}$ **do**
  $G_{i,1}, G_{i,2} \leftarrow$ DIVIDE$(\mathcal{R}_i)$ ▷ divide result into two groups
  $D \leftarrow D \cup \{$DIFFERENCE$(G_{i,1}, G_{i,2})\}$ ▷ calculate the difference between two groups and store the result

series. To automatically obtain additional features from the original time-series or the basic manual features, we used an LSTM autoencoder (Figure 3.3). Since movement modes contained in animal trajectories (e.g., cruising) can be considered as potential representations of motion, concepts similar to movement modes are expected to be obtained by feeding hand-crafted features (i.e., features designed by the researcher) to the autoencoder. The network used in this study consists of an input layer, a hidden LSTM layer using a rectified linear cell activation function, and an output layer (Figure 3.2a). We used the output time-series of each hidden cell (cell in the hidden layer) as the input to the next procedure. The features learned by each hidden unit are called "learned

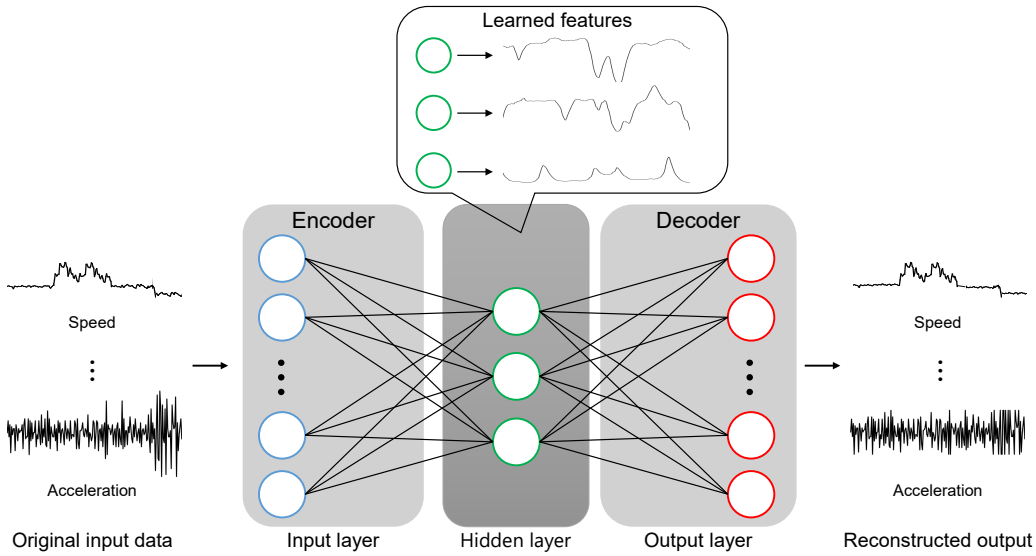


Figure 3.3: Feature learning using an autoencoder. An autoencoder is a neural network that learns the latent representation of an input. The encoder converts the input into the latent representation, the hidden layer contains the latent representation of the input data, and the decoder reconstructs the original input from the latent representation. Each circle is regarded as a unit in the neural network. The number of units in the input layer and that of the output layer are identical to the dimension of the input data. The number of units in the hidden layer is less than that in the input layer. By limiting the number of hidden units, we can compress the input data. Because the compressed representation contains important information necessary to reconstruct the output, the compressed data are considered to represent latent states of an animal (i.e., behavioral modes).

feature". In our study, the input of the encoder and the output of the decoder corresponded to the hand-crafted features. We trained the network using the Adam-based backpropagation method to minimize the average absolute error between the input and output. We performed a feature learning procedure for each sensor mode. For example, we prepared an autoencoder for the GPS data, and the features of the GPS data, such as speed and acceleration, were fed to the autoencoder.

3.3.4 Identifying co-occurrences in behavioral modes and diversification

We computed a ranked list of pairs (co-occurrence of behavioral modes) based on scores (Figure 3.2c) and then removed the similar co-occurrence behavioral modes from the list. We first grouped the co-occurrence behavioral modes from the same features. For each group, we then computed the temporal correlation between each pair of behavioral modes. Given two behavioral modes, $(L^p_{i,\theta_a}, E^q_{j,\theta_b})$ and $(L^r_{i,\theta_c}, E^s_{j,\theta_d})$, we computed $Corr(L^p_{i,\theta_a}, L^r_{i,\theta_c})$ and $Corr(E^q_{j,\theta_b}, E^s_{j,\theta_d})$. Remember that L_i was a trajectory feature time-series and E_j an environment time-series. L^p_i (E^q_j) was p-th (q-th) cluster (behavioral mode) in L_i (E_j), and θ_a (θ_b) was the parameter set. When these two correlation values exceed the threshold, the co-occurrence of behavioral modes with lower scores was discarded.

3.3.5 Identifying the co-occurrence of behavioral modes that differs between groups

After obtaining the ranking of the co-occurrence of behavioral modes, we calculated the correlation differences between the groups in descending order (Figure 3.2d). First, for each co-occurrence behavioral mode, we divided the corresponding animal movement data or learned features into two groups (e.g., group A and group B). Second, we calculated $Corr(L^{p,A}_{i,\theta_n}, E^{q,A}_{j,\theta_m})$ and $Corr(L^{p,B}_{i,\theta_n}, E^{q,B}_{j,\theta_m})$, respectively. Next, we calculated the absolute values of the differences between the two groups and then obtained a ranking table of the differences between the two groups. Finally, the co-occurrence of behavioral modes that differed in frequency between the two groups was output.

3.4 Experiment

3.4.1 Dataset

GPS and bathymetric (water depth) data were collected by attaching the loggers (Axy-Trek; Technosmart, Roma, Italy) to streaked shearwater (*Calonectris leucomelas*) near

Awashima Island (38° 28'N, 139° 14'E; Niigata, Japan) in 2016, 2017, and 2018. Analysis of these sensor data using the proposed method was expected to reveal the co-occurrence of behavioral modes related to the relationship between diving activities and movement modes. For details on the data collection, please refer to [59]. The sampling interval was 1 min for the GPS and 1.0 Hz for the water depth sensor. The number of trajectories was 79, the average duration of the trajectories was 329 hours, and the average number of data points for a track was 14,233. The dataset included information on 37 males (average trajectory duration: 334 hours; the average number of data points in a trajectory: 14,459) and 42 females (average trajectory duration: 325 hours; the average number of data points in a trajectory: 14,034). Because we could obtain a multidimensional time-series for each trajectory (79 time-series in total), we concatenated the 79 time-series into a multidimensional time-series and used them as input.

3.4.2 Feature extraction

We prepared three types of time-series. 1) locomotion features from GPS, 2) the number of dives extracted from bathymetry data, and 3) timestamps. We extracted locomotion features widely used in biological studies by varying their feature parameters (e.g., window size), such as speed [m/s], acceleration [m/s^2], angular speed [rad/s], moving average and variance of speed, acceleration, and angular speed. We computed first passage time (FPT) based on GPS coordinates [28], distance and displacement from the coastline [9, 34]. Table3.1 shows the description of the feature parameters. For example, we calculated the moving average of speed with different window sizes (5, 10, 15, 20, 25, 30) and obtained six time-series of moving average of speed. For example, only one time-series was computed because the distance to the coastline had no characteristic parameters. We also calculated the displacement of GPS data using sliding windows of different window sizes (5, 10, 15, 20, 25, 30) and obtained six time-series of displacement.

We extracted a total of 55 feature time-series data from each trajectory, from which we obtained 32 features learned by the autoencoder. We obtained water depth time-series with sampling intervals of 1 minute and 1 hour by calculating the number of dives per minute and per hour, respectively. In addition, we used a timestamp series based on

Table 3.1: Description of feature parameters. These parameter values are selected to capture short- and long-term behaviors of seabirds.

Features	Feature parameters
Moving average of speed, acceleration and angular speed	window size (min) = 5, 10, 15, 20, 25, and 30.
Moving variance of speed, acceleration and angular speed	window size (min) = 5, 10, 15, 20, 25, and 30.
FPT	Radius (m) = 100, 200, 300, 400, 500, 600, 700, 800, 900, and 1000.
Displacement	window size (min) = 5, 10, 15, 20, 25, and 30.

the hour of the day (e.g., 01:00, 02:00, etc., local time) as the third feature type because we expected to obtain correlations between the diving activities or movement features of seabirds and the hour of the day. Note that when we calculated two feature time-series, they should have the same sampling interval; therefore, we converted the water depth data into a time-series of dive counts so that the sampling interval of the time-series is the same as that of the GPS data (or timestamp series).

3.4.3 Comparison methods and environment

The following methods were used to evaluate the computation time of the proposed method. In this study, we were concerned with the computation time. Generally, researchers design and add new features based on the previous run results, thus iterating the analysis process several times. Therefore, it is crucial to reduce the computational cost of the iterations.

- **Proposed**: the proposed method in this paper.
- **w/o symbol**: the method that without reusing previous SAX results.
- **w/o reduce**: the method that without using a merged similarity graph.

Table 3.2: Evaluation of the efficiency of seabird data: running time [sec])

	Segmentation	Clustering	Total
Proposed	4.30	8.10	12.40
w/o symbol	5.98	8.16	14.14
w/o reduce	4.32	5.61×10^5	5.61×10^5
K-means++	-	-	173.00
HMM	-	-	1.28×10^5

Note that all the above methods had the same output, but different computational time. Furthermore, we omitted cluster pairs not satisfying $Corr(L^p_{i,\theta_n}, E^q_{j,\theta_m}) > \gamma$ in order to filter out behavioral modes with low correlation. Additionally, we set γ to 0.3. We set α_{min} to 4, α_{max} to 20, β_{min} to 2, and β_{max} to 10. These parameters were determined empirically. All methods were implemented in C++, and eigenvectors were calculated by CLAPACK 3.2.1. Moreover, we ran K-means++ (C++) and HMM (Python, hmmlearn 0.2.5) on our data set instead of the combination of SAX and spectral clustering. As these methods do not have the segmentation procedure, we simply varied the number of clusters from 3 to 10. All experiments were conducted on a PC with a 3.4-GHz Intel Core i7 CPU with 16 GB RAM.

3.4.4 Result

Table 3.2 shows the running time of each method. The columns of segmentation and clustering show the computation time of the segmentation and clustering procedures, respectively, indicating the efficiency of the proposed method in terms of computation time compared to other methods. 42 co-occurrence behavioral modes were obtained from the proposed method. The following are the three highest scores of co-occurrence behavioral modes. Note that since the goal of this study was to find the co-occurrence of two behavioral modes, we only focused on these two behavioral modes and ignore the rest of them.

Co-occurrence of behavioral modes with the best score. "A behavioral mode corresponding to small values of the feature learned in the 23rd hidden unit of the LSTM autoencoder" and "behavioral mode of distance from the coastline (from 60 m to 2200 m)" were highly correlated. The $Corr$ were 0.358 and 0.615 for male and female seabirds, respectively. The learned feature was correlated with movement speed, as the feature was highly correlated with moving average of speed (window size: 30 min; Pearson correlation: 0.902); thus, the behavioral mode of the learned feature could be translated to low-speed (between 0.1 and 6 m/s). To determine the meaning of the behavioral mode (e.g., low-speed mode), we simply plotted the distribution of the identified feature and compared it to the distribution of data points belonging to that behavioral mode.

As mentioned above, the low-speed mode and the behavioral mode that close to the coast co-occurred more frequently in females than in males. Figure 3.4 and Figure 3.5 show the entire trajectory of female and male seabirds under the co-occurrence of behavioral modes with the best score. The red segments represent the identified behavioral modes.

Coccurrence of behavioral modes with the 2nd best score. "A behavioral mode of during the daytime (10:00–17:00 in local time)" and "a behavioral mode of moderate frequency dives (10–14 dives per hour)" were highly correlated. The $Corr$ were 0.409 and 0.620 for male and female seabirds, respectively.

As mentioned above, the daytime mode and the behavioral mode of mid-frequency dives co-occurred more frequently in female seabirds than in males. Figure 3.6 and Figure 3.7 show the entire trajectory of female and male seabirds under the co-occurrence of behavioral modes with the 2nd best score. The red segments represent the identified behavioral modes.

Co-occurrence of behavioral modes with the 3rd best score. "A behavioral mode corresponding to the moderate values of the feature learned in the 15th hidden unit of the LSTM autoencoder" and "a behavioral mode of multiple dives (i.e., the behavioral mode corresponding to the time that seabirds make multiple dives per minute)" are highly correlated. The $Corr$ for male and female seabirds were 0.404 and 0.257, respectively. The learned feature was correlated with movement speed, as the feature was highly correlated with moving average of speed (window size: 20 min; Pearson correlation:

0.914), and the behavioral mode from the learned feature was transformed into a high-speed mode ($>$ 5 m/s).

As mentioned above, the high-speed mode and the behavioral mode of multiple dives co-occurred more frequently in males than in female seabirds. Figure 3.8 and Figure 3.9 show the entire trajectories of female and male seabirds under the co-occurrence of behavioral modes with the 3rd best score. The red segments represent the identified behavioral modes.

Figure 3.10 shows a graphical representation of the correlation between females and males under the co-occurrence of behavioral modes with the top three scores. Generalized linear mixed models (GLMMs) [8] with Gaussian distribution was used to analyze the co-occurrence of behavioral modes for the top three highest scores. In the model, we used $Corr$ for each seabird as the independent variable, sex as the response variable, and individual as a random factor. We used the R (version 3.6.0) package lme4 1.1.21 [6] to build the model. There was a significant difference in the co-occurrence of behavioral modes and best scores between males and females (GLMM, $t = -3.515$, $df = 77$, $P < 0.0001$, Figure 3.10a). There was a significant difference in the co-occurrence of behavioral modes with the 2nd best score between males and females (GLMM,$t = -2.788$, $df = 77$, $P < 0.0001$, Figure 3.10b). The co-occurrence of behavioral modes with the 3rd best score varied across genders (GLMM, $t = -2.228$, $df = 77$, $P < 0.0001$, Figure 3.10c).

3.5 Discussion

The proposed method could detect differences in behavioral co-occurrence from multimodal time-series data recorded from wild seabirds (Figure 3.10). In addition, the method significantly reduced the computational time by applying a reduction in the graph size. As shown in Table 3.2, when comparing the proposed method with w/o symbolization, we confirmed that reusing the previous SAX results reduces the computation time associated with segmentation. Because $\alpha_{max} = 20$, the proposed method used the previous SAX results at $\alpha \leq 10$ (as α_{max} increases, we gained the benefit of reusing the previous SAX results).

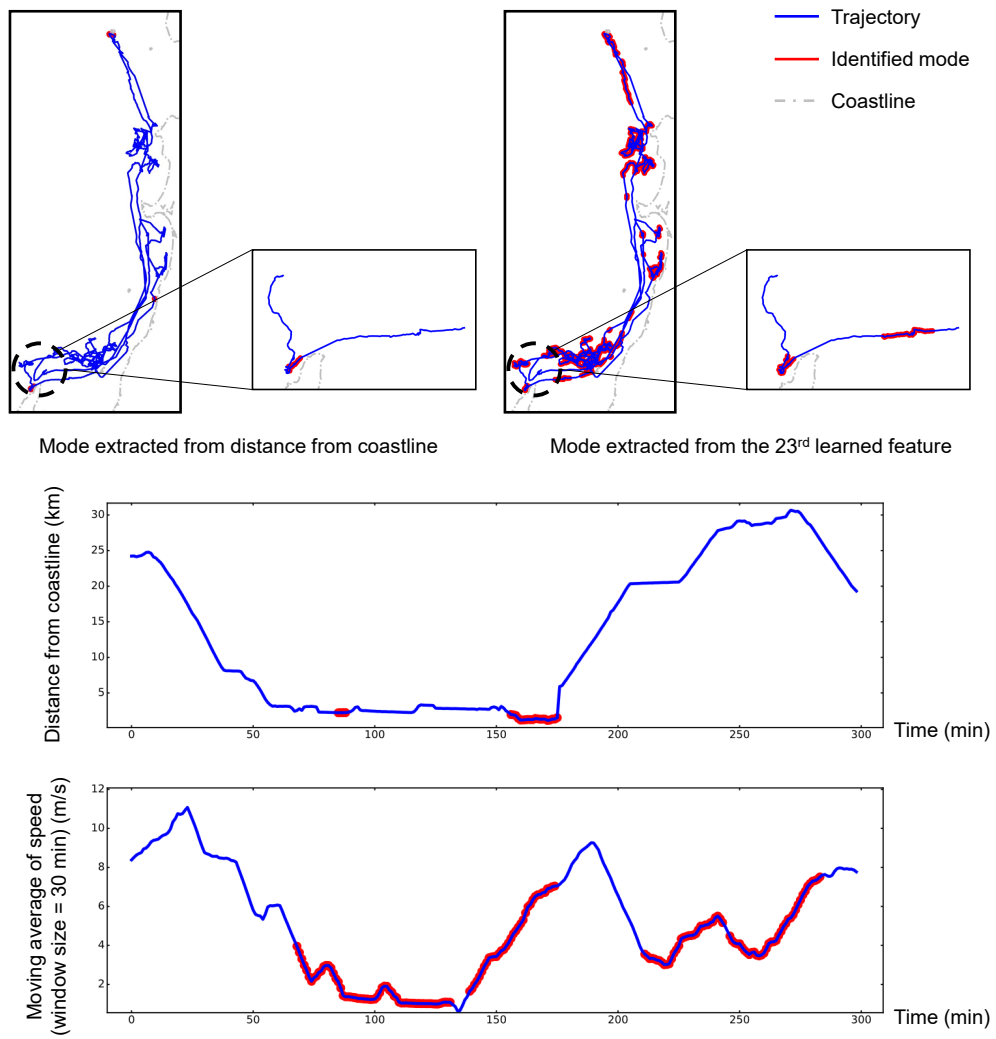


Figure 3.4: Example of a co-occurrence of behavioral modes for female seabirds with the best score. The correlated behavioral modes are the behavioral mode of close to the coast (60-–2200 meters from the coast) from distance from the coastline and the low-speed mode from the 23rd learned feature. The upper maps show bird trajectories. The dashed gray lines show the coastlines, the blue line shows the trajectory, and the red segments represent identified behavioral modes. The lower graphs show the time-series of features, and the red segments show the identified behavioral modes.

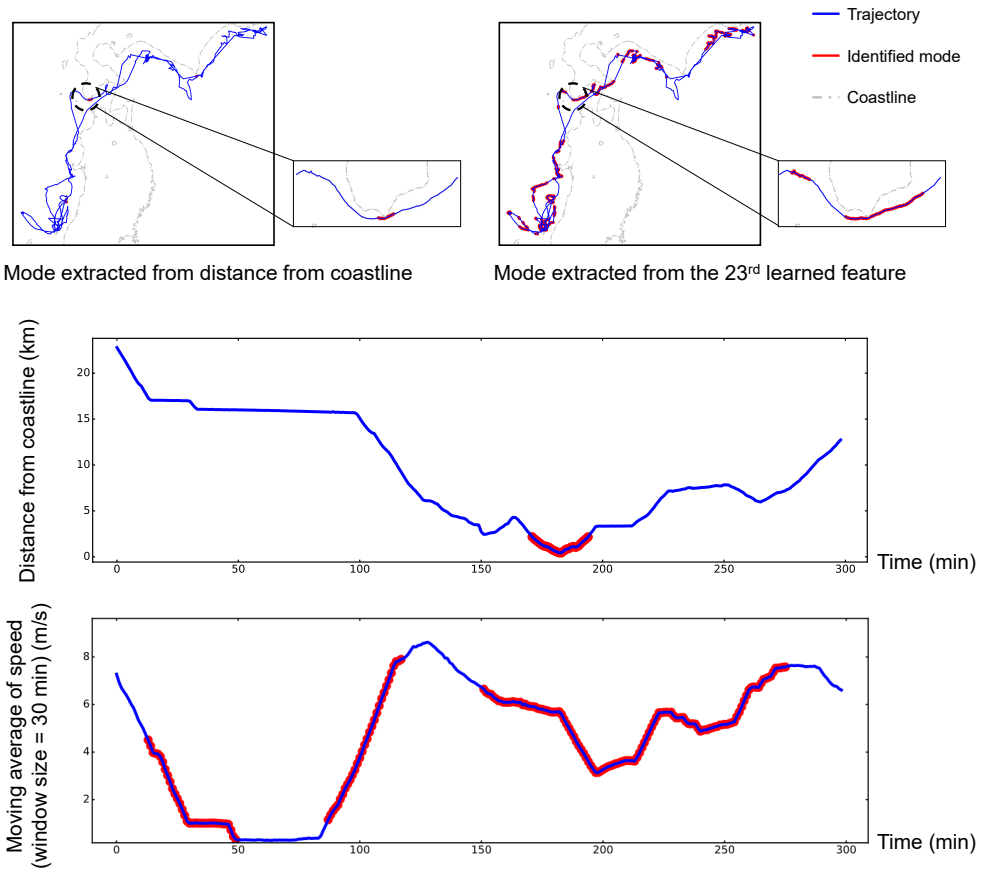


Figure 3.5: Example of a co-occurrence of behavioral modes for male seabirds with the best score. The correlated behavioral modes are the behavioral mode of close to the coast (60—2200 meters from the coast) from distance from the coastline and the low-speed mode from the 23rd learned feature. The upper maps show bird trajectories. The dashed gray lines show the coastlines, the blue line shows the trajectory, and the red segments represent identified behavioral modes. The lower graphs show the time-series of features, and the red segments show the identified behavioral modes.

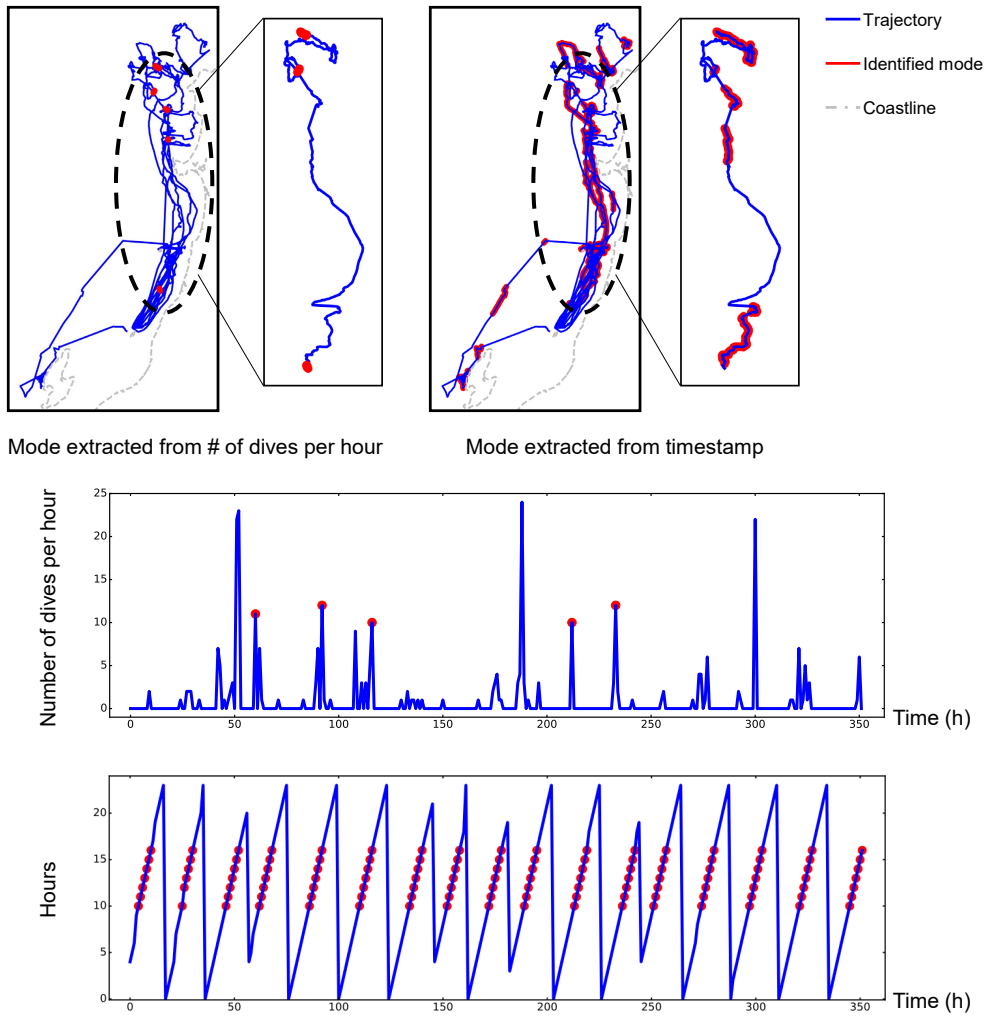


Figure 3.6: Example of a co-occurrence of behavioral modes for female seabirds with the 2nd best score. The correlated behavioral modes are the behavioral mode of frequent dives (between 10 and 14 times per hour) from the number of dives per hour and the daytime mode (10:00–17:00 in local time) from the timestamp. The upper maps show bird trajectories. The dashed gray lines in the map show the coastlines, the blue line shows the trajectory, and the red segments represent identified behavioral modes. The lower graphs show the time-series of features, and the red segments show the identified behavioral modes.

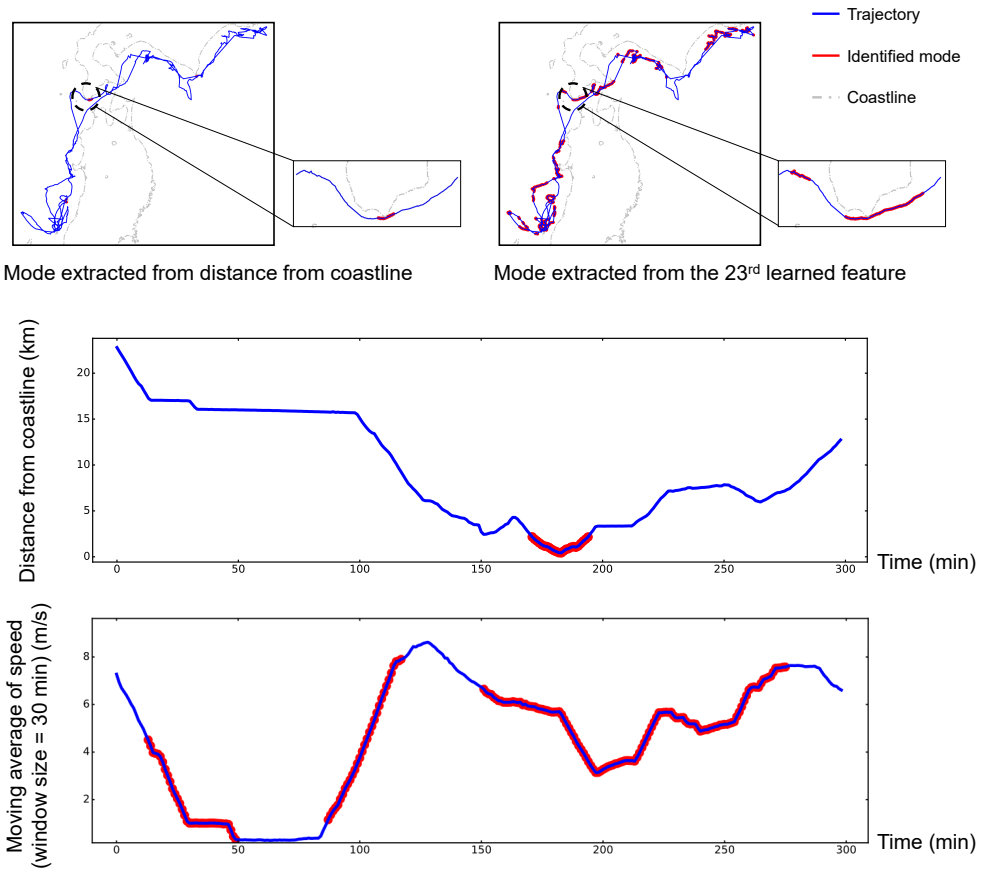


Figure 3.7: Example of a co-occurrence of behavioral modes for male seabirds with the 2nd best score. The correlated behavioral modes are the behavioral mode of frequent dives (between 10 and 14 times per hour) from the number of dives per hour and the daytime mode (10:00–17:00 in local time) from the timestamp. The upper maps show bird trajectories. The dashed gray lines in the map show the coastlines, the blue line shows the trajectory, and the red segments represent identified behavioral modes. The lower graphs show the time-series of features, and the red segments show the identified behavioral modes.

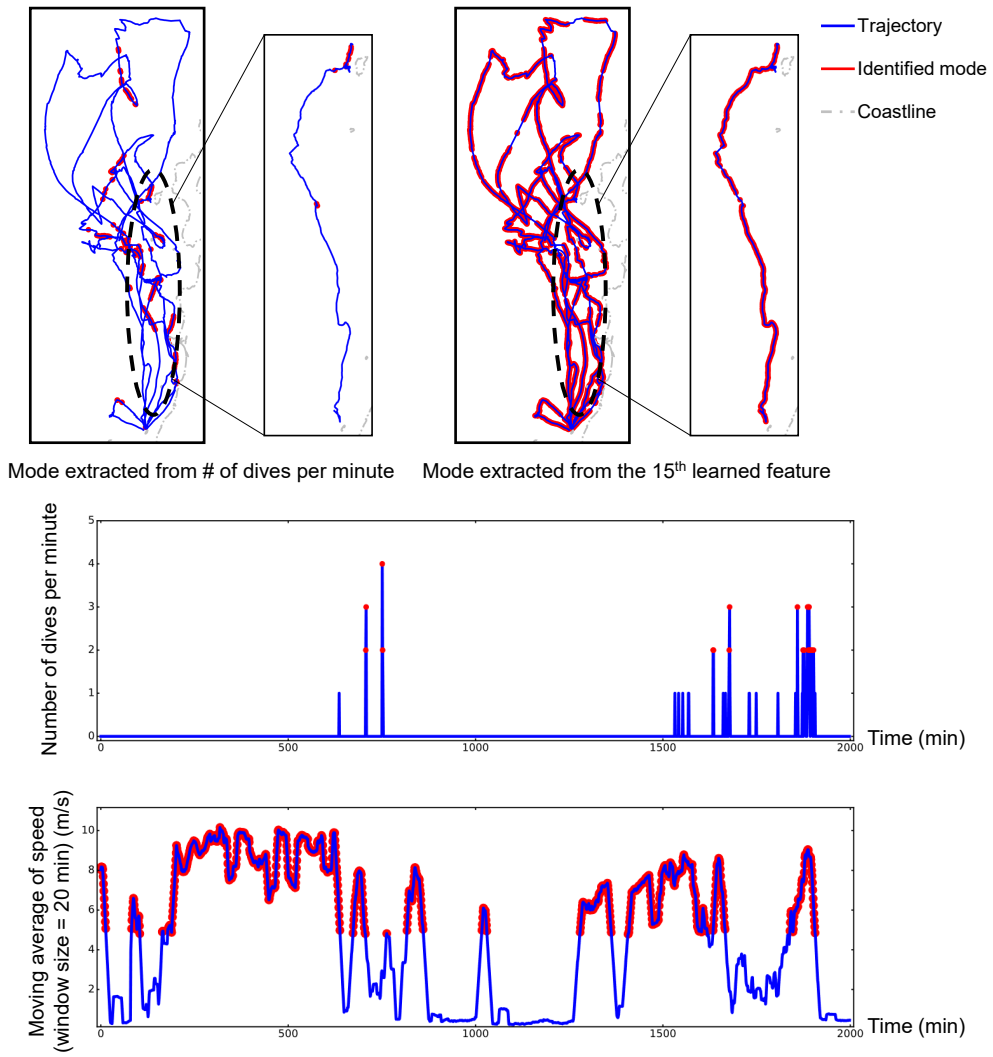


Figure 3.8: Example of a co-occurrence of behavioral modes for female seabirds with the 3rd best score. The correlated behavioral modes are the behavioral mode of multiple dives number of dives per minute and the high-speed mode from the 15th learned feature. The upper maps show bird trajectories. The dashed gray lines in the map show the coastlines, the blue line shows the trajectory, and the red segments represent identified behavioral modes. The lower graphs show the time-series of features, and the red segments show the identified behavioral modes.

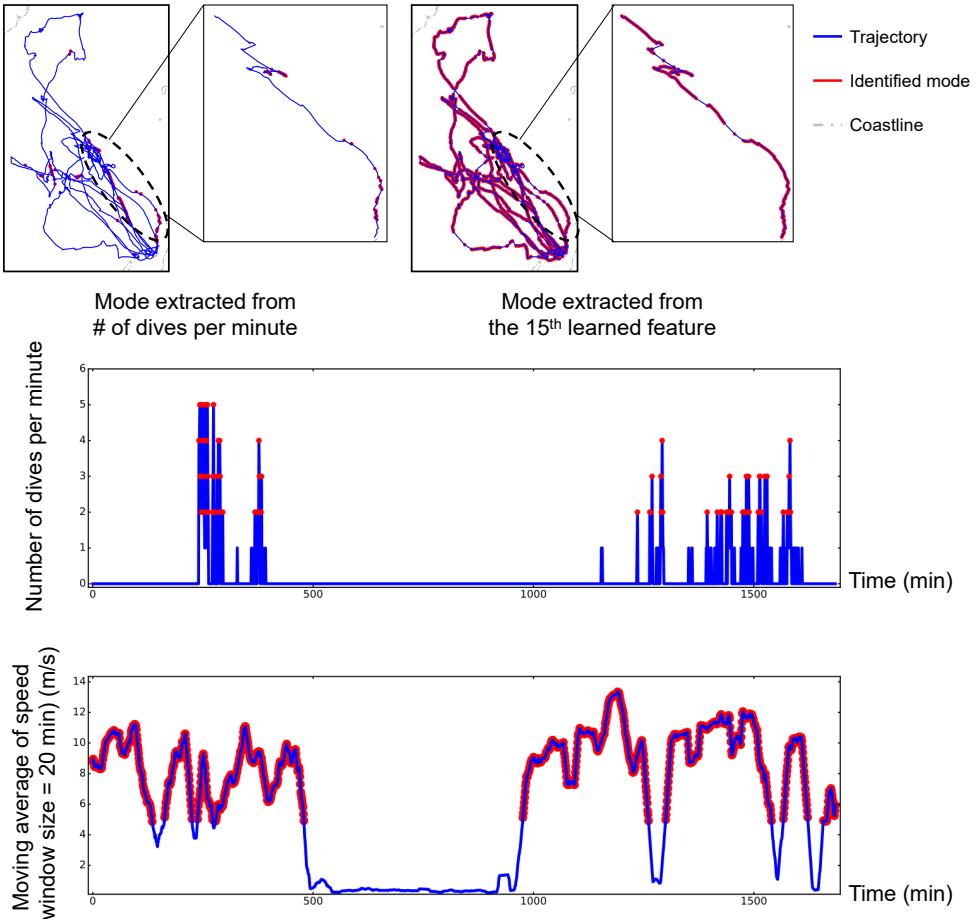


Figure 3.9: Example of a co-occurrence of behavioral modes for male seabirds with the 3rd best score. The correlated behavioral modes are the behavioral mode of multiple dives number of dives per minute and the high-speed mode from the 15th learned feature. The upper maps show bird trajectories. The dashed gray lines in the map show the coastlines, the blue line shows the trajectory, and the red segments represent identified behavioral modes. The lower graphs show the time-series of features, and the red segments show the identified behavioral modes

.

In addition, a comparison of the method without reducing the graph size showed an improvement in efficiency after reducing the clustering procedure. As shown in table 3.2, the proposed method was four times faster after reducing the graph size. These re-

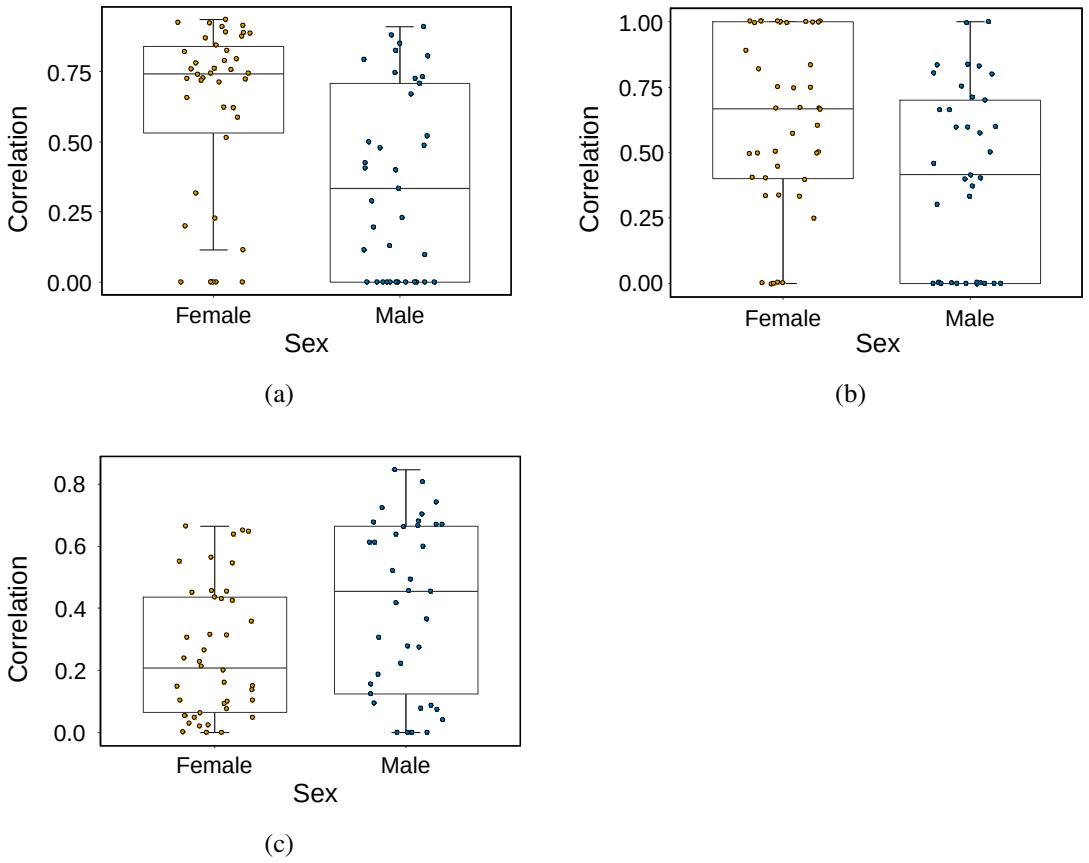


Figure 3.10: Boxplot of Pearson correlation for each co-occurrence of behavioral modes. A significant difference between male and female seabirds was observed by the generalized linear mixed models with Gaussian distributions. Each data point corresponds to a trajectory. (a) Co-occurrence of behavioral modes with the best score ($t = -3.515$, $df = 77$, $P < 0.0001$). (b) Co-occurrence of behavioral modes with the 2nd best score ($t = -2.788$, $df = 77$, $P < 0.0001$). (c) Co-occurrence of behavioral modes with the 3rd best score ($t = 2.668$, $df = 77$, $P < 0.0001$).

sults showed that reducing the size of the graphs significantly affects the computational cost. The proposed method outperformed K-means++ or HMM methods in terms of computation time, indicating that the proposed method is more efficient. Although the computational cost of K-means++ was much smaller than that of HMM, K-means++ could not estimate the temporal regularity of behavioral data.

To the best of our knowledge, this is the first method to detect differences in co-occurrence behavioral modes between groups. While most methods for detecting differences between-group focus on differences in descriptive statistics between groups such as mean and standard deviation, this study first proposed the concept of co-occurrence behavioral modes, where two behavioral modes belonging to different sensor modalities often co-occur. Although clustering methods, such as K-means+ and HMM, can be used to detect behavioral modes, however, it takes a computational time to obtain behavioral modes from big animal behavioral data (Table 3.2). Yeh et al. proposed a method to detect meaningful motifs from multidimensional time-series data [112]. We can use these meaningful motifs to detect co-occurrence behavioral modes (co-occurring motifs) and co-occurrence behavioral modes that differ significantly between groups. However, since the motifs are short, they can only describe an instant animal's behavior; therefore, it is supposed to be difficult to find meaningful co-occurrence behavioral modes by this method.

In the experiments, we iterated 87 time-series by varying the two clustering parameters, resulting in 6,525 runs of the time-series segmentation and clustering process. Thus, we investigated 21,284,550 combinations to find the best time-series and parameter pairs. Our method can help this exhaustive analysis by fast time-series segmentation and clustering.

Investigation of the co-occurrence behavioral modes with the best score showed that the low-speed mode (from 0.1 to 6 m/s) and the behavioral mode that close to shore (60–2200 m from shore) were highly correlated, with higher correlations for females than for males. This co-occurrence of behavioral modes suggests that females fly at lower speed in the range of 60 to 2200 m from the coast, which is more characteristic than males (Figure 3.4 and 3.5). Since females are smaller than males, this suggests that they may prefer to stay closer to the coast, where the wind is not as strong.

The 2nd best score showed that the daytime mode (10:00–17:00, local time) and the behavioral mode of moderate frequency dives (between 10 and 14 dives per hour) were highly correlated, with females showing a higher correlation than males (Figure 3.11 shows the ratio of multiple dives per hour for males and females). This suggests that females dive more frequently than males between 10:00 and 17:00 (Figures 3.6 and 3.7). Differences in diurnal mode between males and females are frequently observed in

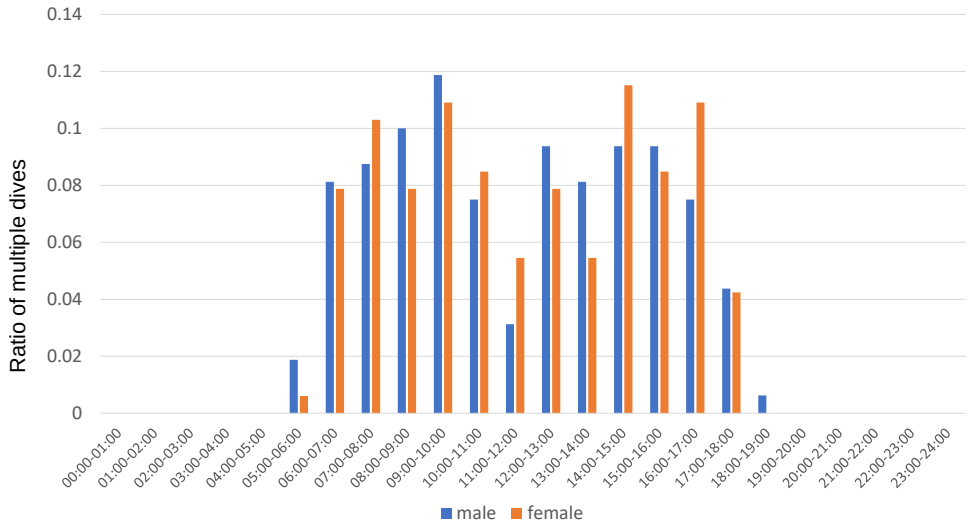


Figure 3.11: Ratio of multiple dives between male and female seabirds per hour.

seabirds and have been interpreted as a consequence of sexual size dimorphism or sex-specificity roles. In the case of streaked shearwaters, females make relatively short trips for their chicks, suggesting that they dive shortly after starting their foraging trips (i.e., in the morning). As mentioned above, new insights related to diving and timestamps of streaked shearwaters are obtained by applying our methods.

The 3rd best score shows that the high-speed mode ($>$ 5 m/s) and the behavioral mode of multiple dives (i.e., corresponding to the time per minute that seabirds make multiple dives) are highly correlated, with males showing a higher correlation than females. This suggests that male seabirds perform multiple dives at higher rates and more frequently than females (Figures 3.8 and 3.9). This may be related to sex differences in foraging behavior. As mentioned above, new insights related to diving in streaked shearwaters are obtained by applying our method to their movement data.

3.6 Conclusion

The proposed method allowed obtaining new insights related to seabirds. Experimental results showed that the proposed method could find co-occurrence of behavioral modes

in different groups and shorter running time than other machine learning methods. As the method aims to mine meaningful co-occurrence from any type of time-series, it has the potential to be widely used to discover relationships between movement modes and foraging activity [105], heart rate and group formation [104], and brain signals and behavior [76]. Our future work will involve validating our findings by measuring sensor data from other modalities (e.g., recording seabird diving activity with a video recorder). In addition, the proposed method can be extended to detect behavioral modes in more than two groups (e.g., juveniles, subadults, and adults).

Chapter 4

NaviMine: A tool for detecting important timing and clues related to animal decision-making

4.1 Introduction

Animals constantly make important decisions during their lives: what to eat, where to go, and how to get there [22]. This animal decision-making plays a crucial role in the animal's navigation, as we mentioned in Chapter 1, because there are more than one destinations, there are more than one routes to the destination, and unexpected situations may arise on the way to the destination. At that point, the animal needs to find the most appropriate one based on some clues (e.g., memory, surrounding environment). For example, the salmon (*Oncorhynchus keta*), the subject of our study, hatch in rivers along the Sanriku coast of Iwate, Japan, and seek out and migrate to their natal rivers after they migrate from the open ocean, i.e., salmon run. The navigation mechanism of salmon from the open ocean to the coastal waters is considered to be different from the migration mechanism from coastal waters to natal rivers [33].

Due to recent advances in sensing technology, the trajectories of moving objects can be easily recorded [114, 115], such as wild animals, and these trajectories can be publicly used for trajectory data mining and/or animal behavior analysis studies. By com-

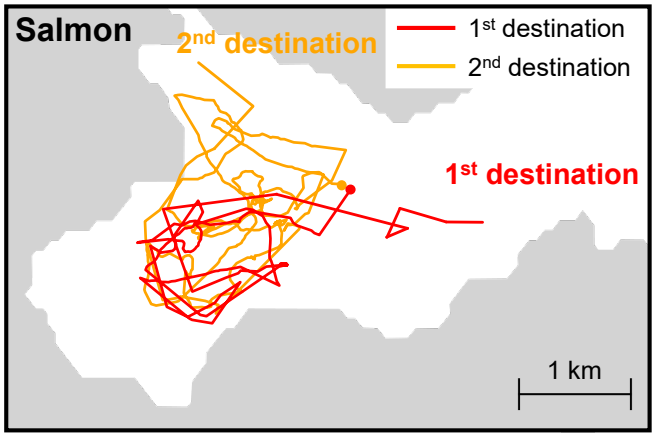


Figure 4.1: An example of trajectories of salmon after they return to Otsuchi Bay, Japan from the open ocean. The circle marks represent the start positions.

bining information about the animal's surroundings, biologists can explain the mechanisms of animal navigation by detecting essential clues related to decision-making. Since animals' movements can reflect their navigation abilities (e.g., destination decisions), studies on analyzing animals' trajectories to reveal their navigation abilities are becoming increasingly popular [57, 111].

However, it is difficult for biologists to find out clues related to destination decision. First, the data is collected for a long time, and it is difficult to detect when an animal makes a decision. Second, a lot of sensor modalities are recorded, it is difficult to find out what clues do animals use to determine their destinations. For example, Figure 4.1 shows the trajectories of our research target: salmon, after they return to the Otsuchi Bay, Japan, from the open ocean. There are two destinations for salmon. The circle marks measure the start positions of salmon. Based on the trajectories, we do not know when the salmon made their decision by looking at it with the naked eye.

Therefore, to support the analysis of animal navigation, we develop NaviMine, a tool that mines trajectory data for navigation studies using destination prediction. NaviMine focuses on the initial short trajectory segment of an animal and uses discriminative classifiers to predict the destination of the animal. For example, if we can predict the destination of the animal by using the first t hours of the initial trajectory segment, it can be assumed that the main reason for deciding the destination is hidden in the first

t hours of the initial segment. NaviMine first finds the times when factors related to finding/selecting destinations may be present. After that, it extracts various features at the time (e.g., first t hours) when important factors may be hidden and compares the distribution of features between different categories (destinations). If the distributions differ significantly depending on the destination, it can be inferred that these feature characteristics are highly relevant to the decision of the destination.

The contributions of this study are as follows.

- We develop a tool to analyze animal decision-making through the use of trajectories. The tool can detect important times and clues by using initial segments to predict the future movements of the animal.
- We validate the tool using actual data obtained from salmon and seabirds, and find some new insights.

The structure of Chapter 4 is as follows. In Section 4.2, we provide a review of some related works. In Section 4.3, we describe detail of our approach. Section 4.4 shows experiments of the proposed method and results. The discussions with biologists are introduce in Section 4.5. Finally, in Section 4.6, we conclude this paper and discuss future work.

4.2 Preliminary

Many studies have used comparative analysis to find factors that may influence animal decision-making. Hernández et al. [36] found that mice's decisions when foraging were related to the difficulty of obtaining food and the risk of predation, and Dunlap et al. [24] found that bees preferred flowers chosen by other bees. Comparative analysis is difficult to apply to wildlife because the natural environment is complex and unpredictable. Many studies have focused on decisions related to destination choice; for example, elephants and dolphins tend to let the most experienced individuals make decisions when migrating or foraging [55, 60]. As mentioned above, research on navigational abilities that reflect the survival strategies of animals has been actively pursued. We believe that computational approaches to large behavioral data of animals will become increasingly important due to recent advances in positioning technology.

Data-driven computational methods for animal behavior analysis have been recently investigated. For example, Yamazaki et al. [111] used decision tree analysis to find the hidden states of animals from trajectory data. Maekawa et al. [57] applied deep learning to comparative analysis to discover new features of animal movements. In contrast, this study focused on destination selection/seeking of animals and used initial segments of trajectories to find factors hidden in trajectories related to destination selection/seeking.

4.3 Proposed method

4.3.1 Assumption

To find the important timings and clues related to decision-making, we set an assumption that animals decide their destinations according to the changes in their surrounding environment and their past events (e.g., foraging activities). If we can use the past trajectories, for example, the initial trajectory segments, to predict future destinations, there may be some clues related to destination determination in the past trajectories. Therefore, we focused on the initial short segments of animals' trajectories and predicted destinations using these segments. If we can predict the destination of animals by using the first t hours of the initial segments, it can be considered that the primary reasons for determining destination are hidden in the first t hours of the initial segments. However, we do not know which t value is appropriate for analysis. Therefore, the proposed method computed prediction accuracies of future destinations by varying different t values. Then, by fusing the prediction accuracy of different t values, we could obtain a series of accuracy. We detected the meaningful time when factors related to destination determination may exist. For example, Figure 4.2 shows a series of accuracy. We can find a sudden increase at the 3rd hour, and we assume that some important events related to destination determination are hidden between the 2nd and the 3rd hour.

4.3.2 Overview

Figure 4.3 shows the overview of the proposed method. First, for each trajectory, we extracted initial t hours segments by varying different values of t (e.g., $t = 1, 2, 3, 4, 5, ...$

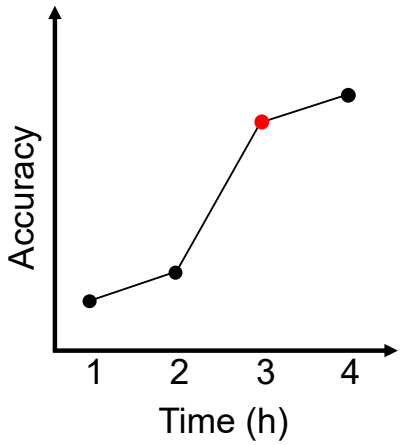


Figure 4.2: An example of series of prediction accuracy. There is a sudden increase between the 2nd and 3rd hour, indicating some important events related to destination determination are hidden between the 2nd and the 3rd hour.

h). Then, time-series features, for example, speed and acceleration time-series, were extracted from each segment (Figure 4.3 i). For each t value, the proposed method estimated labels of segments using the features and calculated the classification accuracies. By fusing the accuracies of different t values, a series of classification accuracies was obtained (Figure 4.3 ii). Then, based on the series of classification accuracies, time t that may contain hidden factors related to the destination finding/selection was detected. After that, the proposed method extracted features focusing on the detected time and built distributions of the features for each class label. Finally, these results were presented to ecologists (Figure 4.3 iii).

4.3.3 Behavior prediction

After we obtained the features (detailed information is presented in Section 4.4), we built a behavior predictor for each time t and computed the classification accuracy. Here, we used the 10-fold cross-validation method to evaluate the performance of each t value. The 10-fold cross-validation method randomly divides the feature vectors into ten groups, using one group as test data and the remaining nine groups as training data. We trained the classifier using the training data and calculated the classification perfor-

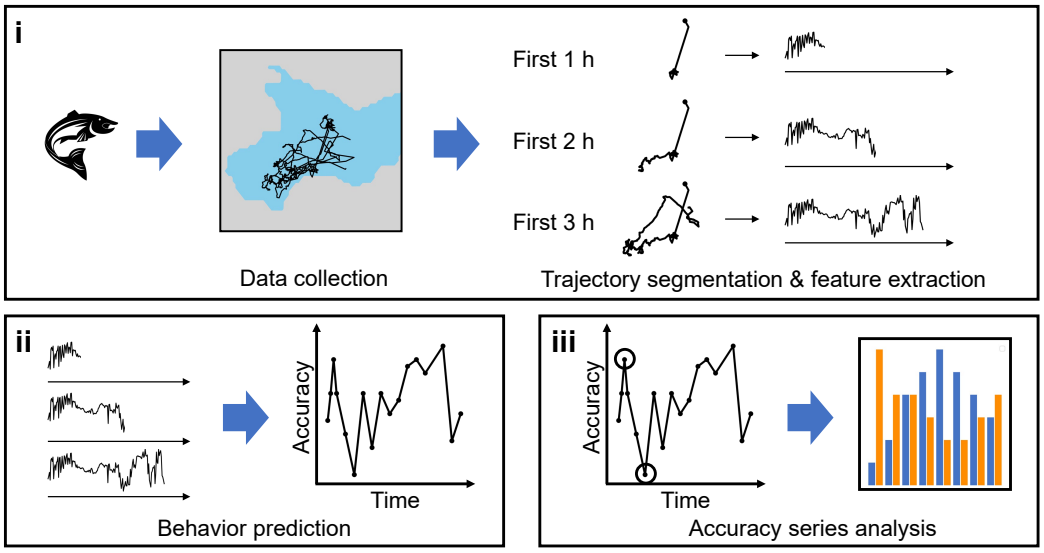


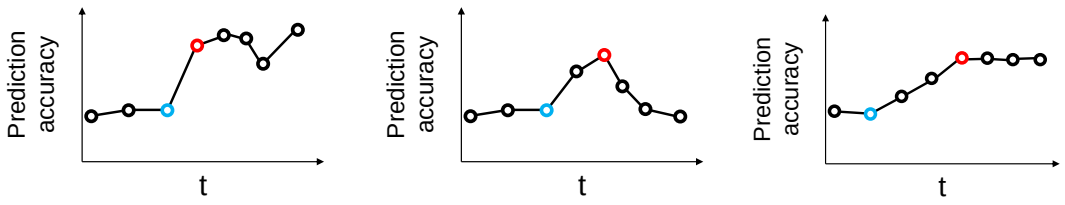
Figure 4.3: Overview of the proposed method.

mance by feeding the test feature vectors into the classifier. We iterated the training and testing ten times by varying the test data set. The average of the classification accuracies obtained by each validation corresponds to the classification accuracy of the value of t.

In this study, we used logistic regression [19] as our behavior predictor and used the macro-averaged F-measure as an indicator of the classification accuracy, since the F-measure is the harmonic mean of recall and precision, measuring the overall accuracy of the predictor. Finally, we obtained the time-series of classification accuracy by fusing the accuracies of different t values. Note that the NaviMine also output a series of classification accuracies for each category, allowing us to analyze a particular label in detail.

4.3.4 Accuracies series analysis

In this study, we focused on three types of timings in the series of accuracies when factors related to destination finding/selection can be hidden: (i) sudden increase, (ii) peak, and (iii) increase before plateau (Figure 4.4). As shown in the figure, we detected these timings and then compared the significant features at these timings with those before the increase of accuracy. Here we explained the ways to detect these timings.



(a) Sudden increase (b) Peak (c) Increase before plateau

Figure 4.4: The process animals deal with information from surrounding environment.

Note that we assumed that a series of prediction accuracies $\mathbf{a} = \{a_{t0}, a_{t1}, \cdots\}$ was given.

Sudden increase

It is considered that something is happening at the time t having a sharp increase in the classification accuracy. Therefore, we focused on the time with a significant increase in the accuracy from the previous moment of the increase (Figure 4.4a).

Algorithm 3 shows the algorithm of this procedure. We first calculated the differential of $\mathbf{a}$, i.e., $\mathbf{a}'$. We then computed the threshold for determining sudden increases from the maximum increase in $\mathbf{a}'$. Finally, we output a set of pairs with each pair consisting of the time of the sudden increase and time just before the increase. In the following procedure, we compared features at the time of sudden increase and the time just before the increase.

Peak

Some hidden factors can be hidden in the time just before the peak of the classification accuracies. Therefore, we focused on the peak and the moment before the increase, as shown in Figure 4.4b.

Algorithm 4 shows the algorithm of this procedure. We first detected peaks in $\mathbf{a}$ [71], and calculated the prominence of each peak [35]. The prominence shows the height of the corresponding peak compared to the surroundings. We then calculated the threshold for determining significant peaks from the maximum prominence value (c_{pr}

Algorithm 3: `Finding sudden increase`

Input: $\mathbf{a}$: a series of prediction accuracies

Output: $\mathcal{P}$: pairs of time corresponding to sudden increase and time just before the increase

```
/* Calculate differential */
```
$\mathbf{a}' \leftarrow \frac{d\mathbf{a}}{dt}$

```
/* Calculate threshold */
```
$a'_{max} \leftarrow \max(\mathbf{a}')$

$th_i = \frac{a'_{max}}{2}$

```
/* Identify sudden increase and time before increase */
```
$\mathcal{P} \leftarrow \emptyset$ ▷ initialize $\mathcal{P}$

for $\forall a'_t \in \mathbf{a}'$ **do**

  if $a'_t > th_i$ **then**

    $\mathcal{P} \leftarrow \mathcal{P} \cup (a'_t.time, a'_{t-1}.time)$ ▷ $a'_t.time$ shows timestamp of a'_t

return $\mathcal{P}$

in Algorithm 4 was a constant value specifying the minimum value of prominence). The significant peaks were defined as peaks whose prominence values were higher than the threshold. After that, we found the time before increase in prediction accuracies for each significant peak (FIND-BEFORE-INCREASE$(\mathbf{a}, r_t.time)$ in Algorithm 4). In the FIND-BEFORE-INCREASE function, we found the time (t_b) using the differential of $\mathbf{a}$, i.e., $\mathbf{a}'$. The time t_b was defined as the latest time when a'_{t_b} was less than or equal to a small constant value before the peak.

Increase before plateau

When the prediction accuracy remains high, the times during the increase may include some critical factors. Therefore, we focused on the starting and ending times of the increase (Figure 4.4c).

Algorithm 5 shows the algorithm of this procedure. To detect the increase, we first calculated the differential of $\mathbf{a}$, i.e., $\mathbf{a}'$. We then detected peaks in $\mathbf{a}'$, and calculated the prominence of each peak. Each peak corresponds to an increase in the prediction accuracy. We calculated the threshold for determining significant peaks (increase) in

Algorithm 4: `Finding peak`

Input: $\mathbf{a}$: a series of prediction accuracies

Output: $\mathcal{P}$: pairs of time corresponding to peak and time before the peak

```
/* Detect peaks in a */
```
$\mathcal{K} \leftarrow$ DETECT-PEAKS$(\mathbf{a})$
```
/* Calculate prominence of peaks */
```
$\mathcal{R} \leftarrow$ CALC-PROMINENCE$(\mathbf{a}, \mathcal{K})$
$th_r \leftarrow \max(\frac{\max(\mathcal{R})}{2}, c_{pr})$ ▷ calculate threshold
```
/* Identify time before peak */
```
$\mathcal{P} \leftarrow \emptyset$ ▷ initialize $\mathcal{P}$
for $\forall r_t \in \mathcal{R}$ **do**
    if $r_t > th_r$ **then**
        $t_b \leftarrow$ FIND-BEFORE-INCREASE$(\mathbf{a}, r_t.time)$ ▷ find time before increase
        $\mathcal{P} \leftarrow \mathcal{P} \cup (r_t.time, t_b)$ ▷ $r_t.time$ shows timestamp of r_t
return $\mathcal{P}$

$\mathbf{a}'$ from the maximum prominence value. (c_{pr} in Algorithm 5 was a constant value specifying the minimum value of prominence.) We also detected peaks in $\mathbf{a}$ ($\mathcal{K}_2$), which were used in the following procedure. After that, we detected significant increase in $\mathcal{K}_1$ (detected peaks in $\mathbf{a}'$). The significant increase had a prominence value higher than the threshold and was not close to peaks in $\mathcal{K}_2$ in time. Therefore, the MINIMUM-DISTANCE function found a peak in $\mathcal{K}_2$, which was closest to a peak in $\mathcal{K}_1$ in time and then computed the absolute temporal difference between the peaks.

After finding the significant increase, we identified the starting and ending times of the increase. Similar to FIND-BEFORE-INCREASE function, the FIND-AFTER-INCREASE function found the time (t_a), which was defined as the earliest time when a'_{t_a} was less than or equal to a small constant value after the peak.

Algorithm 5: `Finding increase before plateau`

Input: $\mathbf{a}$: a series of prediction accuracies

Output: $\mathcal{P}$: pairs of time corresponding to start and end of increase

`/* Calculate differential */`
$\mathbf{a}' \leftarrow \frac{d\mathbf{a}}{dt}$
`/* Detect peaks in` $\mathbf{a}'$ `*/`
$\mathcal{K}_1 \leftarrow$ DETECT-PEAKS$(\mathbf{a}')$
`/* Calculate prominence of peaks */`
$\mathcal{R} \leftarrow$ CALC-PROMINENCE$(\mathbf{a}, \mathcal{K}_1)$
$th_r \leftarrow \max(\frac{\max(\mathcal{R})}{2}, c_{pr})$ ▷ calculate threshold
`/* Detect peaks in` $\mathbf{a}$ `*/`
$\mathcal{K}_2 \leftarrow$ DETECT-PEAKS$(\mathbf{a})$
`/* Identify times before/after increase */`
$\mathcal{P} \leftarrow \emptyset$ ▷ initialize $\mathcal{P}$
for $\forall r_t \in \mathcal{R}$ **do**
  if $r_t > th_r$ & MINIMUM-DISTANCE$(r_t, \mathcal{K}_2) > th_t$ **then**
    $t_b \leftarrow$ FIND-BEFORE-INCREASE$(\mathbf{a}, r_t.time)$ ▷ find time before increase
    $t_a \leftarrow$ FIND-AFTER-INCREASE$(\mathbf{a}, r_t.time)$ ▷ find time after increase
    $\mathcal{P} \leftarrow \mathcal{P} \cup (t_a, t_b)$
return $\mathcal{P}$

4.4 Experiment

4.4.1 Dataset

We applied the proposed method to two kinds of animals: chum salmon (*Oncorhynchus keta*) and streaked shearwaters (*Calonectris leucomelas*).

Salmon

This study used trajectory data collected from chum salmon returning to natal rivers in Otsuchi Bay, Iwate, Japan, for breeding in November and December of 2015, 2016, 2017, and 2018. As shown in Figure 4.5, three rivers, the Otsuchi river, the Kozuchi

river, and the Unosumai river, flow into the Otsuchi Bay. Salmon returning to the bay were captured (star in Figure 4.5), an ultrasonic transmitter (V16-5H, Vemco, Canada) was attached to the salmon (Figure 4.11a), and the salmon were released into the bay (circles in Figure 4.5). The transmitter emits a random transmitter identifier every 30–90 seconds. To receive identifiers emitted by the transmitter, the ultrasonic receivers (VR2W and VR2Tx, Vemco) were installed at the inner part of the bay. Note that 18, 19, 19, and 20 receivers were used in 2015, 2016, 2017, and 2018, respectively. The recovery of transmitters was performed by fishermen. We collected 103 salmon trajectories as a dataset.

In the data preprocessing, we removed outlier trajectories (dead and missing individuals) and trajectories whose data lengths were very short (less than 20 data points). After the preprocessing, the number of salmon (trajectories) returning to the Otsuchi-Kozuchi river and Unosumai river were 28 and 45, respectively. The number of salmon (trajectories) that went out of the bay was 30. The receiver can receive ultrasonic waves from a transmitter within a range of approximately 500 meters. By using the receiver, the location of salmon in the bay could be observed based on trilateration [66]. The end time of each trajectory corresponded to the time of entry into the river (or exit from the bay).

In addition to the trajectory data, environmental data were also used. The environmental data were collected by the Atmosphere and Ocean Research Institute, the University of Tokyo. In this study, water temperature (collected at the triangle in Figure 4.5), ambient temperature, humidity, atmospheric pressure, solar radiation, precipitation, wind direction, and wind speed were used.

Trajectory data for salmon with duration longer than 5 hours were used in this study. We assumed that salmon returning to the Otsuchi or Kozuchi rivers belong to the Otsuchi-Kozuchi class. Therefore, a three-class classification problem was assumed in this study; the Otsuchi-Kozuchi class, the Unosumai class, and the Out-of-Bay class.

Figure 4.6 shows example trajectories used in this study, and Figure 4.7 shows the distribution of the duration of the trajectories.

Although previous researches showed that salmon use their smell to find their natal rivers. In this study, we wanted to find out how the salmon use their sense of smell to identify their natal river.

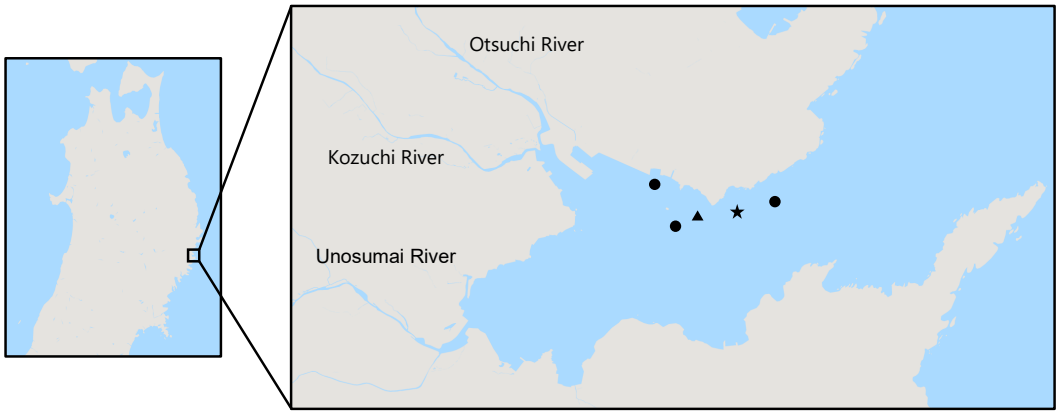


Figure 4.5: Otsuchi bay, Iwate, Japan. The circle shows the release site, the triangle shows the water temperature measurement site and the star shows the salmon capture site.

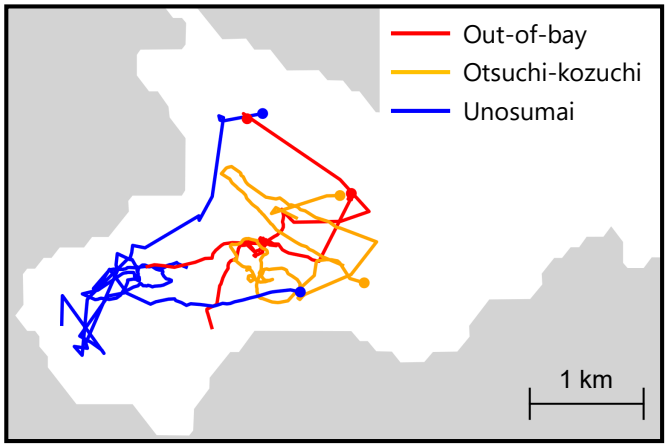


Figure 4.6: Example initial 12 hours trajectories of salmon. We draw two trajectories for each class. The destination of red trajectory is Out-of-bay, the destination of orange trajectory is Otsuchi River or Kozuchi River, and the destination of blue trajectory is Unosumai River. The circles indicate the starting points of the trajectories.

Streaked shearwater

We collected GPS trajectory data of streaked shearwaters from mid-autumn to September in 2016, 2017 and 2018 at Awashima Island, Japan (38°28'N, 139°14'E) [59]. We attached GPS loggers (GiPSy-2, 37×16×4 mm, GiPSy-4, 37×19×6 mm) or GPS, acceleration, and depth loggers (AxyTrek, 55×20×11 mm; TechnoSmArt, Rome, Italy)

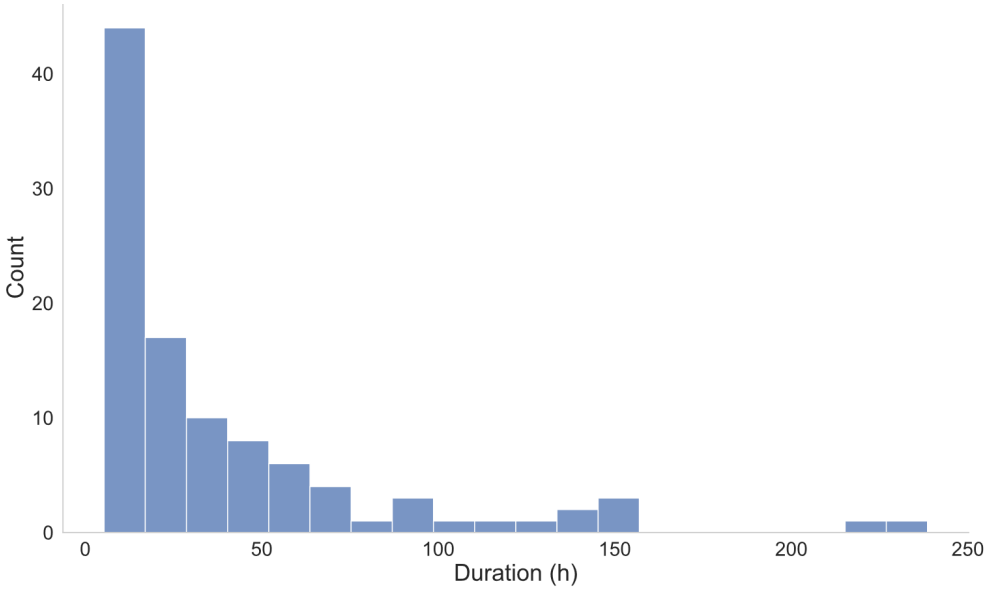


Figure 4.7: The distribution of trajectory duration of salmon.

to the backs of chick-rearing shearwaters (Figure 4.11b) with Tesa® tape (Beiersdorf AG; GmbH, Hamburg, Germany) and cyanoacrylate glue (Loctite® 401; Henkel Ltd., Hatfield, UK), which were set to record one GPS fix per minute. The weight of the device was approximately 25 g, including a waterproof tape or heat-shrinking tube. The device was approximately 5% of the average mass of the birds in our study (mass range: 424–721 g, N=178; males: 621±53 g, range: 513–721 g; females: 503±43 g, range: 424–640 g) [74]. Previous studies have shown that the deployment of similarly sized recorders (such as those in our study) did not adversely affect the behavior of the species, such as trip duration, or the condition of feathers and chicks [80, 113]. In 2016, 2017, and 2018, birds deployed with GPS loggers numbered 58, 70, and 50, respectively.

A trip was defined as the time when a bird was outside the 3 km buffer [14, 69] and over 7.5 hours. The distribution of trip duration (Figure 4.8) indicates that there are two uni-modal distributions of trip duration, and there is a boundary around 24 h that separates the distributions. Based on the trip duration, we had the following definitions: long-term trips equal to or longer than 24 h (maximum: 237.18 h) and short-term trips less than 24 h. We used a valid 198 long-term trips and 301 short-term trips in our analysis.

In addition, the distribution of departure time of trips (Figure 4.9) shows that more

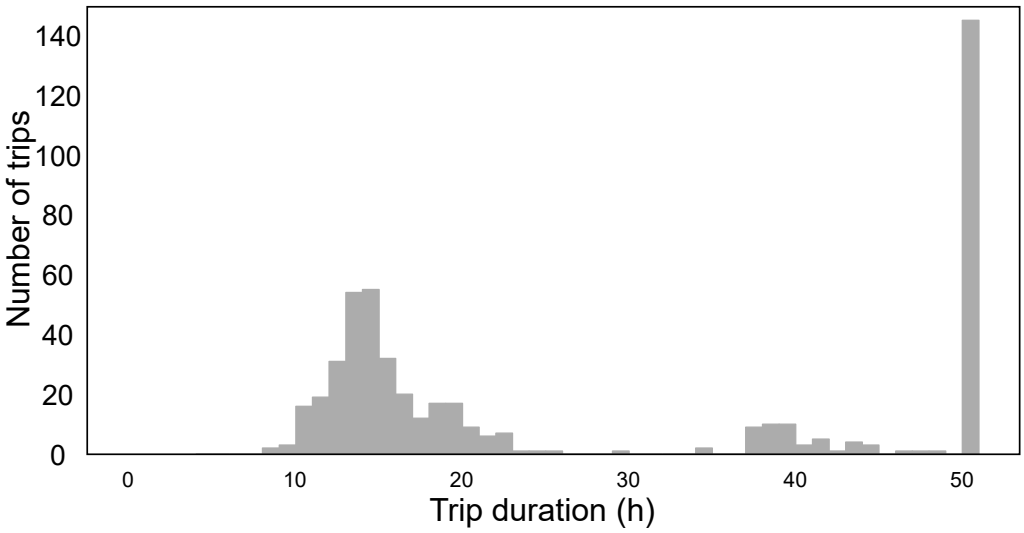


Figure 4.8: The distribution of trip duration of streaked sheawaters.

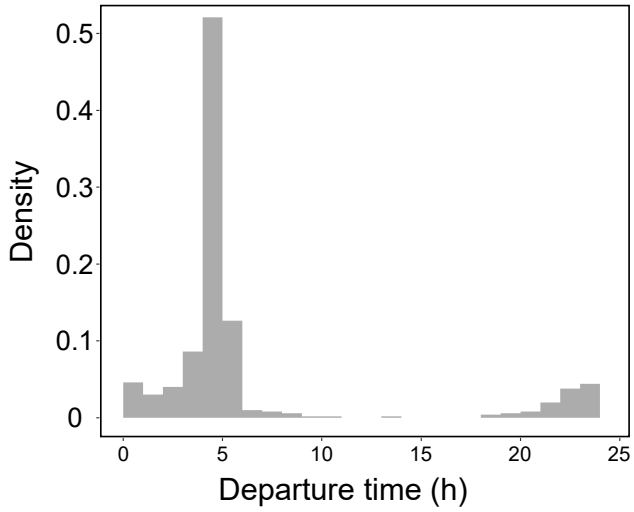
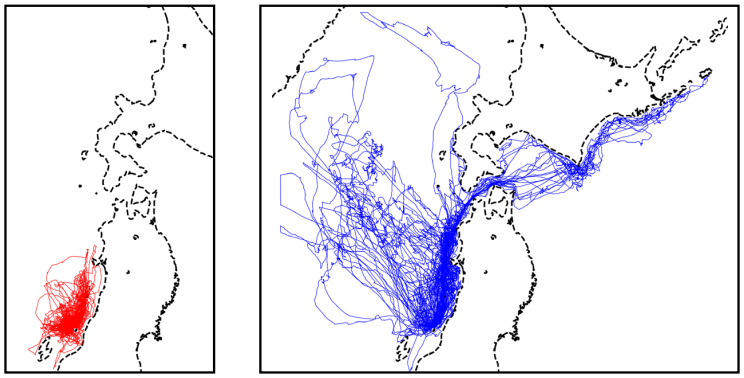


Figure 4.9: The distribution of departure times. The vertical axis shows the normalized frequency.

than half of the shearwaters depart at 04:00 local time. Note that the sunrise time in August and September is between 04:30 and 05:30.



(a) Short-term trip (b) Long-term trip

Figure 4.10: Example trajectories of seabirds. a: Short-term trips. b: Long-term trips.



(a) (b)

Figure 4.11: The picture of animals and devices. a: salmon. b: streaked shearwater.

Figure 4.10 shows the example trips of seabirds used in the experiment. In long-term trips (Figure 4.10b), seabirds fly to Hokkaido for foraging. However, long-term trips consume a lot of energy. In this study, we wanted to find out why the seabirds travel long distances to forage.

4.4.2 Feature extraction

In the feature extraction step, we first extracted initial t hours segments from trajectories by varying t values (e.g., a time-series of GPS coordinates corresponding to 0–3 h of a trip when $t = 3$). After that, features were extracted from the trajectories and envi-

ronmental data contained in each segment (initial t hours). We used the tsfresh library[1] (version: 0.16.0) to extract descriptive statistics (maximum, minimum, median, mean, standard deviation (SD), and range) for each feature time-series. The tsfresh library automatically extracts 763 feature values from each time-series. We concatenated these descriptive statistics to form a feature vector. Each feature vector had a class label; for salmon: the Otsuchi-Kotsuchi class, the Unosumai class, or the Out-of-Bay class; for seabird: short- or long-term trip.

Salmon

We extracted locomotion features such as time-series of speed, acceleration, and displacement from trajectories. We changed the values of t from 30 to 300 minutes to output a series of accuracies.

Streaked shearwater

We calculated time-series of speed, acceleration, orientation, displacement, and first passage time (radius = 100 m, 500 m, 1000 m, and 5000 m) [27], which were widely used to analyze animal trajectories for each initial t h segment. Additionally, we computed the trip distance and orientation between the start and last locations of the initial segment as descriptive statistics. We computed feature vectors by varying the value of t from 1 to 7.5 h.

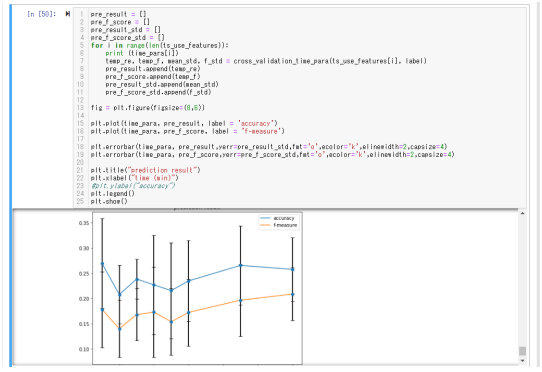
4.4.3 Environment

The tool was implemented in python 3.8, Ubuntu, and all experiments were performed on a computer with a 3.4GHz Intel Core i7 processor and 16GB RAM. Since all the code was written on the jupyter notebook (Figure 4.12).

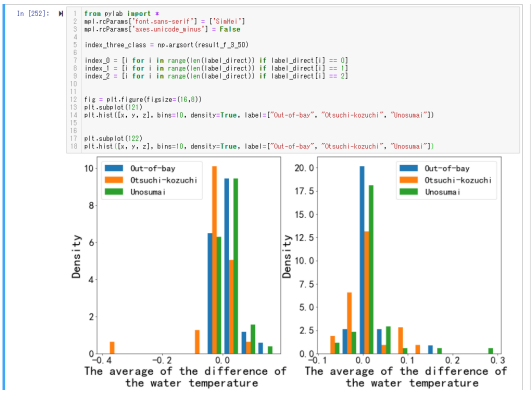
[1] https://github.com/blue-yonder/tsfresh



(a)



(b) Obtain prediction accuracy varying different t value



(c) Analyze important feature's distribution

Figure 4.12: Examples of tools deal with animal behavioral data. (a) Feature extraction. (b) Obtain prediction accuracy varying different t value. (c) Analyze important feature's distribution.

4.4.4 Result

Salmon

Figure 4.13 and Figure 4.14 show the time-series of prediction accurracies and accurracies for each label obtained by the proposed method. The prediction accuracy suddenly increases at $t = 40$ and peaks at $t = 50$ (Figure 4.13). In addition, the prediction accuracy for the Unosumai class suddenly increases at $t = 40$, and the prediction accuracy

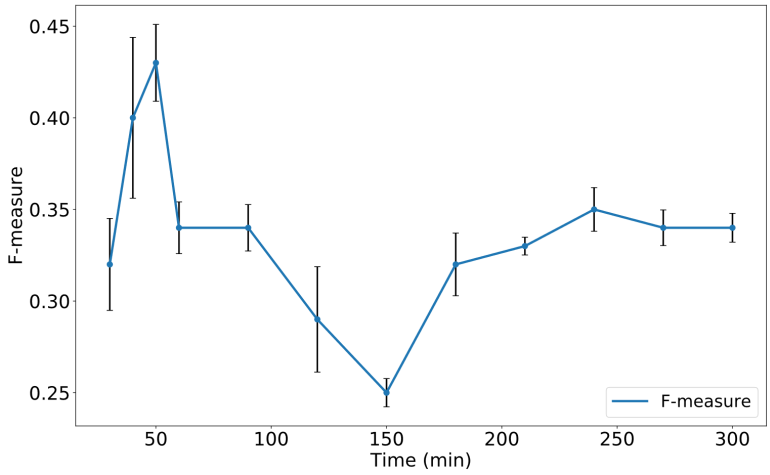


Figure 4.13: The series of accuracies of salmon obtained by our method. The upper and lower whiskers show the maximum and minimum in the cross validation, respectively

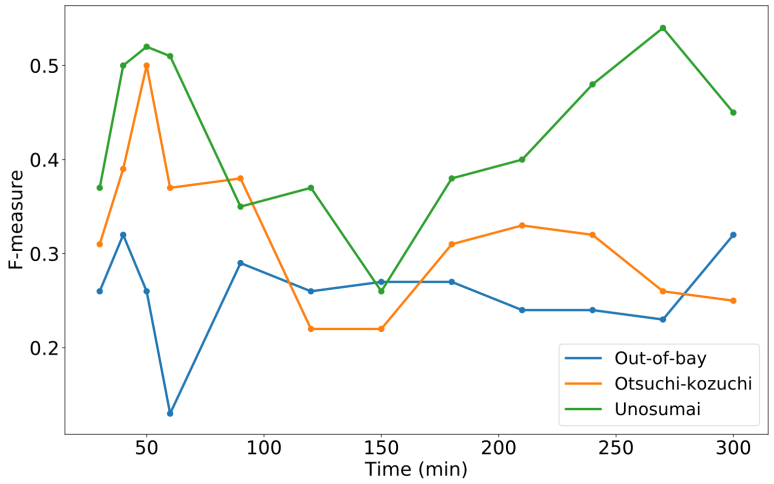
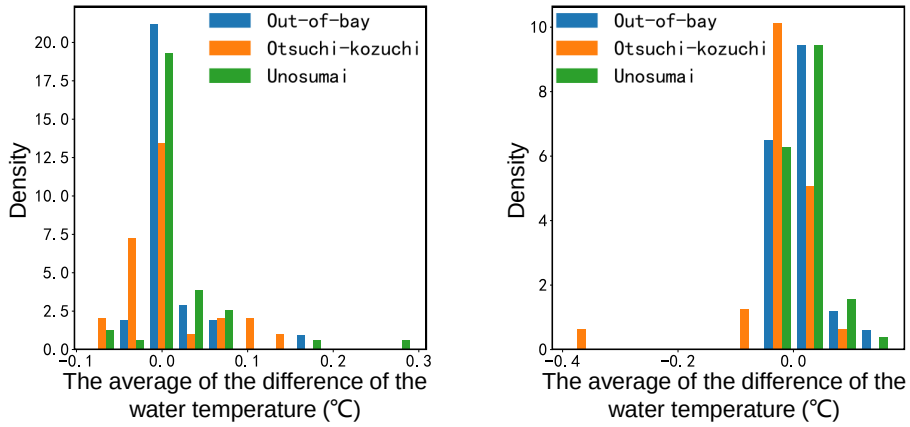


Figure 4.14: The series of accuracies for each class of salmon obtained by our method.

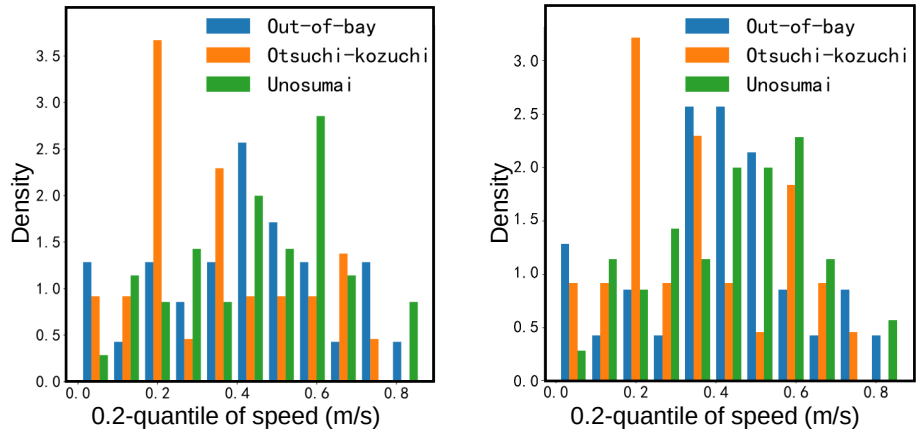
for the Otsuchi-kozuchi class peaks at $t = 50$ (Figure 4.14).

The NaviMine identified the peak at $t = 50$, and output important features and their distributions: "The average of the difference (differential) of the water temperature" (Figure 4.15) and "0.2-quantile of speed" (Figure 4.16).



(a) (b)

Figure 4.15: The distribution of average of the difference (differential) of the water temperature. a: First 30 min data. b: First 50 min data.



(a) (b)

Figure 4.16: The distribution of 0.2-quantile of speed. a: First 30 min data. b: First 40 min data.

Streaked shearwater

Figure 4.17 shows the time-series of prediction accuracies obtained by the proposed method. The prediction accuracy suddenly increases at $t = 5$ (Figure 4.17).

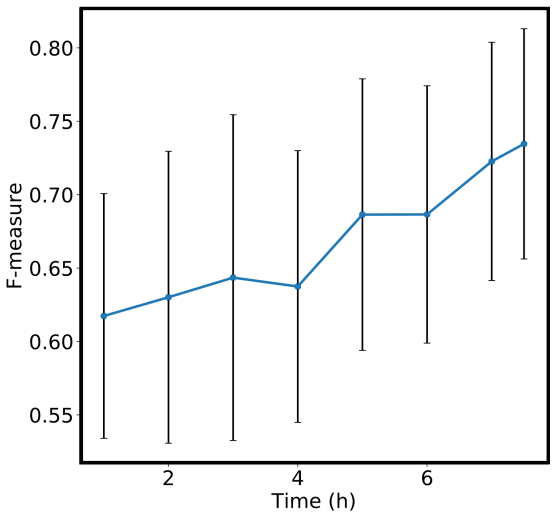


Figure 4.17: The series of accuracies of seabirds obtained by our method. The upper and lower whiskers show the maximum and minimum in the cross validation, respectively

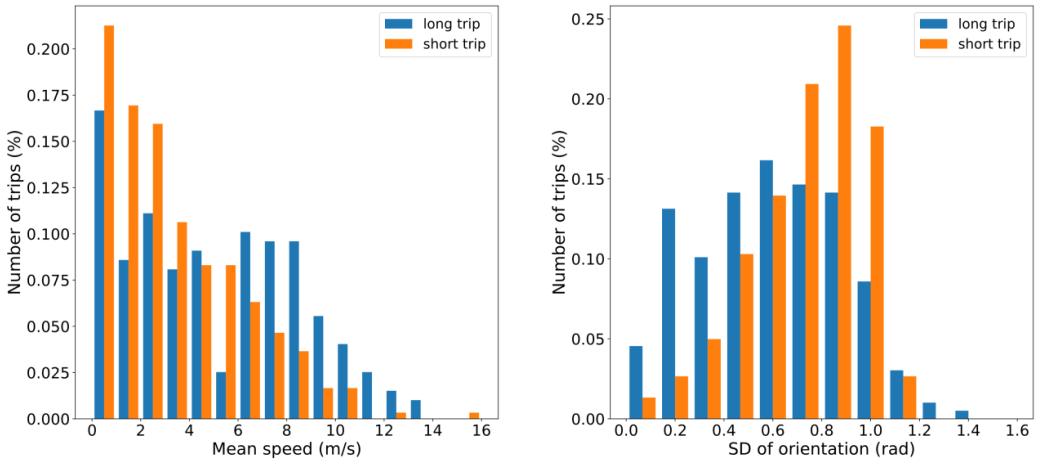
The NaviMine analyzed features between $t = 4$ and $t = 5$, and found out important features at $t = 5$ and output their distributions: "mean speed" (Figure 4.18a) and "SD of orientation" (Figure 4.18b).

4.5 Discussion

Salmon

These results indicated that some clues related to destination finding are hidden around $t = 40, 50$. In addition, these results indicate that characteristic movement features for salmon that would enter the Unosumai river are hidden at $t = 40$. Moreover, characteristic movement features for salmon that would enter the Otsuchi-Kozuchi river may be hidden at $t = 50$.

There is a decreasing trend in water temperature at $t = 30$ compared to the water temperature at $t = 50$ for salmon that would enter the Otsuchi-Kozuchi river (see binning around 0.0 in Figure 4.15). The decrease in water temperature in the bay indicates an increase in river flow, allowing salmon to identify their natal river based on the odor of the water from the river. Therefore, we believe that salmon experiencing a drop in



(a) (b)

Figure 4.18: Analysis results of trips of streaked shearwaters. a: The distribution of mean speed between $t = 4$ and $t = 5$. b: The distribution of SD of orientation between $t = 4$ and $t = 5$.

water temperature (caused by river water) in the early period can identify their natal river and quickly determine their destination. Because water temperature was measured close to the mouth of the Otsuchi-Kozuchi river, the decrease in water temperature could be an important clue for salmon incubated in the Otsuchi-Kozuchi river.

Figure 4.19 shows the relationship between the degree of changes in water temperature before $t = 50$ and the duration of trajectories. The degree of changes in water temperature is defined as the average difference in water temperature (water temperature difference); therefore, the negative value of the degree of changes indicates a decrease in water temperature. As shown in the figure, many salmon belonging to the Otsuchi-Kozuchi class experienced decreased water temperature and entered the Otsuchi-Kozuchi river before 50 hours. This result suggests that salmon entered the river quickly when they were able to identify their natal river due to increased river flow in the early period. Therefore, river odors experienced in the early period can play a crucial role in identifying destinations.

Compared to $t = 30$, the 0.2-quantile of speed of salmon entering the Unosumai

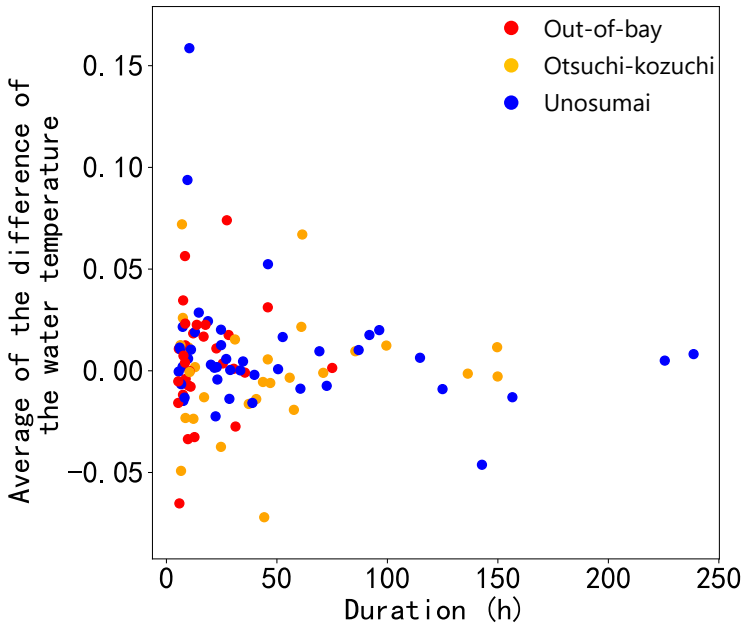


Figure 4.19: The scatter graph showing the relationship between the trajectory duration and the degree of changes in water temperature.

river at $t = 40$ decrease slightly (Figure 4.16, the frequencies of 0.4 and 0.5 increase at $t = 40$; in contrast, the frequencies of higher speed bins decrease at $t = 40$). This result suggests that salmon stay in a certain region(s) at $t = 40$. Figure 4.20 shows the initial 40-minute trajectories belonging to the Unosumai class, indicating that a few salmon (6) stayed in the area close to the estuary of the Unosumai river. From these results, we can assume that salmon belonging to the Unosumai class stay near the mouth of the Unosumai river, using the scent of the river to determine their final destination. This result is consistent with previous studies [66].

Streaked shearwater

The highest increase in series of accuracies was found between the 4th and 5th hour (Figure 4.17), indicating that the segments between $t = 4$ and $t = 5$ may contain important information about the decision-making. . We used GLMM to analyze whether important descriptive statistics differed between $t = 4$ and $t = 5$ during short- and long-term trips. The mean speed (GLMM, $t = -6.548$, $P < 0.0001$, Figure 4.18a) and

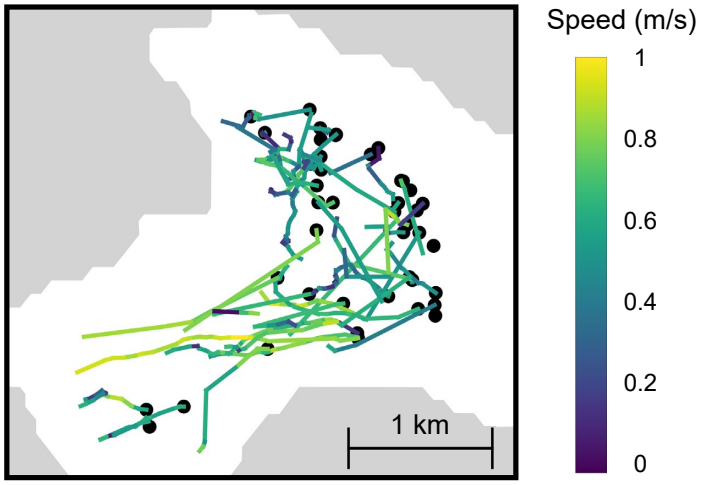
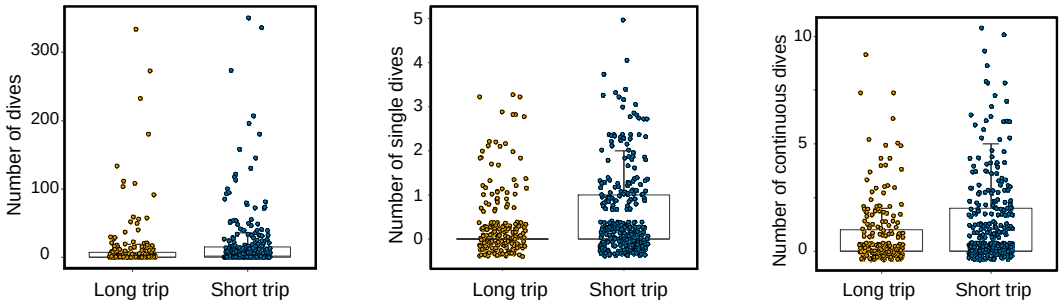


Figure 4.20: Initial 40-min trajectories of salmon belonging to the Unosumai class.

SD of orientation (GLMM, $t = -8.775$, $P < 0.0001$, Figure 4.18b) were significantly different between short- and long-term trips at 4–5 h. The average speed in long-term trips was faster than that in short-term trips (Figure 4.18a), and the SD of the orientation in long-term trips was less than that in short-term trips (Figure 4.18b). Therefore, streaked shearwaters conducting long-term trips changed flight direction less frequently than those conducting short-term trips, while the seabirds that took short-term trips changed directions frequently.

We believe that seabirds frequently change their orientation (large SD of orientation) indicates foraging activities. Therefore, we calculated dive-related features from bathymetric data, including the number of dives, the number of single dives, and the number of continuous dives. A single dive is an isolated dive when there is no other diving activity within 5 min before and after this diving, and a continuous dive involves two or more diving activities, and the time intervals between consecutive diving activities are less than 5 min. The number of dives did not differ between short- and long-term trips (GLMM, $t = -1.704$, $P = 0.0884$, Figure 4.21a). The number of single dives differed significantly among the trip types; shearwaters that undertook short-term trips dived more (GLMM, $t = -2.578$, $P < 0.01$, Figure 4.21b). The number of continuous dives also differed significantly among the trip types; shearwaters that undertook short-term trips dived more (GLMM, $t = -3.161$, $P < 0.01$, Figure 4.21c).

Seabirds determined the type of trips they took at an early period (5 h), as high ac-



(a) Number of dives (b) Number of single dives (c) Number of continuous dives

Figure 4.21: Box plots of dive-related features. a: Box plot of number of dives in short- and long-term trips for the first 5 h of trips (GLMM, $t = -1.704$, $P = 0.09$). b: Box plot of number of single dives in short- and long-term trips for the first 5 h of trips (GLMM, $t = -2.578$, $P < 0.01$). c: Box plot of number of continuous dives in short- and long-term trips for the first 5 h of trips (GLMM, $t = -3.161$, $P < 0.01$).

curacy (70%) in predicting trip type was observed only from the first 5 hours of the trip. Seabirds on short-term trips seemed to focus on foraging activities during the initial hours of trips (5 h), staying in specific areas for long periods of time and frequently changing their flight directions (Figures 4.18b and 4.21c). Seabirds performed short-term trips made more frequent single dives (i.e., searching for prey underwater) and continuous dives (i.e., foraging in prey areas) during the first 5 h than seabirds performing long-term trips. These results suggest that seabirds may make the decision to leave based on such a "win-stay, lose-switch" strategy [11, 85]. Since fish are active in the morning, note that most of the seabirds departed from the colony around 04:00 (Figure 4.9), if a seabird cannot catch fish in the initial 5 hours, the seabird seems to select a long-term trip.

4.6 Conclusion

This study proposed a data mining tool for analyzing trajectory data of moving objects. The tool was mainly proposed based on our hypothesis that animals will determine their

future behavior based on past events (e.g., foraging activities). Therefore, we used the initial t time trajectory of the animals and the data of their surroundings to predict their following behavior. If we can predict the animals' behavior with high accuracy, we can assume that the factors affecting the animals' decisions are within the initial t time. To find the exact t, we first predicted the animal's behavior using every possible value of t to obtain a series of prediction accuracies. Second, the tool detected three important timings by analyzing the accuracy series. We analyzed the distribution of the features under each label within the important timings to find the factors associated with the animal's decision. We applied the tool to salmon and seabirds, and discussions with biologists revealed new findings related to navigation by these animals. Specifically, the tool helps find i) timings of decision making from long-duration behavioral data and ii) sensor data differences between different classes focusing on the detected timings. The tool provides a new way to analyze animal decision-making, and the tool does not require knowledge of the species being studied; therefore, it can be applied to many species. Note that, there are other tools available for big data analysis, such as data search tools (e.g., Elasticsearch (ES)) and business intelligence tools (BI, e.g., PowerBI and Tableau). ES allows quick access to data from documents and real-time data analysis, while the BI tools are complete solutions for effectively integrating existing data in an enterprise, providing fast and accurate reporting and decision basis to help enterprises make informed business decisions. In contrast, the proposed method does not focus on the speed of data analysis, but automatically digs deeper into the critical factors related to the animal's decision-making by employing classifiers that predict animals' future behaviors.

Chapter 5

Summary

5.1 Summary of contributions

In this thesis, we described how to detect important information (e.g., sensor modalities and timings) from big animal behavioral data to support biologists better understand animal navigation.

In Chapter 1, we introduced the rapidly changing science and technology that provide biologists with more detailed data for analyzing the navigation of animals. At the same time, the large amount of collected data has created problems that prevent biologists from performing their analysis effectively, such as a large number of sensor modalities and long recording periods. In the task of analyzing frequent co-occurrence of behavioral modes, we proposed a method to efficiently find important sensor modalities. In the task of analyzing decision-making of animals, we proposed a method to find a moment of decision-making.

Analyzing frequent co-occurrence behavioral modes can help us understand the relationship between animals' behavior and their external or internal environment. Different behavioral modes exist in different sensor modalities, for example, foraging and cruising modes can be extracted from speed time-series, and relaxation and tension modes can be extracted from heart rate data. Time-series segmentation and clustering methods have been used to extract behavioral modes in prior studies. However, parameters (sensor modalities and clustering parameters) used in the previous methods were selected by

biologists based on their past experiences. In contrast, to find frequent co-occurrence behavioral modes, this study analyzed all possible behavioral modes and parameters, taking substantial computational time. Therefore, in Chapter 2, we proposed a frequent co-occurrence behavioral modes detection method that enables high-speed clustering and finds frequent co-occurrence behavioral modes. In the proposed method, we first segmented the time-series using SAX, which is a symbolization method, to convert a series of numerical values into a series of symbols. After segmenting the time series, we performed spectral clustering to cluster the segments. We proposed two ideas for reducing the clustering time: 1) we reuse the previous results when segmenting with SAX; 2) when performing spectral clustering, we merge segments with the same symbol into one segment. We applied the proposed method to trajectory data from bats to analyze their foraging behaviors. After discussing the results with biologists, we found that bats use their uropatagium to slow down before capturing insects, which in turn allows for better control of the body.

We continued our study on frequent co-occurrence behavioral modes in Chapter 3. Since there are individual differences between animals, we focused on detecting frequent co-occurrence behavioral modes that differ significantly between groups (e.g., male vs. female groups) in this chapter. This means that we introduced comparative analysis into the method introduced in Chapter 2. By calculating the differences in the time correlations of co-occurred behavioral modes between groups, we were able to identify co-occurrence behavioral modes that differ significantly between groups. We applied the proposed method to trajectory data from streaked shearwaters (seabirds) to analyze how sex-specificity (e.g., body size, roles in breeding) might affect their behavior. The experiment demonstrated that our proposed method could successfully extract hidden knowledge from actual animal behavioral data, showing the contributions of our method to the computer science and biology domains. Because the method is designed for any types of time-series, we believe that the method can be applied to various applications such as analysis of violations in driving and time-series gene expression.

In Chapter 4, we developed a tool to identify the timings and clues associated with animal decision-making. Finding clues related to decision-making is important since it can help us understand the navigation mechanisms of animals. However, it is difficult for biologists to find out clues related to decision-making. First, the data is collected

for a long time, making it difficult to detect when an animal makes a decision. Second, a lot of sensor modalities are recorded, making it difficult to find out what clues do animals use to determine their destination. The tool could find the timing of animal decision-making through behavioral prediction and factors associated with decision-making by comparing the distributions of features across labels. We applied the tool to salmon and seabird data,and the tool enabled us to discover new knowledge from actual data. Specifically, the tool helps find i) timings of decision making from long-duration behavioral data and ii) sensor data differences between different classes focusing on the detected timings. Note that, there are other tools available for big data analysis, such as data search tools (e.g., Elasticsearch (ES)) and business intelligence tools (BI, e.g., PowerBI and Tableau). ES allows quick access to data from documents and real-time data analysis, while the BI tools are complete solutions for effectively integrating existing data in an enterprise, providing fast and accurate reporting and decision basis to help enterprises make informed business decisions. In contrast, the proposed method does not focus on the speed of data analysis, but automatically digs deeper into the critical factors related to the animal's decision-making by employing classifiers that predict animals' future behaviors.

In summary, our study contributed to detect frequent co-occurrence behavioral modes and the co-occurrence behavioral modes that differ significantly between groups, as well as to identify the crucial timings and clues related to animals' decision-making. By applying the techniques to different animals, we could obtain new insights. Therefore, our approach has been proven to help biologists detect important information from long period multi-modal sensor data.

5.2 Future work

Although the goal of this study is to help biologists analyze animal navigation effectively, some areas could still be studied in depth.

Fieldwork. Our results were based on the analysis of behavioral data collected from the animal in advance. We need to verify our conclusions by comparing our findings with the actual behavior of animals. For this purpose, for example, we plan to attach sensors

with cameras to the animals studied in our thesis and validate our findings by recording videos of co-occurrence behavioral modes when they happen.

In-depth analysis of salmon. In Chapter 4, we have found that river odors experienced early period play an essential role in identifying the destination of salmon. When salmon are able to identify their natal river due to increased early river flow, they quickly enter the river. However, Figure 4.19 shows that salmon belonging to the Otsuchi-Kozuchi class entered the river before 50 hours, indicating that there is a delay between identified and entered the natal river. Therefore, as a part of our future work, we plan to conduct an in-depth analysis of salmon movements related to the water temperature experienced in the early period. The first step in our in-depth study is to verify whether early changes in water temperature played an essential role in the salmon's destination decisions. We plan to mount thermometers at the mouths of both rivers to record changes in water temperature, attach loggers with temperature acquisition, and video recording capabilities to the salmon to record their surrounding water temperature in real-time using multi-modal sensor devices developed in our research group [45]. After the salmon are captured, the tool proposed in Chapter 4 will be applied to the salmon entering the Unosumai River to verify whether changes in water temperature influence the salmon's destination decisions. Second, for salmon entering the Unosumai river, we compare the time of salmon entering the natal river with the time of decision-making to detect if there is also a delay between identified and entered the natal river. By analyzing the recorded video and trajectories, we analyze the behavior of salmon from the time they make their decision to the time they swim to the mouth of the natal river.

Acknowledgement

Time flies, it is now my sixth year in Japan, and there are only a few months left for my PhD career. On the occasion of completing my PhD thesis, I would like to express my most sincere gratitude to my teachers, family, colleagues, and friends who have been caring for my academic and scientific research for a long time.

First and foremost, I would like to sincerely acknowledge my instructive professor, Professor Takuya Maekawa, for his careful teaching over the past five years. Prof. Maekawa is a serious and responsible instructor, and when I encountered difficulties, he would always discuss and consider solutions with me. No matter how late or busy he was, Prof. Maekawa always replied to me in time, and I was grateful and warm when I saw his emails in the early morning. In the process of completing my thesis, Prof. Maekawa helped me revise everything, from the innovative expression of the thesis, chapter structure to the refinement of each sentence, from each word of the abstract to the format of each reference. Without His advice and guidance, this thesis would not have completed. I have significantly benefited from Prof. Maekawa's rigor and care, and it is an honor to be his student.

I would like to express my sincere gratitude to my adviser, Professor Takahiro Hara, for choosing me over many other applicants and allowing me to come to Osaka University to pursue my study at this excellent institution. He is rigorous and severe in research and has clear thinking. He can always explain complex matters in two or three sentences. He is very approachable in life and provided a lot of help to me when I first arrived in Japan. It is a lifelong blessing to be able to enter Hara laboratory. I will remember his teachings and continue to learn and improve.

I would like to express my sincere gratitude to the committee members for my thesis, Professor Makoto Onizuka and Professor Shinji Shimojo, for their comments that made

this thesis even better. I would like to thank Professor Yasuyuki Matsushita and Professor Toru Fujiwara, and all the professors at the Department of Multimedia Engineering of the Graduate School of Information Science and Technology of Osaka University, for their supervision and guidance.

I would like to sincerely appreciate Professor Daichi Amagata for his unfailing help in my life and research during my time in the lab.

I would like to express my sincere gratitude to Professor Shizuko Hiryu at Faculty of Life and Medical Sciences Department of Biomedical Information of Doshisha University, Professor Ken Yoda at Graduate School of Environmental Studies of Nagoya University, and Professor Takashi Kitagawa at Atmosphere and Ocean Research Institute of Tokyo University, for their help in my research. Their rich expertise made the research effective and efficient.

I would like to express my sincere gratitude to Mr. Masayuki Fujiwara from Daikin Industries, for his help during my tenure as a research assistant. In the beginning, I had no idea about what I was going to do, and it was only under his careful guidance that I was able to adapt to the project quickly.

I would like to sincerely thank Dr. Boqi Gao, and Mr. Shunhei Hayashida for providing me with great help in my research as well as in my life when I first came to Japan, and helping me integrate into the lab quickly. I would also like to thank the past and present members of my research group, Dr. Tatsuya Nakamura, Dr. Syunya Nishio, Mr. Tomoya Nakatani, Mr. Naoya Yoshimura, Mr. Dissanayake Thilina Madushan, Mr. Daiki Higashide, Mr. Shinya Kamiya, Mr. Hiroki Tsujimoto, Mr. Kim Heng, Mr. Zesheng Cai, Mr. Kenta Murakami, Ms. Yuka Tanno, Mr. Yuuki Nishino, Mr. Tomoya Moritoh and Ms. Teoh Tze Chuin. I would like to thank them for the help they provided to my research. On behalf of a member of Hara laboratory, every member from the 4th-year bachelor students to the most senior doctoral students in the laboratory, has provided me a wonderful experience for a couple of years here. I would like to thank all the students and professors at Systems Science of Bio-Navigation, and I was able to interact with students and professors from different fields and learn additional knowledge. I would like to express my sincere gratitude to the secretaries of Hara laboratory, Ms. Kyoko Shimomura and Ms. Makiko Higashinaka. It was because they were taking care of the daily chores that I could concentrate on my research. Thank

you to the Chinese who were and are studying at Hara Research, Mr. Cheng Chen, Mr. Bunki Cao, Mr. Yuan Lyu, Mr. Hanxin Wang, Mr. Zhi Li, Mr. Heng Zhou, Ms. Qingxin Xia, Mr. Yuchen Ji, and Ms. Yue Zhao. It is the communication with you that makes me no longer feel that this is a foreign country.

I would like to express my sincere gratitude to my parents for their constant companionship, trust, understanding, and support. Thank you for your kindness in raising me. Your education and guidance are the most solid foundation for me to obtain my PhD degree.

Thank you to everyone who has helped and cared for me. I know that I could never have achieved anything on my own. Thank you to those who have helped me to improve a little. Thank you to those who cared for me and gave me some warmth when I was helpless.

I want to thank the perseverance, indomitable myself. Your struggle and hard work eventually led to a PhD degree. I hope you have dreams in your heart, light in your eyes, and expectations for the future. In the future, when you are confused and disillusioned, please open this thesis again, and you will still be the same persevering and unstoppable teenager.

Be positive and move on.

REFERENCE

[1] T. Adam, C. A. Griffiths, V. Leos-Barajas, E. N. Meese, C. G. Lowe, P. G. Blackwell, D. Righton, and R. Langrock. Joint modelling of multi-scale animal movement data using hierarchical hidden markov models. *Methods in Ecology and Evolution*, 10(9):1536–1550, 2019.

[2] S. Aghabozorgi, A. S. Shirkhorshidi, and T. Y. Wah. Time-series clustering - a decade review. *Information Systems*, 53:16–38, 2015.

[3] S. Aghabozorgi and T. Y. Wah. Clustering of large time series datasets. *Intelligent Data Analysis*, 18(5):793–817, 2014.

[4] S. Åkesson, J. Boström, M. Liedvogel, and R. Muheim. Animal navigation. *Animal Movement Across Scales*, 21:151–178, 2014.

[5] D. Arthur and S. Vassilvitskii. k-means++: The advantages of careful seeding. In *Proceedings of the 18th Annual ACM-SIAM Symposium on Discrete Algorithms*, pages 1027–1035, 2007.

[6] D. Bates, M. Mächler, B. Bolker, and S. Walker. Fitting linear mixed-effects models using lme4. *Journal of Statistical Software, ARTICLEs*, 67(1):1–48, 2015.

[7] A. Bennison, S. Bearhop, T. W. Bodey, S. C. Votier, W. J. Grecian, E. D. Wakefield, K. C. Hamer, and M. Jessopp. Search and foraging behaviors from movement data: a comparison of methods. *Ecology and Evolution*, 8(1):13–24, 2018.

[8] N. E. Breslow and D. G. Clayton. Approximate inference in generalized linear mixed models. *Journal of the American Statistical Association*, 88(421):9–25, 1993.

[9] R. M. Bryce and K. B. Sprague. Revisiting detrended fluctuation analysis. *Scientific Reports*, 2:315, 2012.

[10] T. Burt, R. Holland, and T. Guilford. Further evidence for visual landmark involvement in the pigeon's familiar area map. *Animal Behaviour*, 53(6):1203–1209, 1997.

[11] G. Carroll, R. Harcourt, B. J. Pitcher, D. Slip, and I. Jonsen. Recent prey capture experience and dynamic habitat quality mediate short-term foraging site fidelity in a seabird. *Proceedings of the Royal Society B: Biological Sciences*, 285(1883):20180788, 2018.

[12] D. M. Christopher, R. Prabhakar, and S. Hinrich. Introduction to information retrieval. *An Introduction To Information Retrieval*, 151:177, 2008.

[13] J. G. Clapp, J. D. Holbrook, and D. J. Thompson. Gpseqclus: An r package for sequential clustering of animal location data for model building, model application and field site investigations. *Methods in Ecology and Evolution*, 12(5):787–793, 2021.

[14] T. A. Clay, S. Oppel, J. L. Lavers, R. A. Phillips, and M. d. L. Brooke. Divergent foraging strategies during incubation of an unusually wide-ranging seabird, the murphy's petrel. *Marine Biology*, 166(1):1–14, 2019.

[15] J. F. Cohn, J. Campoy, Z. Ambadar, and F. D. la Torre. Temporal segmentation of facial behavior. In *Proceedings of the 11th IEEE International Conference on Computer Vision*, pages 1–8, 2007.

[16] T. S. Collett. The use of visual landmarks by gerbils: reaching a goal when landmarks are displaced. *Journal of Comparative Physiology. A, Sensory, Neural, and Behavioral Physiology*, 160(1):109——113, January 1987.

[17] T. S. Collett, M. Collett, and R. Wehner. The guidance of desert ants by extended landmarks. *Journal of Experimental Biology*, 204(9):1635–1639, 2001.

[18] L. Conradt and T. J. Roper. Deciding group movements: where and when to go. *Behavioural Processes*, 84(3):675–677, 2010.

[19] D. R. Cox. The regression analysis of binary sequences. *Journal of the Royal Statistical Society: Series B (Methodological)*, 20(2):215–232, 1958.

[20] M. L. Damiani, H. Issa, G. Fotino, M. Heurich, and F. Cagnacci. Introducing 'presence'and 'stationarity index'to study partial migration patterns: an application of a spatio-temporal clustering technique. *International Journal of Geographical Information Science*, 30(5):907–928, 2016.

[21] N. de Weerd, F. van Langevelde, H. van Oeveren, B. A. Nolet, A. Kölzsch, H. H. Prins, and W. F. de Boer. Deriving animal behaviour from high-frequency gps: tracking cows in open and forested habitat. *Plos one*, 10(6):e0129030, 2015.

[22] L. M. Dill. Animal decision making and its ecological consequences: the future of aquatic ecology and behaviour. *Canadian Journal of Zoology*, 65(4):803–811, 1987.

[23] A. Dittman and T. Quinn. Homing in pacific salmon: mechanisms and ecological basis. *Journal of Experimental Biology*, 199(1):83–91, 1996.

[24] A. S. Dunlap, M. E. Nielsen, A. Dornhaus, and D. R. Papaj. Foraging bumble bees weigh the reliability of personal and social information. *Current Biology*, 26(9):1195–1199, 2016.

[25] S. T. Emlen. Migratory orientation in the indigo bunting, passerina cyanea: part i: evidence for use of celestial cues. *The Auk*, 84(3):309–342, 1967.

[26] S. T. Emlen. Migratory orientation in the indigo bunting, passerina cyanea. part ii: mechanism of celestial orientation. *The Auk*, 84(4):463–489, 1967.

[27] P. Fauchald and T. Tveraa. Using first-passage time in the analysis of area-restricted search and habitat selection. *Ecology*, 84(2):282–288, 2003.

[28] P. Fauchald and T. Tveraa. Using first-passage time in the analysis of area-restricted search and habitat selection. *Ecology*, 84(2):282–288, 2003.

[29] E. Fujioka, I. Aihara, S. Watanabe, M. Sumiya, S. Hiryu, J. A. Simmons, H. Riquimaroux, and Y. Watanabe. Rapid shifts of sonar attention by pipistrellus

abramus during natural hunting for multiple prey. *The Journal of the Acoustical Society of America*, 136(6):3389–3400, 2014.

[30] A. Gionis and H. Mannila. Finding recurrent sources in sequences. In *Proceedings of the 7th Annual International Conference on Research in Computational Molecular Biology*, pages 123–130. ACM, 2003.

[31] A. Gomez-Marin, J. J. Paton, A. R. Kampff, R. M. Costa, and Z. F. Mainen. Big behavioral data: psychology, ethology and the foundations of neuroscience. *Nature Neuroscience*, 17:1455–1462, 2014.

[32] L. Hagen and A. B. Kahng. New spectral methods for ratio cut partitioning and clustering. *IEEE Transactions on Computer-Aided Design of Integrated Circuits and Systems*, 11(9):1074–1085, 2006.

[33] L. Hansen, N. Jonsson, and B. Jonsson. Oceanic migration in homing atlantic salmon. *Animal Behaviour*, 45:927–941, 05 1993.

[34] J. A. Helmuth, C. J. Burckhardt, P. Koumoutsakos, U. F. Greber, and I. F. Sbalzarini. A novel supervised trajectory segmentation algorithm identifies distinct types of human adenovirus motion in host cells. *Journal of Structural Biology*, 159(3):347–358, 2007.

[35] Y. D. Heman-Ackah, D. D. Michael, M. M. Baroody, R. Ostrowski, J. Hillenbrand, R. J. Heuer, M. Horman, and R. T. Sataloff. Cepstral peak prominence: A more reliable measure of dysphonia. *Annals of Otology, Rhinology & Laryngology*, 112(4):324–333, 2003.

[36] M. C. Hernández, Á. Navarro-Castilla, and I. Barja. Wood mouse feeding effort and decision-making when encountering a restricted unknown food source. *Plos one*, 14(6):e0212716, 2019.

[37] S. Hochreiter and J. Schmidhuber. Long short-term memory. *Neural Computation*, 9(8):1735–1780, 1997.

[38] A. K. Jain, M. N. Murty, and P. J. Flynn. Data clustering: A review. *ACM Computing Surveys*, 31(3):264–323, sep 1999.

[39] N. W. Jankowski. Exploring e-science: an introduction. *Journal of Computer-Mediated Communication*, 12(2):549–562, 01 2007.

[40] A. R. Johnson, J. A. Wiens, B. T. Milne, and T. O. Crist. Animal movements and population dynamics in heterogeneous landscapes. *Landscape Ecology*, 7(1):63–75, 1992.

[41] M. J. Johnson and A. S. Willsky. Bayesian nonparametric hidden semi-markov models. *Journal of Machine Learning Research*, 14(1):673–701, 2013.

[42] G. Jones and J. Rayner. Flight performance, foraging tactics and echolocation in free-living Daubenton's bats Myotis daubentoni (Chiroptera: Vespertilionidae). *Journal of Zoology*, 215(1):113–132, 1988.

[43] G. Jones and J. Rayner. Flight performance, foraging tactics and echolocation in the trawling insectivorous bat Myotis adversus (Chiroptera: Vespertilionidae). *Journal of Zoology*, 225(3):393–412, 1991.

[44] A. K. Kalan and C. Boesch. Audience effects in chimpanzee food calls and their potential for recruiting others. *Behavioral Ecology and Sociobiology*, 69:1701–1712, 08 2015.

[45] J. Korpela, H. Suzuki, S. Matsumoto, Y. Mizutani, M. Samejima, T. Maekawa, J. Nakai, and K. Yoda. Machine learning enables improved runtime and precision for bio-loggers on seabirds. *Communications biology*, 3(1):1–9, 2020.

[46] G. Kramer. Weitere analyse der faktoren, welche die zugaktivität des gekäfigten vogels orientieren. *Naturwissenschaften*, 37(16):377–378, 1950.

[47] G. Kramer. Experiments on bird orientation and their interpretation. *Ibis*, 94(2):265–285, 1952.

[48] R. J. Larsen and M. L. Marx. *An introduction to mathematical statistics*. Prentice Hall, 2005.

[49] L. Li and B. A. Prakash. Time series clustering: Complex is simpler! In *Proceedings of the 28th International Conference on International Conference on Machine Learning*, pages 185–192, 2011.

[50] T. W. Liao. Clustering of time series data - a survey. *Pattern Recognition*, 38(11):1857–1874, 2005.

[51] J. Lin, E. Keogh, L. Wei, and S. Lonardi. Experiencing SAX: a novel symbolic representation of time series. *Data Mining and Knowledge Discovery*, 15(2):107–144, 2007.

[52] C.-Y. Liou, W.-C. Cheng, J.-W. Liou, and D.-R. Liou. Autoencoder for words. *Neurocomputing*, 139:84–96, 2014.

[53] C.-Y. Liou, J.-C. Huang, and W.-C. Yang. Modeling word perception using the elman network. *Neurocomputing*, 71(16-18):3150–3157, 2008.

[54] J. Liu, C. Wang, M. Danilevsky, and J. Han. Large-scale spectral clustering on graphs. In *Proceeding of the 23rd International Joint Conference on Artifcial Intelligence*, pages 1486–1492, 2013.

[55] D. Lusseau and L. Conradt. The emergence of unshared consensus decisions in bottlenose dolphins. *Behavioral Ecology and Sociobiology*, 63(7):1067–1077, 2009.

[56] H. Lutkepohl. Handbook of matrices. *Computational Statistics and Data Analysis*, 25(2):243, 1997.

[57] T. Maekawa, K. Ohara, Y. Zhang, M. Fukutomi, S. Matsumoto, K. Matsumura, H. Shidara, S. J. Yamazaki, R. Fujisawa, K. Ide, et al. Deep learning-assisted comparative analysis of animal trajectories with DeepHL. *Nature Communications*, 11(5316), 2020.

[58] P. Malhotra, A. Ramakrishnan, G. Anand, L. Vig, P. Agarwal, and G. Shroff. Lstm-based encoder-decoder for multi-sensor anomaly detection. *arXiv preprint arXiv:1607.00148*, 2016.

[59] S. Matsumoto, T. Yamamoto, M. Yamamoto, C. B. Zavalaga, and K. Yoda. Sex-related differences in the foraging movement of streaked shearwaters *Calonectris leucomelas* breeding on awashima island in the sea of japan. *Ornithological Science*, 16(1):23–32, 2017.

[60] K. McComb, G. Shannon, S. M. Durant, K. Sayialel, R. Slotow, J. Poole, and C. Moss. Leadership in elephants: the adaptive value of age. *Proceedings of the Royal Society B: Biological Sciences*, 278(1722):3270–3276, 2011.

[61] J. M. McNamara, Z. Barta, M. Klaassen, and S. Bauer. Cues and the optimal timing of activities under environmental changes. *Ecology Letters*, 14(12):1183–1190, 2011.

[62] F. Mörchen, A. Ultsch, and O. Hoos. Extracting interpretable muscle activation patterns with time series knowledge mining. *International Journal of Knowledge-based and Intelligent Engineering Systems*, 9(3):197–208, 2005.

[63] H. Mouritsen and T. Ritz. Magnetoreception and its use in bird navigation. *Current Opinion in Neurobiology*, 15(4):406–414, 2005.

[64] R. Nathan, W. M. Getz, E. Revilla, M. Holyoak, R. Kadmon, D. Saltz, and P. E. Smouse. A movement ecology paradigm for unifying organismal movement research. *Proceedings of the National Academy of Sciences*, 105(49):19052–19059, 2008.

[65] A. Y. Ng, M. I. Jordan, and Y. Weiss. On spectral clustering: analysis and an algorithm. *Advances in Neural Information Processing Systems*, pages 849—-856, 04 2002.

[66] S. Nobata, T. Kitagawa, K. Tanaka, K. Komatsu, Y. Aoki, K. Sato, Y. Takei, and S. Hyodo. Spreading of river water guides migratory behavior of homing chum salmon *Oncorhynchus keta* in otsuchi bay, a narrow inlet with multiple river flows. *Zoological Science*, 36(6):449–457, 2019.

[67] U. M. Norberg. *Vertebrate flight: mechanics, physiology, morphology, ecology and evolution*, volume 27. Springer Science & Business Media, 2012.

[68] S. M. Oksanen, M. Niemi, M. P. Ahola, and M. Kunnasranta. Identifying foraging habitats of baltic ringed seals using movement data. *Movement Ecology*, 3(1):33, 2015.

[69] S. Oppel, A. Beard, D. Fox, E. Mackley, E. Leat, L. Henry, E. Clingham, N. Fowler, J. Sim, J. Sommerfeld, et al. Foraging distribution of a tropical seabird supports ashmole's hypothesis of population regulation. *Behavioral Ecology and Sociobiology*, 69(6):915–926, 2015.

[70] I. P. Owens and I. R. Hartley. Sexual dimorphism in birds: why are there so many different forms of dimorphism? *Proceedings of the Royal Society of London. Series B: Biological Sciences*, 265(1394):397–407, 1998.

[71] G. Palshikar et al. Simple algorithms for peak detection in time-series. In *Proceedings of the 1st International Conference Advanced Data Analysis, Business Analytics and Intelligence*, volume 122, 2009.

[72] T. D. Pereira, D. E. Aldarondo, L. Willmore, M. Kislin, S. S.-H. Wang, M. Murthy, and J. W. Shaevitz. Fast animal pose estimation using deep neural networks. *Nature Methods*, 16(1):117–125, 2019.

[73] A. Pérez-Escudero, J. Vicente-Page, R. C. Hinz, S. Arganda, and G. G. de Polavieja. idtracker: tracking individuals in a group by automatic identification of unmarked animals. *Nature Methods*, 11:743–748, 2014.

[74] R. A. Phillips, J. C. Xavier, and J. P. Croxall. Effects of satellite transmitters on albatrosses and petrels. *The Auk*, 120(4):1082–1090, 2003.

[75] T. P. Quinn and E. L. Brannon. The use of celestial and magnetic cues by orienting sockeye salmon smolts. *Journal of Comparative Physiology*, 147(4):547–552, 1982.

[76] N. C. Rattenborg, B. Voirin, S. M. Cruz, R. Tisdale, G. Dell'Omo, H.-P. Lipp, M. Wikelski, and A. L. Vyssotski. Evidence that birds sleep in mid-flight. *Nature Communications*, 7:1–9, 2016.

[77] B. Rensch. Die abhängigkeit der relativen sexualdifferenz von der körpergrösse. *Bonner Zoologische Beiträge*, 1:58–69, 1950.

[78] Y. S. Resheff, S. Rotics, R. Harel, O. Spiegel, and R. Nathan. Accelerater: a web application for supervised learning of behavioral modes from acceleration measurements. *Movement Ecology*, 2(1):27, 2014.

[79] H.-U. Schnitzler, E. Kalko, L. Miller, and A. Surlykke. The echolocation and hunting behavior of the bat, Pipistrellus kuhli. *Journal of Comparative Physiology A: Neuroethology, Sensory, Neural, and Behavioral Physiology*, 161(2):267–274, 1987.

[80] K. Shiomi, K. Yoda, N. Katsumata, and K. Sato. Temporal tuning of homeward flights in seabirds. *Animal Behaviour*, 83(2):355–359, 2012.

[81] R. V. Short, E. Balaban, et al. *The differences between the sexes*. Cambridge University Press, 1994.

[82] N. Srivastava, E. Mansimov, and R. Salakhudinov. Unsupervised learning of video representations using lstms. In *Proceedings of the 32nd International Conference on Machine Learning*, pages 843–852. PMLR, 2015.

[83] E. K. Studd, M. Landry-Cuerrier, A. K. Menzies, S. Boutin, A. G. McAdam, J. E. Lane, and M. M. Humphries. Behavioral classification of low-frequency acceleration and temperature data from a free-ranging small mammal. *Ecology and Evolution*, 9(1):619–630, 2019.

[84] A. Surlykke and E. K. Kalko. Echolocating bats cry out loud to detect their prey. *PLoS one*, 3(4):1–10, 2008.

[85] P. V. Switzer. Site fidelity in predictable and unpredictable habitats. *Evolutionary Ecology*, 7(6):533–555, 1993.

[86] M. Teimouri, U. G. Indahl, H. Sickel, and H. Tveite. Deriving animal movement behaviors using movement parameters extracted from location data. *ISPRS International Journal of Geo-Information*, 7(2):78, 2018.

[87] Y. Tian, T. Maekawa, D. Amagata, T. Hara, S. Matsumoto, K. Yoda, E. Fujioka, F. Hamai, D. Fukui, and S. Hiryu. Discovery and verification of frequent rules in migration behavior data of streaked shearwater and japanese large-footed bat. In *Proceedings of ZSJ*, 2018.

[88] Y. Tian, T. Maekawa, D. Amagata, T. Hara, S. Matsumoto, K. Yoda, E. Fujioka, F. Hamai, D. Fukui, and S. Hiryu. Preliminary investigation of co-occurrence rule extraction from multi-modal animal locomotion data. In *Proceedings of IPSJ*, 2018.

[89] Y. Tian, T. Maekawa, D. Amagata, T. Hara, S. Matsumoto, K. Yoda, E. Fujioka, F. Hamai, D. Fukui, and S. Hiryu. A study on fast extraction of frequent co-occurrence rules from animal movement behavior data. In *Proceedings of DEIM Forum*, 2018.

[90] Y. Tian, T. Maekawa, D. Amagata, T. Hara, S. Matsumoto, K. Yoda, E. Fujioka, F. Hamai, D. Fukui, and S. Hiryu. Discovering frequent co-occurrence rules from multi-modal animal locomotion data. *IPSJ Journal*, 60(3):859–869, 2019.

[91] Y. Tian, T. Maekawa, T. Hara, S. Matsumoto, and K. Yoda. A study on the discovery of factors involved in decision-making in animals using behavioral prediction. In *Proceedings of SICE*, 2020.

[92] Y. Tian, T. Maekawa, T. Hara, Y. Yokomori, and T. Kitagawa. Navimine: A tool for mining trajectories through behavior prediction. In *Proceedings of PerCom2021 Workshop on Pervasive Information Flow*, 2021.

[93] Y. Tian, T. Maekawa, J. Korpela, D. Amagata, T. Hara, S. Matsumoto, and K. Yoda. Preliminary investigation of co-occurrence rule extraction for sex-specific behavior of streaked shearwater. In *Proceedings of ACML2019 Workshop on Machine Learning for Trajectory, Activity, and Behavior*, 2019.

[94] Y. Tian, T. Maekawa, J. Korpela, D. Amagata, T. Hara, S. Matsumoto, and K. Yoda. Automatic identification of differences in behavioral co-occurrence between groups, animal biotelemetry (accepted). *Animal Biotelemetry*, 9(21):1–15, 2021.

[95] N. Tinbergen and W. Kruyt. Über die orientierung des bienenwolfes (philanthus triangulum fabr.). *Zeitschrift für vergleichende Physiologie*, 25(3):292–334, 1938.

[96] P. Turchin. *Quantitative analysis of movement: measuring and modeling population redistribution in animals and plants*. Sinauer Associates, 1998.

[97] A. Ultsch and F. Mörchen. Esom-maps: tools for clustering, visualization, and classification with emergent som. Technical report, DATA BIONICS RESEARCH GROUP, UNIVERSITY OF MARBURG, 2005.

[98] J. J. Valletta, C. Torney, M. Kings, A. Thornton, and J. Madden. Applications of machine learning in animal behaviour studies. *Animal Behaviour*, 124:203–220, 2017.

[99] M. Vartak, S. Madden, A. Parameswaran, and N. Polyzotis. Seedb: Automatically generating query visualizations. *VLDB Endowment*, 7:1581–1584, 08 2014.

[100] M. Vartak, S. Rahman, S. Madden, A. Parameswaran, and N. Polyzotis. Seedb: Efficient data-driven visualization recommendations to support visual analytics. *Proc. VLDB Endow.*, 8(13):2182—-2193, Sept. 2015.

[101] N. J. Vickers. Mechanisms of animal navigation in odor plumes. *The Biological Bulletin*, 198(2):203–212, 2000.

[102] U. von Luxburg. A tutorial on spectral clustering. *Statistics and Computing*, 17(4):395–416, 2007.

[103] H. Wagner and F. Sauer. Die sternenorientierung nächtlich ziehender grasmücken (sylvia atricapilla, borin und curruca) 1. *Zeitschrift für Tierpsychologie*, 14(1):29–70, 1957.

[104] H. Weimerskirch, J. Martin, Y. Clerquin, P. Alexandre, and S. Jiraskova. Energy saving in flight formation. *Nature*, 413(6857):697–698, 2001.

[105] H. Weimerskirch, D. Pinaud, F. Pawlowski, and C. Bost. Does prey capture induce area-restricted search? a fine-scale study using gps in a marine predator, the wandering albatross. *The American Naturalist*, 170:734–743, 12 2007.

[106] WHO. Who calls for further studies, data on origin of sars-cov-2 virus, reiterates that all hypotheses remain open. `https://www.who.int/news/item/30-03-2021-who-calls-for-further-studies-data-on-origin-of-sars-cov-2-virus-reiterates-that-all-hypotheses-remain-open`.

[107] R. Wiltschko and W. Wiltschko. *Magnetic Orientation in Animals*. Springer, 1995.

[108] W. Wiltschko, K. Stapput, P. Thalau, and R. Wiltschko. Avian magnetic compass: fast adjustment to intensities outside the normal functional window. *Naturwissenschaften*, 93(6):300–304, 2006.

[109] W. Wiltschko and R. Wiltschko. Magnetic orientation and magnetoreception in birds and other animals. *Journal of Comparative Physiology A: Neuroethology, Sensory, Neural, and Behavioral Physiology*, 191(8):675–693, 2005.

[110] W. J. Wisby and A. D. Hasler. Effect of olfactory occlusion on migrating silver salmon (o. kisutch). *Journal of the Fisheries Board of Canada*, 11(4):472–478, 1954.

[111] S. J. Yamazaki, K. Ohara, K. Ito, N. Kokubun, T. Kitanishi, D. Takaichi, Y. Yamada, Y. Ikejiri, F. Hiramatsu, K. Fujita, et al. STEFTR: A hybrid versatile method for state estimation and feature extraction from the trajectory of animal behavior. *Frontiers in Neuroscience*, 13:626, 2019.

[112] C.-C. M. Yeh, N. Kavantzas, and E. Keogh. Matrix profile vi: Meaningful multidimensional motif discovery. In *2017 IEEE international conference on data mining (ICDM)*, pages 565–574. IEEE, 2017.

[113] K. Yoda, K. Shiomi, and K. Sato. Foraging spots of streaked shearwaters in relation to ocean surface currents as identified using their drift movements. *Progress in Oceanography*, 122:54–64, 2014.

[114] J. Yuan, Y. Zheng, X. Xie, and G. Sun. Driving with knowledge from the physical world. *Proceedings of the 17th ACM SIGKDD International Conference on Knowledge Discovery and Data Mining*, pages 316–324, 2011.

[115] J. Yuan, Y. Zheng, C. Zhang, W. Xie, X. Xie, G. Sun, and Y. Huang. T-drive: driving directions based on taxi trajectories. *Proceedings of the 18th SIGSPATIAL International Conference on Advances in Geographic Information Systems*, pages 99–108, 2010.

[116] F. Zhou, F. D. la Torre Frade, and J. K. Hodgins. Aligned cluster analysis for temporal segmentation of human motion. In *Proceedings of the 8th IEEE International Conference on Automatic Face Gesture Recognition*, pages 1–7, 2008.

[117] F. Zhou, F. D. la Torre Frade, and J. K. Hodgins. Hierarchical aligned cluster analysis (haca) for temporal clustering of human motion. *IEEE Transactions on Pattern Analysis and Machine Intelligence*, 35(3):582 – 596, March 2013.

[118] J. Zi, X. Yu, Y. Li, X. Hu, C. Xu, X. Wang, X. Liu, and R. Fu. Coloration strategies in peacock feathers. *Proceedings of the National Academy of Sciences*, 100(22):12576–12578, 2003.

[119] R. K. Zimmer-Faust, C. M. Finelli, N. D. Pentcheff, and D. S. Wethey. Odor plumes and animal navigation in turbulent water flow: a field study. *The Biological Bulletin*, 188(2):111–116, 1995.